PHYSICOCHEMICAL STUDIES OF TRIAZOLYL BENZOATE AMPHIPHILE AND THE EFFECTS OF DIFFERENT GLYCOLIPIDS TOWARDS ITS CRITICAL MICELLAR CONCENTRATION

NURUL FAIEZIN BINTI ZUL

FACULTY OF SCIENCE
UNIVERSITI MALAYA
KUALA LUMPUR

2021

PHYSICOCHEMICAL STUDIES OF TRIAZOLYL BENZOATE AMPHIPHILE AND THE EFFECTS OF DIFFERENT GLYCOLIPIDS TOWARDS ITS CRITICAL MICELLAR CONCENTRATION

NURUL FAIEZIN BINTI ZUL

DISSERTATION SUBMITTED IN FULFILMENT OF THE REQUIREMENTS FOR THE DEGREE OF MASTER OF SCIENCE

DEPARTMENT OF CHEMISTRY
FACULTY OF SCIENCE
UNIVERSITI MALAYA
KUALA LUMPUR

2021

UNIVERSITI MALAYA

ORIGINAL LITERARY WORK DECLARATION

Name of Candidate: **NURUL FAIEZIN BINTI ZUL**

Matric No: **17006177/2**

Name of Degree: **MASTER OF SCIENCE**

Title Dissertation ("this Work"):

PHYSICOCHEMICAL STUDIES OF TRIAZOLYL BENZOATE AMPHIPHILE AND THE EFFECTS OF DIFFERENT GLYCOLIPIDS TOWARDS ITS CRITICAL MICELLAR CONCENTRATION

Field of Study: **PHYSICAL CHEMISTRY**

I do solemnly and sincerely declare that:

(1) I am the sole author/writer of this Work;
(2) This Work is original;
(3) Any use of any work in which copyright exists was done by way of fair dealing and for permitted purposes and any excerpt or extract from, or reference to or reproduction of any copyright work has been disclosed expressly and sufficiently and the title of the Work and its authorship have been acknowledged in this Work;
(4) I do not have any actual knowledge nor do I ought reasonably to know that the making of this work constitutes an infringement of any copyright work;
(5) I hereby assign all and every rights in the copyright to this Work to the University of Malaya ("UM"), who henceforth shall be owner of the copyright in this Work and that any reproduction or use in any form or by any means whatsoever is prohibited without the written consent of UM having been first had and obtained;
(6) I am fully aware that if in the course of making this Work I have infringed any copyright whether intentionally or otherwise, I may be subject to legal action or any other action as may be determined by UM.

Candidate's Signature Date:

Subscribed and solemnly declared before,

Witness's Signature Date:

Name:

Designation:

PHYSICOCHEMICAL STUDIES OF TRIAZOLYL BENZOATE AMPHIPHILE AND THE EFFECTS OF DIFFERENT GLYCOLIPIDS TOWARDS ITS CRITICAL MICELLAR CONCENTRATION

ABSTRACT

Basic molecular structure of natural fatty acids consisted of polar carboxylic acid headgroup (hydrophilic) connected to non-polar hydrocarbon tail (hydrophobic). However, the addition of a heteroaromatic as a linker between the regions and how they interact within the molecules in self-assembling structure were not well explored. The structure has inspired us to prepare and investigated a synthetic amphiphile constructed from the similar headgroup and alkyl chain but connected by triazolyl group, named as *para*-decyloxymethyl triazolyl benzoate (*p*-DMTB). The triazolyl was sufficiently produced from Copper(I)-catalyzed cycloaddition between 4-azidobenzoic acid and alkyl acetylene. Purity and molecular elucidation of the amphiphile were analyzed from ^{1}H and ^{13}C Nuclear Magnetic Resonance (NMR) Spectroscopy, Fourier-Transform Infra-Red (FT-IR) Spectroscopy, Liquid Chromatography-Mass Spectrometry (LC-MS) and elemental analysis. Self-aggregation of *p*-DMTB in basic condition has been investigated by using various methods such as surface tension, electrical conductivity, absorbance and emission intensity. The results showed that the amphiphile self-aggregated at extremely low concentration (0.10 mM) influenced by the heterocyclic and aromatic moieties in the amphiphile structure. The amphiphile was then investigated in the presence of glycolipids with three different alkyl chain lengths: octyl-*β*-D-glucopyranoside (OG), decyl-*β*-D-glucopyranoside (DG) and dodecyl-*β*-D-glucopyranoside (DDG). Series of mixed *p*-DMTB-glycolipids solutions have been prepared with a fixed-volume ratio of 9 to 1. The samples were analyzed using surface tension, turbidity and fluorescence spectroscopy measurements. The results suggested that the presence of OG, DG and DDG have disturbed the aggregation of *p*-DMTB in the mixture solution by increasing the Critical

Micellar Concentration (CMC) value of *p*-DTMB. Consistent with the earlier part of the investigation, *p*-DMTB without glycolipids was stable due to the headgroup and hydrophobic interactions with additional interaction from aromatic phenyl and heterocyclic triazolyl. However, the presence of glycolipids within *p*-DMTB aggregation has reduced the effectiveness of interactions that exist within the amphiphile molecules. Therefore, additional interactions such as hydrogen bonding and π-π interaction within *p*-DMTB molecule could be another co-factor for the amphiphile to self-aggregate more effectively without the presence or help from the glycolipid co-surfactant.

Keywords: Self-aggregation, Triazole, Glycolipids, Micelle, Vesicle.

KAJIAN FIZIKOKIMIA AMFIFIL TRIAZOLIL BENZOAT DAN KESAN GLIKOLIPID YANG BERLAINAN TERHADAP KEPEKATAN KRITIKAL MISEL

ABSTRAK

Struktur molekul asas asid lemak semulajadi terdiri daripada kumpulan kepala asid karboksilik polar (hidrofilik) dan rantaian hidrokarbon bukan polar (hidrofobik). Bagaimanapun, tambahan suatu heterosiklik sebagai kumpulan penyambung antara kedua lingkungan kawasan serta bagaimana heterosiklik itu berhubung di dalam struktur swaaggregat masih samar. Struktur ini telah memberi ilham kepada kami untuk mensintesis dan mengkaji satu amfifil sintetik yang terdiri daripada kumpulan kepala dan satu rantaian alkil yang serupa yang dihubungkan oleh kumpulan triazolil, iaitu *para*-desiloksimetil triazolil benzoat (*p*-DMTB). Triazolil ini telah dihasilkan daripada penambahan siklo bermangkinkan Kuprum (I) di antara asid 4-azidobenzoik dan asetilena alkil dengan hasil yang tinggi. Ketulenan dan pencirian molekul amfifil tersebut dianalisis melalui ^{1}H dan ^{13}C Spektroskopi Nuklear Magnetik Resonans (NMR), Spektroskopi Inframerah Transformasi Fourier (FT-IR), Kromatografi Cecair-Spektrometer Jisim (LC-MS) dan analisis elemen. Swaagregat *p*-DMTB di dalam keadaan beralkali telah dikaji dengan menggunakan pelbagai kaedah seperti tegangan permukaan, kekonduksian elektrik, penyerapan dan pelepasan intensiti. Hasil kajian menunjukkan bahawa amfifil ini membentuk struktur agregat pada kepekatan yang sangat rendah (0.10 mM) yang dipengaruhi oleh kumpulan heterosiklik dan aromatik dalam struktur amfifil. Amfifil ini seterusnya dikaji dengan kehadiran tiga glikolipid yang berlainan kepanjangan ekor: oktil-*β*-D-glukopiranoksida (OG), desil-*β*-D-glukopiranoksida (DG) dan dodesil-*β*-D-glukopiranoksida (DDG). Siri larutan campuran *p*-DMTB-glikolipid telah disediakan dengan nisbah tetap 9 kepada 1. Sampel tersebut dianalisis menggunakan pengukuran tegangan permukaan, kekeruhan dan spektroskopi pendarfluor. Hasil kajian menunjukkan

bahawa kehadiran OG, DG dan DDG mengganggu agregasi *p*-DMTB di dalam larutan campuran dengan meningkatkan nilai Kepekatan Kritikal Misel (CMC) *p*-DMTB. Selaras dengan bahagian awal penyelidikan, *p*-DMTB tanpa glikolipid adalah stabil disebabkan oleh interaksi kumpulan kepala dan hidrofobik dengan interaksi tambahan daripada fenil aromatik dan triazolil heterosiklik. Walau bagaimanapun, kehadiran glikolipid dalam agregasi *p*-DMTB telah mengurangkan keberkesanan interaksi yang terdapat di antara molekul amfifil. Oleh itu, interaksi tambahan seperti ikatan hidrogen dan interaksi π-π di antara molekul *p*-DMTB boleh menjadi factor bersama lain bagi amfifil tersebut mampu swaagregat dengan lebih berkesan tanpa kehadiran ataupun bantuan daripada surfaktan bersama glikolipid.

Kata kunci: Swaagregat, Triazol, Glikolipid, Misel, Vesikel

ACKNOWLEDGEMENTS

First and foremost, I thank Allah the Almighty for all His help and providence while carrying out this research successfully. Indeed, Allah has guided me always along the way throughout my studies. He knows everything and His plan is the best for me. To complete this thesis, I have overcome a lot of challenges that have taught me to be patient and determined. I may not be able to face my obstacles alone without getting assisted by many people around me especially my beloved parents (Zul bin Md Nir and Rashidah binti Abdul Rashid) and siblings (Nurul Farah Ain, Muhammad Aliff Zikry and Nur Fasya Aqilah) for their care, support and encouragement. To them, I express my most profound appreciation and love.

My sincere gratitude goes to both of my supervisors, Associate Professor Dr. Hairul Anuar Tajuddin and Dr. Noraini Ahmad for their precious time, enlightening insights, and uplifting discussions throughout my master's study. I am grateful for their unending great support and invaluable emotional support that has boosted my confidence in conducting the research work, as well as preparing the required scientific article and thesis. Once again, thank you very much for being patient with me.

Besides that, special appreciation to Associate Professor Dr. Zul Hazrin Zainal Abidin, Professor Dr. Zanariah Abdullah and my irreplaceable friends, Amnani, Nadia Chan, Nurulain Nadia, Bayhaki, Shameer, Lidya, Phoebe, Idayu, Yatie, Sopia, Shida, Fatin, Anas, Akmal, Fatirah, Mardhiah, Fadhilah, and other postgraduates friends for their beautiful souls that have helped me during my ups and downs throughout my master's journey. Thank you for all the assistance and memories we have shared together. My heartfelt appreciation also goes out also to all lecturers and staff in the Department of Chemistry, Faculty of Science, as well as the management of the University of Malaya for their diligence, dedication and support.

I am very grateful for the financial support provided by the Ministry of Higher Education (MOHE) grants MO002-2014, Fundamental Research Grant Scheme (FP046-2014A), and the University of Malaya under Research University grant – Faculty Program (RF027B-2018). Finally, I address this thesis to those who seek knowledge about the synthesis of heterocyclic surfactants, surfactant self-assembly and physical chemistry.

TABLE OF CONTENTS

LIST OF FIGURES

LIST OF TABLES

LIST OF EQUATIONS

LIST OF SCHEMES

LIST OF SYMBOLS AND ABBREVIATIONS

α	:	Alpha
β	:	Beta
κ	:	Conductivity
E	:	Energy
v	:	Frequency
l	:	Length
Λ	:	Molar conductivity
h	:	Planck constant
γ	:	Surface tension
F	:	Tensile force
τ	:	Turbidity
λ	:	Wavelength
CMC	:	Critical Micellar Concentration
CPP	:	Critical Packing Parameter
CVC	:	Critical Vesicular Concentration
DG	:	Decyl-β-D-glucopyranoside
DDG	:	Dodecyl-β-D-glucopyranoside
FT-IR	:	Fourier-Transform Infra-Red
GUV	:	Giant Unilamellar Vesicle
Gly	:	Glycolipids
g	:	Gram
LUV	:	Large Unilamellar Vesicle
LC-MS	:	Liquid Chromatography-Mass Spectrometry
μm	:	Micrometer

ml	:	Milliliter
mM	:	Millimolar
M	:	Molar
nm	:	Nanometer
NMR	:	Nuclear Magnetic Resonance
OG	:	Octyl-*β*-D-glucopyranoside
OPM	:	Optical polarizing microscope
p-DMTB	:	*Para*-decyloxymethyl triazolyl benzoate
p-DMTBA	:	*Para*-decyloxymethyl triazolyl benzoic acid
SUV	:	Small Unilamellar Vesicle
TLC	:	Thin Layer Chromatography
TEM	:	Transmission Electron Micrograph
UV-VIS	:	Ultraviolet-Visible

LIST OF APPENDICES

CHAPTER 1: INTRODUCTION

1.1 Introduction to the research

Self-assembly of amphiphilic molecules can be described as a spontaneous aggregation process which driven by non-covalent interactions such as hydrogen bonding, electrostatic, hydrophobic interaction, van der Waals and metal-ligand coordination bonding. Hydrophobic interaction occurred between the hydrocarbon tails would be the primary driving force for surfactants to self-assembling. Meanwhile, electrostatic and hydrogen bonding attractions between headgroups may further stabilize the aggregation. Combinations of the interactions can also drive the amphiphilic molecules into various shapes besides their packing parameters. For example, the shapes could be spherical, cylindrical, or rod-like micelles (Fisher & Oakenfull, 1977). Another fascinating self-aggregated surfactant shape is vesicles (Hoffmann et al., 1999; Maibaum et al., 2004).

The shapes of some surfactants can be produced by using various methods such as sonication (Akbarzadeh et al., 2013), mechanical extrusion under high-pressure conditions (Frisken et al., 2000; Hunter & Frisken, 1998) as well as from a mixture of different types of surfactants (Fukuda et al., 1990; Gabriel & Roberts, 1984; Kaler et al., 1989; Kondo et al., 1995). Example of a common approach to convert micelle-to-vesicle shapes is by using pH titration mainly observed in natural fatty acids. Large sizes of vesicles up to 10 μm have been reported by this approach (Chen et al., 2017; Fameau et al., 2014; Kanicky & Shah, 2003). Unfortunately, the large size vesicles usually are less stable than the smaller size vesicle. Therefore, the presence of non-covalent interactions between the surfactant molecule, typically electrostatic and hydrophobic interactions could help to form and stabilize such vesicles.

Besides these common interactions, other non-covalent interactions can induce or enhance self-aggregation mechanisms. The incorporation of a heteroaromatic group within an amphiphilic molecular structure can create additional interactions. For example, hydrogen bonding has been reported to occur in the porphyrin group through its four amino groups that interact intramolecularly that leads to the formation of a highly ordered array (Liu et al., 2014). Another example of a heteroaromatic group that shows similar interactions to porphyrin is triazole. In recent years, triazole has attracted considerable interest due to its straightforward synthesis from Click chemistry reaction (Han et al., 2018; Ozkal et al., 2014; Rostovtsev et al., 2002; Sharpless et al., 2008; Tornoe et al., 2002). The triazole moiety has been recognized to influence the overall structure of certain foldamers from the C-H position particularly through ion complexation, e.g. palladium (Yuasa et al., 2017) and chloride (Hua & Flood, 2010; Juwarker et al., 2008). Although the C-H groups are the typical weaker donors of hydrogen bonds than hydrogens bound to heteroatoms, CH---N / O interactions may play a role to help in molecular assembly (Leigh et al., 2013).

Molecular self-assembly also can be driven by π–π interaction occurred between aromatic moieties. There are reports suggesting the π–π interaction stabilizing self-aggregated structures such as in phenylene ethynylene (Pickholz & Stafström, 2001) and proteins (Gazit, 2002). Moreover, π–π interaction has been an indicator to determine the orientation of self-assembly in parallel, face-to-face or edge-to-face (Hunter & Sanders, 1990).

The non-covalent interactions described above could be additional factors to influence the self-assembly of heteroaromatic-contained amphiphiles. We aim to explore the triazole self-assembly in detail using different approaches like surface tension, conductivity, absorbance intensity, fluorescence emission and optical properties.

Meanwhile, hydrogen bonding and π-π interactions could be deduced and proven from Nuclear Magnetic Resonance (NMR). The work will be then employed for the main study involving the addition of co-surfactants, which are glycolipids with different alkyl chains in aqueous solution.

1.2 Introduction to amphiphile

Amphiphile is derived from the Greek word *amphi,* meaning both, in which the amphiphile is composed of two regions; polar and non-polar. The polar part has a strong attraction to polar solvent such as aqueous (hydrophilic) while non-polar repels from the aqueous solvent (hydrophobic). **Figure 1.1** below shows the basic structure of amphiphile. When amphiphiles are dissolved in water, the hydrophobic group distorts the water structure in such to decrease the entropy of the system. Some of the molecules expelled from the bulk of the solvent and adsorbed at the air-water interfaces. Meanwhile, hydrophilic keeps them in solution and prevents them from separating as another phase.

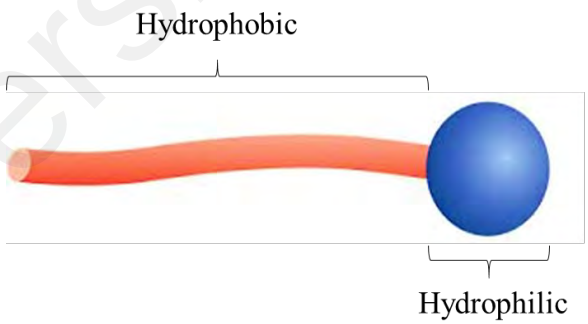

Figure 1.1: A schematic diagram of amphiphile. Redrawn from (Myers, 1999).

Amphiphile can be categorized into four general types based on the headgroup (Butt et al., 2004) including positive (cationic), negative (anionic), positive and negative (amphoteric) and without charge (nonionic). The most common examples of cationic, anionic, amphoteric and nonionic amphiphile are cetyltrimethylammonium bromide

(CTAB), decanoic acid, N-dodecyl-N,N-dimethyl-3-ammonio-1-propanesulfonate and Tween 60, respectively. They can be summarized as **Table 1.1** below:

Table 1.1: Types of amphiphiles.

Types	Characters	Examples	References
Anionic	Hydrophilic group with a negative charge	Carboxyl ($RCOO^{-}$ M^{+}), sulfonate (RSO^{-}_{3} M^{+}), or sulfate ($ROSO^{-}_{3}$ M^{+})	(Rustan & Drevon, 2005)
Cationic	Hydrophilic group with a positive charge	Quarternary ammonium halides (R_4N^{+} X^{-})	(Verma & Ghosh, 2011)
Nonionic	No charge	Polyoxyethylene, Glycolipids	(Wanka et al., 1994)
Amphoteric	Both charges at the hydrophilic group	Betaine	(Kronberg et al., 2014)

1.2.1 Structure of amphiphilic molecule aggregates

Basic idea about the aggregation of amphiphiles has been introduced (Tanford, 1974). The concept is about two opposing forces that control self-aggregation. The two forces involved are attractive interfacial terms from hydrocarbon/water interactions and repulsion terms that arise from headgroup-headgroup interactions.

Israelachvili et al., (1976) have quantified the basic idea proposed by Tanford (1974) for amphiphile aggregation to be controlled by the balanced geometry of the amphiphile molecule. The balanced geometry of the amphiphile relates the overall free energy of association into three variables of the molecule, which are the effective area of headgroup, a_o, the volume of hydrophobic tails, V, and the length of hydrophobic tails, l_c. From those three variables, as shown in **Figure 1.2**, it allows a simple and estimation into the

aggregation of amphiphile phenomenon, which is known as a critical packing parameter (CPP) (Israelachvili et al., 1976). CPP is defined as in **Equation 1.1**.

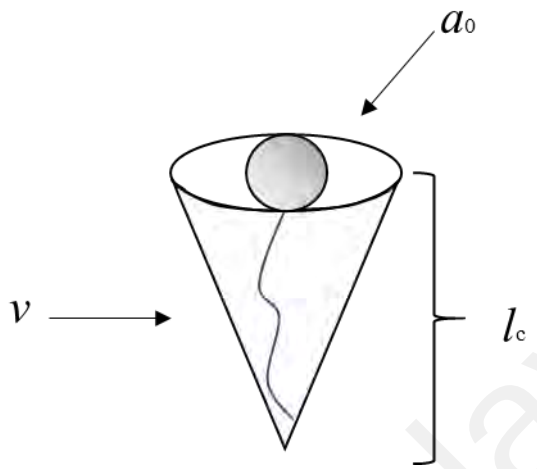

Figure 1.2: Illustration to determine the packing parameter of amphiphile.

$$\boldsymbol{CPP} = \frac{\boldsymbol{v}}{\boldsymbol{a_o l_c}} \tag{1.1}$$

where V is the volume of hydrophobic tails, l_c denotes as the length of hydrophobic tail and a_o is the effective area of headgroup.

Based on the CPP equation, CPP value increases if a_o is a small value, and V is a large input. This would change the amphiphile aggregate structure from spherical to cylindrical micelles. As a result, the transformation from cylindrical micelles to bilayers is expected to happen.

Modification of the solution conditions, such as adding salt to ionic amphiphile and increasing temperature for nonionic amphiphile, can reduce the repulsion force at the headgroup. Thus, a_o decreases and CPP value will increase. Besides that, the hydrophobic tail from single to double chains resulting in the packing parameter twice compared to single chain molecule. Therefore, double chain amphiphile can self-assemble to bilayer

aggregates while the corresponding single chain amphiphile into spherical or cylindrical micelles (Nagarajan, 2002).

Several types of amphiphilic aggregates structures can be estimated from CPP value such as spherical micelle, cylindrical micelle, vesicles, planar bilayers and inverted micelles. Based on **Table 1.2**, if the CPP value is less than 1/3, the amphiphile structure will form spherical micelles. If 1/3 < CPP < 1/2, cylindrical micelles are formed, such as CTAB in high salt concentration (Hoffmann & Ebert, 1988). Vesicles will form with CPP value in range 1/2 to 1, and as CPP is approximate to 1, planar bilayers are formed. More than 1 of the CPP value will induce amphiphiles to form inverted micelles (Kontogeorgis & Kiil, 2016).

Table 1.2: Type of structure formed with CPP values.

CPP value	Structure formed	Examples	Reference
<1/3 	Spherical micelle	Single chain surfactants, e.g. SDS in low salt concentration	(Kontogeorgis & Kiil, 2016)
1/3 – 1/2 	Cylindrical micelle	Single chain surfactants with small headgroup areas, e.g. CTAB and SDS in high salt concentrations, nonionic surfactants	(Butt et al., 2004)
1/2 – 1 	Flexible bilayers	Double – chain surfactants with large headgroup areas, e.g. lecithin, dihexadecyl phosphate	(Butt et al., 2004)
~ 1 	Planar bilayers	Double chain surfactants with small headgroup areas. Anionic surfactant in high salt concentrations, e.g. phosphatidyl ethanolamine	(Kontogeorgis & Kiil, 2016)
> 1 	Inverted micelles	Double – chain surfactants with small headgroup areas. Nonionic surfactants and anionic surfactants in high salt concentrations, e.g. cardiolipin + Ca^{2+}.	(Kontogeorgis & Kiil, 2016)

1.2.2 Applications of amphiphiles

Aggregation of amphiphiles has led to many applications. They are widely applied in industrial and pharmaceutical platforms. Several examples of amphiphiles used in industry are alcohol ethoxylates, alkylbenzene sulfonates, sulfates and ether sulfates, which become major components of personal care products, household and laundry detergents. In pharmaceutical application, amphiphile act as an enhancer for percutaneous absorption (Nishihata et al., 1988), for respiratory distress therapy (Logan & Moya, 2009), flocculating agents (Li et al., 2009) and mouthwashes (Reshad et al., 2009).

Besides, another potential of amphiphiles is in the biochemistry aspect when amphiphiles act as a solubilizing agent to determine molecular structure in membrane proteins (Ek et al., 1983). Meanwhile, in the electrophoresis aspect, amphiphile is needed for transferring in membrane proteins to identify the hydrophobic region in proteins (Ek et al., 1983). The rise of amphiphiles application has also driven the scientist to study the physical and chemical investigation in mixed amphiphile system.

1.2.3 Micelle

The simple aggregate formed by surfactant in aqueous solution is micelles. Critical micellar concentration (CMC) is the concentration of surfactant when the micelle spontaneously forms in solution. General pertinent techniques characterize the formation of micelles is by determining changes in surface tension value, the turbidity of the amphiphile solution with varying surfactant concentration, and measurement of ion conductivity in the solution. Experimentally, the CMC value is deduced by plotting a graph of suitable physical property as a function of surfactant concentration. From the graph, a discontinuity in system properties marks the CMC.

Figure 1.3 is a schematic representation showing the discontinuity of physical properties such as osmotic pressure, turbidity, surface tension and molar conductivity with increasing surfactant concentration. These parameters and many other types of measurement serve as evidence for the formation of aggregates in solutions of surfactant at relatively well-determined concentrations. Besides the types of analysis used to determine the aggregation of amphiphiles, several factors affect the value of CMC in solution.

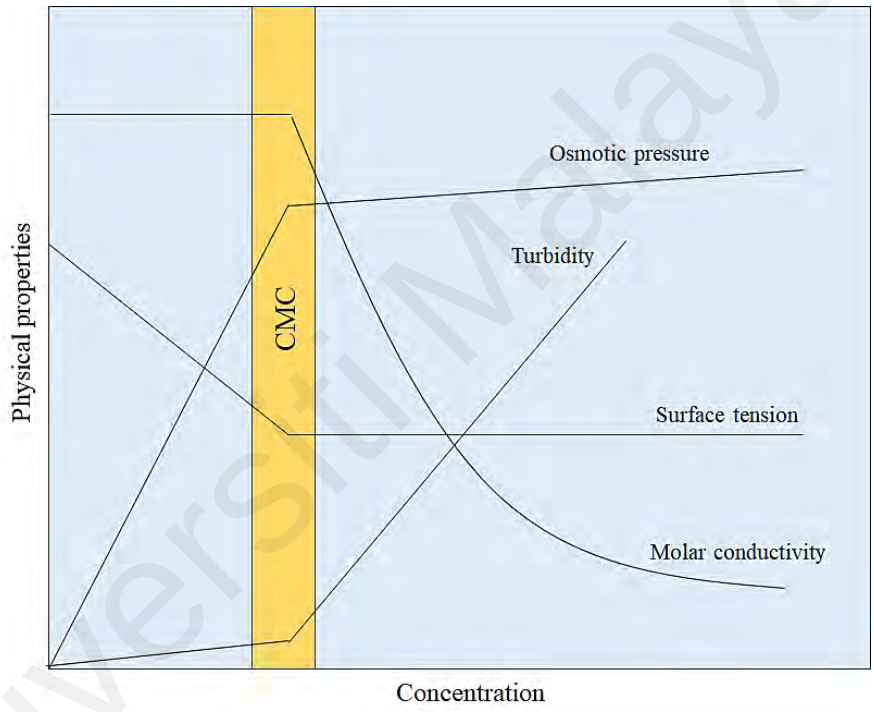

Figure 1.3: The CMC determination using selected physical properties against concentration of amphiphile. Redrawn from (Holmberg et al., 2003).

Factors that affect the CMC value are (1) structure of the amphiphile, (2) the presence of added electrolyte in solution, and (3) temperature of the solution. The hydrophilic headgroup and hydrophobic tails indicate regions in the amphiphile. Hydrophobic tails are divided by length, branching and unsaturation properties. In general, as the length of hydrophobic tails increases, the CMC value is decreased (Mukerjee, 1967). Longer hydrophobic tails may increase the tendency of amphiphile to form micelle. For example,

homologous series of alkyl trimethylammonium bromide with 12, 14 and 16 alkyl chain length significantly reduced the CMC value from 0.0017 M to 0.0009 M (Peterson & Marzzacco, 2007).

In case of branched hydrophobic chain, the branching causes an increase in CMC due to low free energy arise from the aggregation. Besides, unsaturation at hydrophobic tails contributes to increasing the CMC value by a factor of 3-4 compared to saturated tails. Meanwhile, *cis* isomer generally has higher CMC value than *trans* isomer. These observations could be due to the steric factor in micelle formation (Rosen, 1972). Therefore, the short length of the alkyl chain, branching and unsaturation at hydrophobic tails causes the formation of the bulky hydrophobic group, thus resulting in higher CMC value and restrict the formation of aggregates.

Nevertheless, CMC value also could be changed by different types of hydrophilic groups. For example, ionic surfactants have higher CMC than nonionic surfactants with equivalent hydrophobic groups. However, zwitterionic surfactants have slightly smaller CMC than ionic with the same number of carbons at the tail group. Position of the hydrophilic group also gives a prominent effect to the CMC (Rosen, 2004).

As the position of the hydrophilic group moves towards the middle of the molecule, the CMC increases. Such an effect could be similar to a branched hydrophobic group which leads to a steric effect on the micellar formation (Evans, 1956). Micelle formation in the ionic surfactant is closely related to the interaction of the solvent with the ionic headgroup. The degree of ionization would influence the value of CMC and aggregation number. Such an effect is attributed to the presence of additives in the solution.

Addition of additives gives a dramatic effect to lower the CMC of shorter chain to more extended chain surfactants. A variation of CMC for several carbons in the alkyl chains with high salt concentration is much stronger than without the addition of salt (Rosen, 2004). The effect of added salt strongly depends on the valency of the ions.

Besides additives in the solution, temperature also is one factor that affects the CMC value of amphiphiles. Effect of temperature to CMC is related to hydration of hydrophobic and hydrophilic amphiphiles in aqueous solution. At low temperatures, hydration for both parts of amphiphile is possible because of the monomer state. Nevertheless, the hydrations are disturbed with the rise in temperature. An increase in temperature causes low hydration at the hydrophilic part by disruption of water structure surrounds the amphiphiles. The micelle is disrupted at a higher temperature, hence increasing the CMC value.

1.2.4 Vesicles

Self-organizing of amphiphile with the hydrophilic group oriented toward bulk water while the hydrophobic group builds the inner part of bilayer leads to the formation of self-closed lipid bilayers known as vesicles. A typical example of the natural vesicle is a phospholipid that is a major component in the cell membrane. Phospholipid structures that were initially discovered by Theodore Nicolas Gobley in 1847 are composed of two fatty acid chains as the hydrophobic group, while phosphate derivatives, such as phosphocholine, are the hydrophilic group with glycerol connector (Hensing, 2004).

Formation of vesicles occurs with CPP value between 1/2 to 1 due to the increase in the volume of the hydrophobic group. Vesicles are often spherical but can also exist in different shapes. They can be different sizes and types of bilayers, such as unilamellar and multilamellar. Unilamellar can be divided into three sizes, which are small, large and giant. Small unilamellar vesicle (SUV) is ranging from 20 to 100 nm while large

unilamellar vesicle (LUV) is between 0.1 to 1 µm and giant unilamellar vesicle (GUV) has a diameter size up to 50 µm.

Various methods can be applied to induce the formation of vesicles, such as mechanical and sonication. Mechanical extrusion approach can produce monodisperse vesicle suspension as a result of energy dissipating shearing forces that are generated when lipid suspension is repeatedly passed through cylindrical pores of polycarbonate membrane filters under high-pressure condition. Although extrusion offers reproducibility, it is slow and causes sample material loss during the extrusion process. By contrast, sonication uses acoustic energy that breaks the multilamellar to unilamellar structure. Sonication will produce a distribution of lipids vesicle with known size. Both extrusion and sonication methods can be applied to break the vesicles into a smaller size.

Formation of large size of vesicles is induced by the addition of salt to amphiphile solution. The salt could influence the growth rate and vesicle diameter. For example, the diameter of vesicles of sodium dodecyl benzenesulfonate (SDBS) was increased with salinity due to compression of the salt on polar headgroup that reduce the volume and curvature of the vesicles (Zhai et al., 2005).

Other than that, another method to induce vesicles is by changes of pH. pH would alter the counterions in the amphiphile solution that leads to the production of vesicles in a specific range of pH. Titration with acid produces a turbid solution that indicates the formation of large particle such as vesicle. Those methods mentioned above are commonly for a single surfactant system.

Gabriel and Robert (1984) have reported vesicles can also be produced by mixing of two surfactants. Two fatty acids with mismatch chain length were mixed in aqueous suspension and produced unilamellar vesicles (Gabriel & Roberts, 1984). Other than that,

two oppositely charged single-tailed surfactants were mixed in various molar ratios to form vesicles in radius ranging from 30 to 80 nm without a mechanical approach (Kaler et al., 1989). A fixed molar ratio of cationic surfactant and single-tailed fatty acid was then reported to produce translucent vesicles with a size of 200 nm observed under transmission electron micrograph (TEM) (Fukuda et al., 1990).

1.3 Mixed amphiphiles

Mixed amphiphiles are a mixture of two components systems with the presence of added components (such as co-surfactant or salt). It would directly affect the properties of amphiphiles system (Ohta et al., 2001; Rosen & Sulthana, 2001; Zhang et al., 2004). A mixture of amphiphiles frequently gives superior performance over a single or pure amphiphile due to its synergistic interaction between the amphiphiles.

The synergism would affect the properties of amphiphile in terms of aggregation, solubility, wetting, foaming and detergency (Nishikido, 1992; Palla & Shah, 2000). Aggregation properties of mixed amphiphiles might be determined either in between or outside the two single amphiphile solutions value.

Mixing of two types of surfactants can be either for ionic/ionic, ionic/nonionic or nonionic/nonionic surfactants. The mixture of ionic/ionic surfactants are generally not compatible due to strong interaction and lead to precipitation in aqueous solution. Besides that, a mixture of nonionic/nonionic surfactants tends to behave ideally as they provide decent solubility in polar solvents such as water. However, ionic/nonionic mixture surfactants are commonly selected because they exhibit excellent aggregation properties compared to their component alone and reduce electrostatic interaction at the ionic surfactant headgroup. Thus, the mixture of ionic/nonionic surfactants is selected to be further discussed.

Interaction between anionic and nonionic surfactants presents in the self-assembly structures is due to intramolecular interactions from hydrophobic interactions between hydrocarbon chains and ion-dipole interaction of the headgroups (Zhang et al., 2004). Paulo and his teams have reported that repulsion between sulfate headgroup of sodium dodecyl sulfate (SDS) was reduced by a factor of 5 by intercalating the nonionic surfactant (Brij 30) from 0 - 0.5 mol fraction between SDS monomers (Moises de Oliviera & H., 2002).

The property such as critical vesicular concentration (CVC) of mixture is better than individual components as they can form a stable vesicle. One interesting finding has been reported about the interaction between natural fatty acid with additional co-surfactant like glycolipids by varying the number of alkyl chain length (Ahmad et al., 2014). It has been observed that interaction between natural fatty acid like decanoic acid and glycolipids were in synergism. That means the presence of co-surfactant was helping in the self-aggregation of both surfactants. The decanoic acid solution with dodecyl-*β*-D-glucopyranoside shifted the CVC value to 0.010 M compared to decanoic acid solution alone (0.020 M) due to the presence of glucosyl as headgroup that increases the size of the polar region (Ahmad et al., 2014). Besides that, the molecular structure of surfactants whether in long, unrigid and not bulky hydrophobic tails may also be resulting in synergism effect to mixed amphiphiles (Rosen & Zhou, 2001).

From all the studies, this drives us to investigate further the mixed system of amphiphile embedded with heterocyclic and aromatic moiety in the presence of glycolipids as co-surfactant.

1.4 Problem statement

One of the popular amphiphiles that can be found in many applications and well self-aggregate is a natural fatty acid. However, synthetic amphiphile has become known because they can be synthesized and used for comparison with natural fatty acid. Even though the headgroup is same, which is the carboxylate group but by having different alkyl chain functional groups and additional aromatic ring influence the CMC value obtained (Hatzopoulos et al., 2011; Kanicky & Shah, 2003).

Nowadays, Click Chemistry has been applied to synthesize heteroaromatic group. The process is straightforward, which enables researchers to obtain a high yield of products. An example of a common heteroaromatic group is triazole synthesized from Click Chemistry. Triazole is widely used as a linker in the supramolecule structure. However, the influence of the triazole in the aggregation of simple molecular structure and mono amphiphile system is still not well understood.

Because of that, a synthetic amphiphile comprising of aromatic and heteroaromatic groups is embedded in the middle part of the molecular structure with carboxylic acid as the headgroup and straight alkyl chain as the tail group as shown in **Figure 1.4**. The influence of both aromatic and heteroaromatic groups to the amphiphile aggregation behavior in aqueous solution will be discussed further.

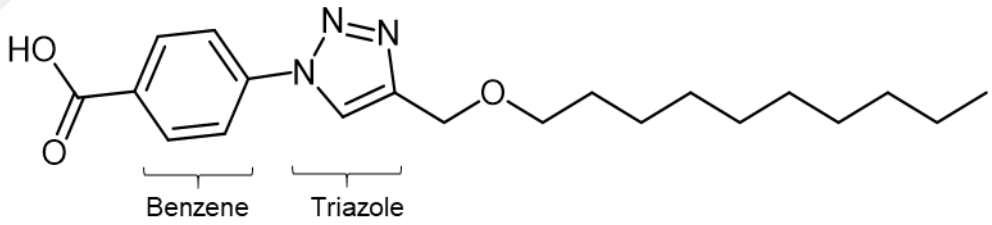

Figure 1.4: Benzene and triazole are in the middle part of the molecular structure.

Afterward, the aggregation of the amphiphile will be determined in the presence of co-surfactant glycolipids. This approach is driven by a report that the aggregation value of natural fatty acid was improved with the presence of glycolipids (Ahmad et al., 2014). **Figure 1.5** shows the possibilities of *p*-DMTB-glycolipids mixture arrangement to micellize. **Figure 1.5**(a) shows *p*-DMTB and glycolipids molecules form micelle by themselves. **Figure 1.5**(b) represent combination of *p*-DMTB and glycolipids in micellar structure whereas *p*-DMTB micelle and unaggregated glycolipids are presented in **Figure 1.5**(c). These possibilities will be discussed in result and discussion part.

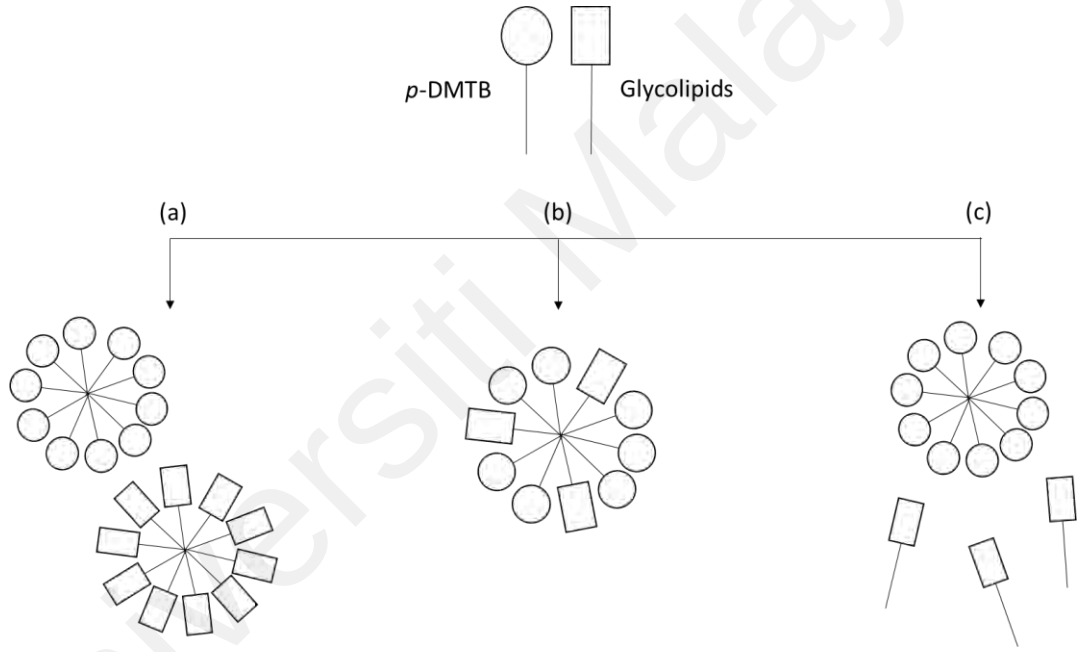

Figure 1.5: Possible micellization arrangement of *p*-DMTB-glycolipids in aqueous solution. (a) Separated *p*-DMTB and glycolipids micelle, (b) Combination of *p*-DMTB and glycolipid as micelle and (c) *p*-DMTB micelle and unaggregated glycolipids.

1.5 Objectives of the research

The main research objective is to characterize the chemical and the physical properties of triazolyl benzoate amphiphile, namely *para*-decyloxymethyl triazolyl benzoic acid (*p*-DMTBA) or *para*-decyloxymethyl triazolyl benzoate (*p*-DMTB). *p*-DMTBA acronym is used in synthesizing parts while *p*-DMTB is when the amphiphile is in aqueous solution form. Consequently, the effects of *p*-DMTB when mixed with glycolipids was studied. In summary, the objectives of this research were as follows:

1. To synthesize and characterize triazolyl benzoate amphiphile.
2. To investigate micellar formation and phase transition of the triazolyl benzoate amphiphile.
3. To investigate the effect of glycolipids towards micellar formation of the triazolyl benzoate amphiphile.

1.6 Significance of the research

The research started by acknowledging uses of natural fatty acid that abundantly been found in human body, industrial and formulation applications. Natural fatty acid can self-aggregate in aqueous solution due to the existing groups which are alkyl chain and carboxylic acid. Based on the two groups, hydrophobic and electrostatic interactions are playing the self-aggregation role for the natural fatty acid, however, those two groups could not provide auxiliary information such as emission study. Thus, additional chromophore moiety needs to be embedded to provide such information.

Synthetic amphiphile was synthesized by Click Chemistry approach that are high yielding and commonly versatile in incorporating moieties such as triazole and phenyl. Self-aggregation of the amphiphile was further investigated in aqueous solution. Triazole act as a chromophore and indicator during self-aggregation process by inducing emission intensity and providing intermolecular hydrogen bonding. Moreover, phenyl group has also been an indicator for other type of interaction which is π-π interaction.

Self-aggregation of the amphiphile was significantly lower than natural fatty acid at 0.10 mM based on spectroscopy analysis like absorbance, fluorescence, conductivity and surface tension. NMR spectroscopy approach also has been applied to interpret hydrogen bonding at C5 to N2 of triazole and protons at phenyl group. Based on the result obtained, existing interaction like electrostatic and hydrophobic interactions are important for self-aggregation of the amphiphile to occur meanwhile hydrogen bonding and π-π interaction act as extra role by promoting the aggregation process.

1.7 Dissertation outline

Chapter 1 describes the general introduction of overall research. It covers topics such as introduction to amphiphile, the structure of amphiphile, applications of amphiphiles, micelle, vesicle and mixed amphiphiles. Besides that, chapter 1 also provide problem statement, objectives, significance and outline of the dissertation.

Chapter 2 represents the literature review and more in-depth discussion of the research. It covers the introduction of reaction that was used in synthesizing *p*-DMTBA, details of choosing aromatic and heteroaromatic groups to be embedded in the amphiphile, and glycolipids as co-surfactant.

Chapter 3 describes the materials and instrumentations used throughout this research. It also explained the experimental techniques used in this work.

Chapter 4 is the results and discussions of the synthesizing *p*-DMTBA on the phase transition and CMC of *p*-DMTB solution. Effect of glycolipids on the micellar formation of *p*-DMTB is also being discussed. The glycolipids that have been used in this research were octyl-*β*-D-glucopyranoside, decyl-*β*-D-glucopyranoside and dodecyl-*β*-D-glucopyranoside.

Chapter 5 gives general conclusions, including some ideas and recommendations for future research.

CHAPTER 2: LITERATURE REVIEW

2.1 Fatty acids

One of the simplest and popular amphiphiles in many applications and very well self-aggregated is natural fatty acid (Averko-Antonovich et al., 2004). Natural fatty acids are used in various purposes as the acids themselves or form of their derivatives such as soap, amides, esters or alcohol. They are composed of hydrocarbon tail of various lengths with a terminal carboxyl group and categorized under anionic amphiphile. The hydrophobic tail of the fatty acid is divided into saturated and unsaturated groups, as shown in **Figure 2.1**. Saturated fats are usually solid at ambient temperature, whereas unsaturated fats are liquid at room temperature. Examples of saturated fats are palmitic acid and stearic acid; meanwhile, the most common example in unsaturated fat is linoleic acid (Anneken et al., 2006).

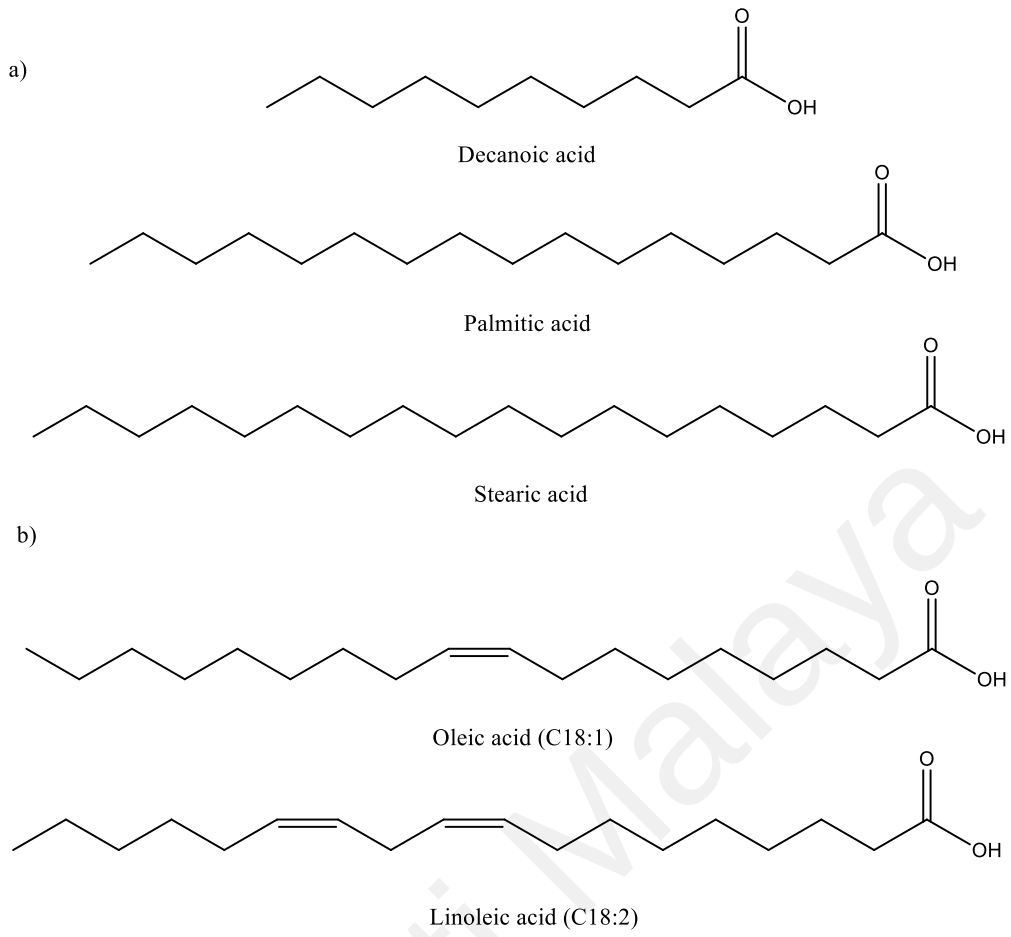

Figure 2.1: Examples of fatty acid with (a) saturated and (b) unsaturated chain lengths. Adapted from (Anneken et al., 2006).

In 1979, a quantification of monocarboxylic acid has been abundantly found in carbonaceous meteorites such as ethanoic acid, hexanoic acid and decanoic acid (Lawless & Yuen, 1979). Decanoic acid has been reported been used as prototypical prebiotic fatty acid due to it is long enough to form vesicles (Hargreaves & Deamer, 1978). Formation of vesicles was determined at various pH depending chain length of the fatty acids. For example, decanoic acid formed vesicles at pH 8 with the incorporation of decanol at molar ratio 1:1 (Hargreaves & Deamer, 1978). Formation of stable fatty acid vesicles was determined by hydrogen bonding $RCOO^{-}$---HOOCR networks in the presence of both ionized and neutral acids and hydrogen bonding acids $RCOO^{-}$ with alcohol HOR (Apel et al., 2002).

Fatty acids are sensitive to pH changes, incompatible with acidic or very basic solutions and relatively insoluble in aqueous. An important parameter to consider with the fatty acid molecule is the pKa value that represents ionic environment of the solution where 50% of the carboxylic group are replaced by existing OH^- in the solution (Shinoda, 1954). Kanicky & Shah (2003) have reported that short-chain fatty acids such as sodium caproate (C6), sodium caprylate (C8), sodium decanoate (C10) and sodium laurate (C12) have limitation in solubility which they need enough amount of sodium hydroxide to solubilize the samples before analysis (Kanicky & Shah, 2003). Large organic counterion, choline has been used to enhance the solubility of the fatty acids by ion-pairing (Klein et al., 2008).

2.2 Amphiphiles with additional aromatic or heteroaromatic groups

Hydrotropes are an amphiphilic organic compound with similar molecular structures as fatty acid. *p*-*n*-alkyl benzoates with various alkyl chain length have been synthesized and examined with conductivity, surface tension and ^{1}H-NMR by incorporating benzene ring in between terminal carboxyl and alkyl chain (Hatzopoulos et al., 2011). **Figure 2.2** shows a schematic diagram of the *p*-*n*-alkyl benzoates. Hatzopoulus et al,. (2011) have determined that critical aggregation concentrations (CAC) of C_nBenz with alkyl chain from C0 to C8 decrease from 0.48 M to 0.011 M. The study has suggested hydrotropes exhibited similar aggregation behavior like other surfactants.

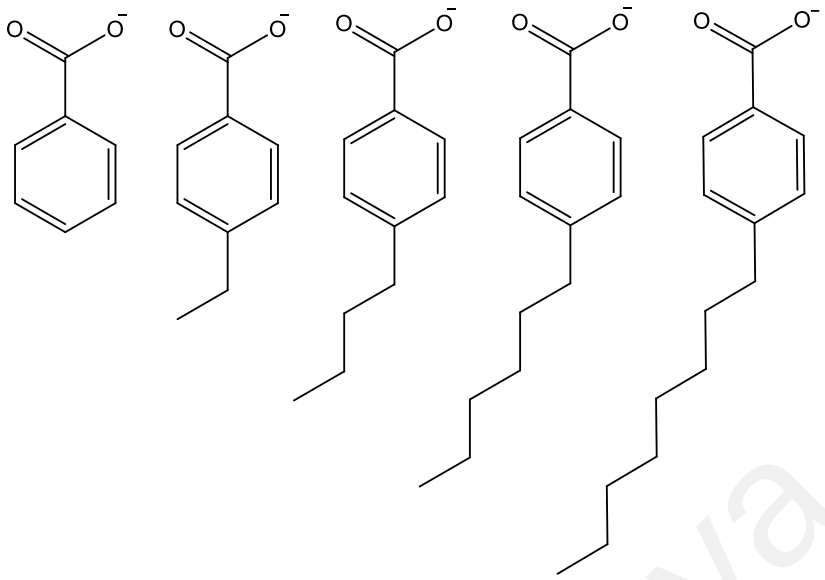

Figure 2.2: A schematic diagram of *p-n*-alkyl benzoates with various alkyl chain lengths. Adapted from (Hatzopoulos et al., 2011).

Figure 2.3 shows cationic amphiphile with 1,4-dioxyphenylene units located at different positions within a long alkyl chain (De et al., 2010). The phenyl location played a significant role in the micellization behavior of the synthetic amphiphiles. The micellization concentration was decreased monotonically from 23 mM to 3 mM as the phenyl group moves from tail to head end. Besides, phenyl position at tail has low solubility in water at room temperature, thus need a higher temperature to make it solubilize before the measurement is performed.

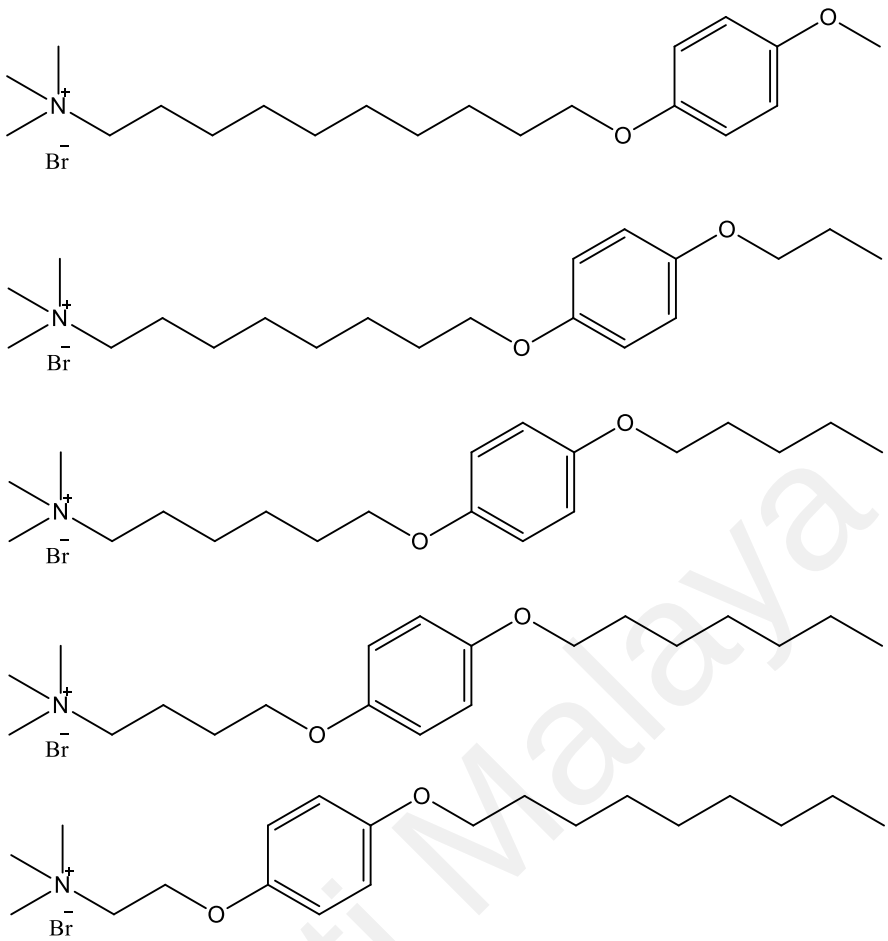

Figure 2.3: A schematic diagram of amphiphile molecule carrying 1,4-dioxyphenylene unit at different locations within hydrophobic segment. Adapted from (De et al., 2010).

Effect of benzene ring was furthered studied by Rabah A Khalil & Saadoon (2015) in terms of viscosity studies (Khalil & Saadoon, 2015). They compared the transformation of one-dimensional aggregate wormlike micelle, a rheological property for sodium dodecyl sulphate (SDS) and sodium dodecylbenzenesulfonate (SDBS) (**Figure 2.4)** and also their mixtures with cationic cetyltrimethylammonium bromide (CTAB) and Triton X-100. Presence of benzene ring causes a negative effect towards formation of one-dimensional aggregate wormlike micelle which increases the Gibbs free energy (ΔG°) from -11.1 to -4.9 kJ mol^{-1}. Previously, they also have reported on the theory of critical intermolecular forces (CIF) (Khalil & Hammad, 2014). CIF described the formation of a wormlike micelle occurred by the aid of dispersion energy between hydrophobic chains

of surfactants, electrostatic attraction between opposite charged polar headgroup, and the formation of excess of hydrogen bond between the water molecules due to the hydrophobic effect. Therefore, in other words, presence of benzene ring did not disturb the formation of wormlike micelles.

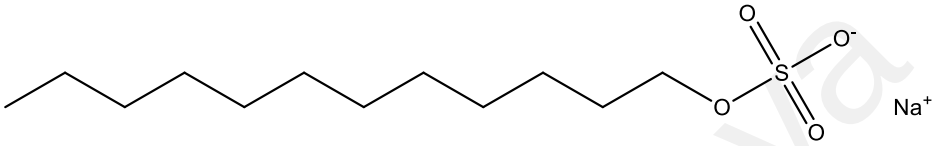

Sodium Dodecyl Sulphate (SDS)

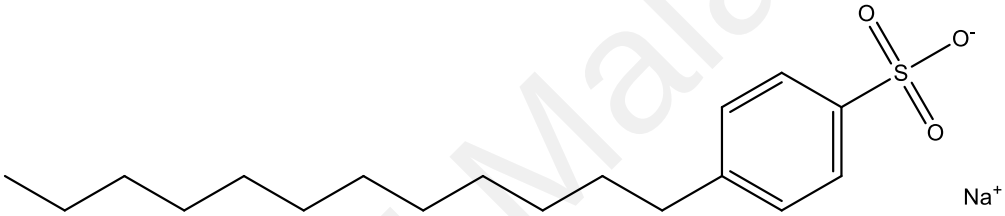

Sodium Dodecylbenzenesulfonate (SDBS)

Figure 2.4: Chemical structures of sodium dodecyl sulphate (SDS) and sodium dodecylbenzenesulfonate (SDBS). Redrawn from (Khalil & Saadoon, 2015).

The next example is a surfactant with a benzene ring synthesized by Li et al., (2005). They have synthesized nonionic surfactant poly(oxyethylene) glycol alkyl ether with the presence of benzene ring at the hydrophobic chain, moves from hydrophobic terminal chain towards the headgroup (Li et al., 2005). Introduction of benzene ring and adamantane at the hydrophobic chain led to steric hindrance that inhibits aggregation. However, the existence of π-π interaction among adjacent phenyl group favors the surfactant to aggregate, especially when the phenyl group moves toward the headgroup. Besides that, even number of carbon atoms at the hydrophobic chain also contributed to the hydrophobic interaction among the hydrophobic chain compared to the odd number of carbon atoms.

Presence of aromatic group within amphiphile structure has been well studied. Beside the aromatic group, heteroaromatic based amphiphile has also been investigated. Example of the heteroaromatic is triazole that is commonly synthesis via a reaction called Click chemistry.

2.3 Click chemistry

'Click' chemistry is a type of reaction that is easy to perform and work up, has high yielding and is tolerant of water or oxygen. One reaction known as Huisgen 1,3-dipolar cycloaddition arises from the field. Huisgen 1,3-dipolar cycloaddition is a reaction of a terminal acetylene (a dipolarophile) with an azide (a 1,3-dipole) to produce a 1,2,3-triazole. '1,3' refers to the atoms of the dipole that undergo reaction whereas [3 + 2] refers to the number of members provided by reactant to form the new ring. Copper(I) catalyst is used and determined to speed up the reaction and regio specificity with formation 1,4-triazole. **Figure 2.5** demonstrates the formation of 1,2,3-triazole by cycloaddition of azide and terminal alkyne with a different parameter such as thermal or catalyst. Thermal cycloaddition shows no regio specificity meanwhile Copper(I)-catalyzed shows regio specificity for 1,4 triazole.

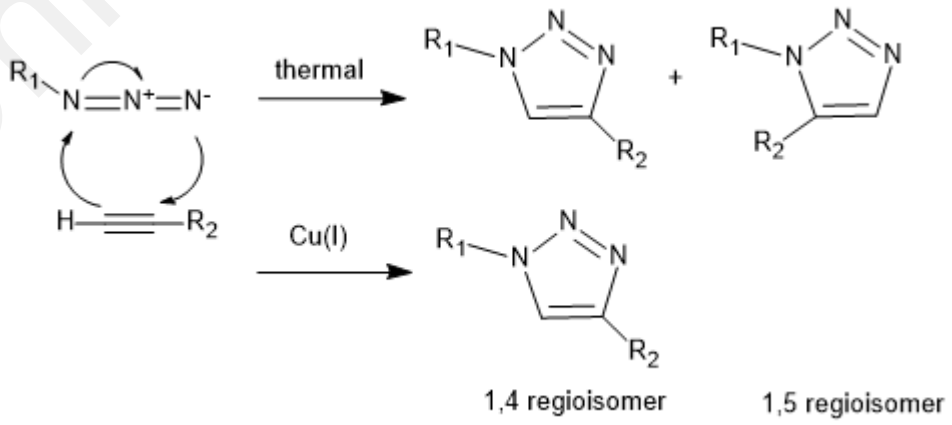

Figure 2.5: Formation of 1,2,3-triazole via thermal and Copper(I) catalyzed.

Triazole has received huge attention since revisited using Copper(I)-catalyzed (Han et al., 2018; Rostovtsev et al., 2002; Sharpless et al., 2008; Tornoe et al., 2002). Triazolyl moiety comprises the N-coordination site that makes it possible to act as a linker (Horne et al., 2004) with metal due to the substantial polarization property of the π system. As a matter of fact of this unique property of triazole, it can be incorporated in fatty acids for the surfactant formation. Examples of triazolyl fatty acid based surfactant include alkyl 1,2,3-triazole carboxylic acids (Fu et al., 2017), 1-(R-phenyl)-5-(R-methyl)-1H-1,2,3-triazole-4-carboxylic acids (Pokhodylo et al., 2010) and 1-phenyl-1H-1,2,3-triazole-4 carboxylic acid (Zhang et al., 2017a) as shown in **Figure 2.6**. However, the example of triazolyl fatty acid was based on the synthesizing part and biological aspect instead of aggregation.

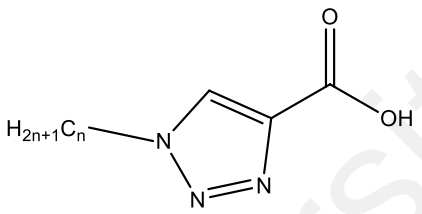

Alkyl 1,2,3-triazole carboxylic acid

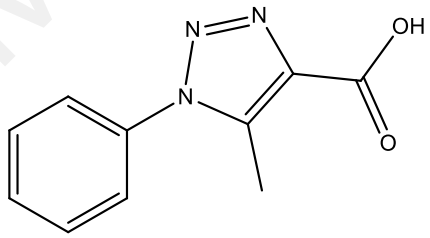

1-(R-phenyl)-5-(R-methyl)-1H-1,2,3-triazole-4-carboxylic acid

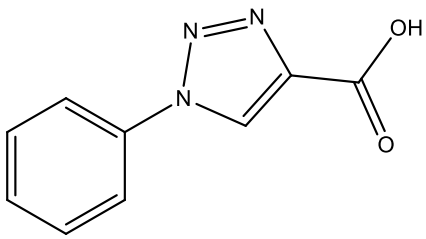

1-phenyl-1H-1,2,3-triazole-4 carboxylic acid

Figure 2.6: Examples of triazolyl carboxylic acid structure synthesized via Click reaction.

Besides that, Sani et al., (2012) have reported a study of triazole that linked between sugar headgroup and alkyl chain. They have determined and compared critical micellar concentration (CMC) values of alkyl triazolyl glycoside (ATGs) with alkyl glucoside. The CMC values of ATGs with 12 carbon alkyl chains and above were in good agreement with those of corresponding alkyl glucosides. However, the trend of CMC upon chain length mismatched with typical surfactant behavior (Sani et al., 2012). Triazole in the ATG structure was furthered studied by Han et al., (2017). They found that triazole has enabled easiness for coupling of sugar headgroup without effecting surface activity and emulsifying properties of the ATG (Han et al., 2017).

Other than that, triazole had also induced inhibitory performance of xanthine oxidase for production of uric acid (Zhang et al., 2017a) and carbon steel corrosion (Resende et al., 2019). Besides, triazole containing alkyl *β*-D-xylopyranoside surfactant has induced stable monolayer at the air-water interface while exhibited low cytotoxicity in mammalian cells (Oldham et al., 2013). Thus, these examples made triazole as an excellent linker in synthesis and various applications.

In another aspect, triazole was applied in optical properties that give blue fluorescence usually when excited at the UV region. The intensity of blue fluorescence triazole significantly increases for N-2-aryl isomer compared to N-1-aryl isomer (Yan et al., 2011). Different isomers of hydroxyphenyl substituted 1,2,3-triazole molecules display emission color shifted when the hydroxyl group is deprotonated in basic condition (Meisner et al., 2018). These examples show the potential of triazole moieties in optical property particularly for fluorescence behavior.

Another example was the starburst triphenylamine molecule connected by triazole produces deep blue fluorescence in chloroform (Zhang et al., 2009). The emission wavelength of the molecule is red-shifted in solid form when excited at 350 nm. Triazole

links between triphenylamine with different electron donating groups and allows the intramolecular charge transfer (Kautny et al., 2017). The degree of charge transfer in the molecules does allow the solvatochromic behavior but 1,5-substituted triazole exhibits greater red-shifted emission.

Triazole has been reported in influencing the overall structure of the supramolecular system. A transition of disordered oil droplets into ordered micelle was promoted by the production of triazole containing-surfactant (TS) and prompt to gelation formation through complex formation with palladium (II) (Yuasa et al., 2017). Besides that, triazole has been widely used in oligomer study about anion binding. Juwarker et al., (2008) have demonstrated proton at carbon five of the triazole unit able to interact strongly with chloride with the increasing generation of triazole-containing oligomer (Juwarker et al., 2008). C---H groups are typically the weaker donor of hydrogen bonding than hydrogens bound to heteroatoms. CH---N or CH---O may play a significant effect in a molecular assembly such as reported in (Leigh et al., 2013). They reported that the introduction of triazole had replaced NH---N hydrogen bond of the supramolecular complexes to CH---N interactions.

2.4 Glycolipids as co-surfactant

Glycolipids are one of the examples under nonionic surfactant. Glycolipids are associated with the cell membrane and essential in providing energy and serve as markers for cellular recognition. They can be categorized into natural or synthetic glycolipids. Natural glycolipids are consisting of glycosphingolipids and glycoglycerolipids while sucrose ester, sorbitan ester and glycosides are characterized as synthetic glycolipids.

Glycosides are formed when one or more monosaccharide groups are bound by a glycosidic linkage to a hydrophobic group. Two known examples of glycosides are alkyl glucoside and alkyl maltoside, as shown in **Figure 2.7**. They were synthesized through

condensation of long-chain alcohol and glucose. Among the two examples of glycolipids, it was shown that alkyl glucoside shows greater surface adsorption efficiency than alkyl maltoside. Rosen & Sulthana (2001) have reported that decyl-β-glucoside (C10G) has a stronger interaction than the corresponding maltoside, decyl-β-maltoside (C10M) with surface tension value of 28.1 mN m^{-1} and 36.6 mN m^{-1}, respectively (Rosen & Sulthana, 2001). They also had correlated the large size of hydrophilic headgroups of C10M could not accommodate at planar air/water interface based on a small value of surface excess concentration, Γ_{max}.

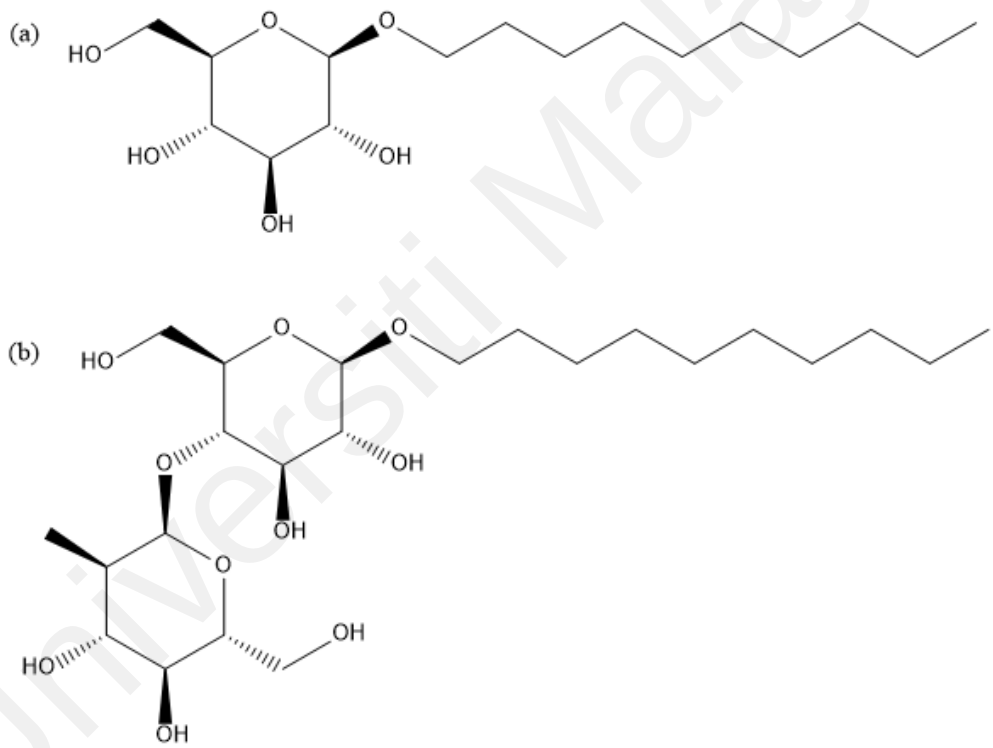

Figure 2.7: Examples of molecular structure of (a) alkyl glucoside and (b) alkyl maltoside.

Optically active fluorescent probe, (4Z,15Z)-bilirubin-IX (BR) has been used to determine alkyl glucoside, C_nG and alkyl maltoside, C_nM micelles. C_nG micelle was determined to have more fluid interiors and less polar surfaces compared to C_nM micelle due to large maltopyranoside residue. Because of the large headgroup, C_nM micelles are

more hydrated and more water molecules are located at the micellar surface. Therefore, water molecules have bound with maltopyranosides headgroup and restricted mobility and reduce rates of solubility of C_nM (Kano & Ishimura, 1995). Between alkyl glucoside and alkyl maltoside, it has been shown that alkyl glucoside is a more useful type of glycolipids that we can focus on. A few literature surveys have been reviewed to understand this effect. Firstly, we focus on the differences in the anomeric configuration of *α* and *β*-D-glucosides.

Brown et al., (1970) have reported a comparison of solubility and micellization properties of *α*-D-glucoside and *β*-D-glucoside. They reported that the solubility of *β*-D-alkyl glucoside was seven times greater than that of *α*-D-glucosides as proven by the formation of micelle at 0.025 mole/liter and 0.01 mole/liter, respectively (Brown et al., 1970). Formation of *α*-octyl glucoside micelle was confirmed by Schmidt and co-researchers could not be determined by isothermal titration calorimetry (ITC) method due to water solubility problem (Schmidt-Lassen & Lindhorst, 2014). Besides that, both anomeric are found to exhibit different solid-state properties, in which crystallizing *α*-anomers are easier than *β*-anomers (Gaudin et al., 2017; Van Koningsveld et al., 1988).

Due to water solubility problem, we only consider using alkyl-*β*-D-glucoside. There are various alkyl chain lengths of *β*-D-glucosides. The most popular and commonly used are octyl-*β*-D-glucoside (OG), decyl-*β*-D-glucoside (DG) and dodecyl-*β*-D-glucoside (DDG). CMC values of those three glucosides have been reported by surface tension study using drop weight method (Shinoda et al., 1961). The obtained CMC values were 0.025, 0.0022 and 0.00019 mol/liter for octyl, decyl and dodecyl-*β*-D-glucosides, respectively.

Difference in *β*-D-glucoside alkyl chain lengths has also been reported able to solubilize or saturate the phosphatidylcholine (PC) liposomes (López et al., 2001). Octyl-*β*-D-glucoside shows maximum activity to saturate or solubilize PC liposomes. Meanwhile, dodecyl-*β*-D-glucoside showed the highest portioning coefficient into liposomes due to its surface activity.

Therefore, from the above discussion, *β*-D-glucosides with eight, ten and twelve alkyl chain length are selected to be used as a co-surfactant mix with *p*-DMTB in aqueous solution.

2.5 NMR studies to elucidate possible forces present in the aggregates

The characterization of micellar structure by NMR was started from the 1970s. Development of NMR techniques makes it a multifunctional tool competitive over other spectroscopic method. Its resolution is superior to other methods in which different molecules in a multi-component system can be studied simultaneously (Hanzhen et al., 1999).

For example, NMR techniques was applied to determine CMC value for octanoic, decanoic, lauric and myristic acid in 95.5% sulfuric acid and laurylammonium salts of butyric, caprylic and lauric acids in CCl_4 at 35°C. They have determined through slopes of the concentration curves above CMC of the acids that showed chain length dependence with decanoic acid having anomalous behavior. Relative loss and gain of structure breaking and polarization factors involved NMR sensitive protons. Inverse micelle was interpreted by large upfield chemical shift for the butyrate salt on micelle formation through large loss of proton polarization. Small chemical shift at the CMC of butyrate salt also has been determined due to solubilization of the water in the outer region of the micelles (Yan & Palmer, 1969).

Ring current effect also had been disclosed by Du Vernet and Boekelheide (1974) where they found that low field signal of quaternary carbons of a series of bridged annulenes in the carbon magnetic resonance. The ring current effect based on carbon-13 obtained were same with protons where they occupied the same position in space relative to the aromatic π-electron cloud (Du Vernet & Boekelheide, 1974).

Quantitative analysis from surfactant solution such as NMR chemical shift have been analyzed for anionic surfactant, SDS of protons H1 and H5 and self-diffusion coefficients in D2O. Since fast exchange of surfactant molecule between aqueous and micellar pseudo-phase, the observed shift is weighted by concentration of micellized surfactants and determination of CMC was obtained from straight lines drawn through experimental points (Al-Soufi et al., 2012). Based on chemical shift obtained through NMR, CMC value obtained gave clearly a too low CMC value that was mentioned previously but did not justified in (Cui et al., 2008). Nevertheless, the data serve to demonstrating the application of the concentration model instead of critical evaluation of the values.

2.6 Aggregation Induced Emission (AIE)

Materials that display AIE are strongly emissive in aggregate or solid state but turn out to be very strong emitters when they are in the aggregate form either as powders or nanoaggregates.

Various factors that contribute to attain induced emission and emission enhancement properties in a functional fluorophore such as close molecular stacking with a short interplanar distance that restrict intramolecular rotation either through bulky substitution, hydrogen bonding or metal chelation (Mei et al., 2015), weak intermolecular face-to-face π-π interactions that can prevent the formation of excimer enhancing emission (Deng et al., 2011), hydrogen bonding assisted enhancement (Zhou et al., 2009), restricted intramolecular vibrations (RIV) or restricted intramolecular motions (RIM) and

establishment of J/H type aggregates that can block non-radiative decay pathways leading to AIE (Yang et al., 2013).

For example, AIE happen from restriction of intramolecular rotation of the peripheral phenyl groups attached to the conjugated cores in solid state or in solid matrices. Lipophilic AIE compound was poorly soluble in water but highly soluble in organic solvents. Driven by hydrophilic-hydrophobic interactions, the lipophilic AIE molecules will enter and aggregate in the hydrophobic cores of the micelles. As result, amplified FL will be recorded (Tang et al., 2009).

Next, detection of CMC of cationic and anionic surfactants was detected based on AIE property of hexaphenyl silole derivatives (Tang et al., 2009). Molecules showing AIE property usually display very weak FL in good solvents but emit efficiently when they are in a certain aggregation state (Kagatikar & Sunil, 2019). Thus, according to factors mentioned earlier, restriction of molecules during aggregation process become one of the indicators for an amphiphile as chromophore that induced emission intensity.

CHAPTER 3: METHODOLOGY

3.1 Materials

4-aminobenzoic acid (99%), sodium nitrite (99%), sodium azide (98%), 1-decanol (99%), sodium hydride (99%), propargyl bromide (80% w/w in toluene), copper (I) chloride (98%), ethanol (98%), tetrahydrofuran (98%), diethyl ether (98%) and silica gel 60 (0.063 – 0.200 mm) were purchased from Merck & Co (U.S.A). Hydrochloric acid (with fuming 37%), sodium hydroxide pellet (97%), dodecyl-*β*-D-glucopyranoside (98%), decyl-*β*-D-glucopyranoside (98%), octyl-*β*-D-glucopyranoside (98%) were all purchased from Sigma Aldrich Co (U.S.A). All chemicals were used as received without further purification except if stated otherwise. Deionized water was from *Sartorius* with ionic conductivity of 18.2 μS cm^{-1} was used for all sample preparations. CMC for dodecyl-*β*-D-glucopyranoside (DDG), decyl-*β*-D-glucopyranoside (DG) and octyl-*β*-D-glucopyranoside (OG) in water were 0.19 mM, 2.20 mM and 18-20 mM, respectively.

3.2 Methodology

The whole research works involved into the following parts:

1) The synthesis of *para*-decyloxymethyl triazolyl benzoic acid (*p*-DMTBA) in three steps reaction as shown in **Figure 3.1**. Characterization of *p*-DMTBA was analyzed using Nuclear Magnetic Resonance (NMR) spectroscopy, Fourier-Transform Infrared (FT-IR) spectroscopy and elemental analyzer.
2) The sample solutions of basic (NaOH), *p*-DMTB, DDG, DG, OG and mixture of *p*-DMTB-glycolipids solutions were prepared before physicochemical investigation of (i) *p*-DMTB and (ii) the mixture between *p*-DMTB and glycolipids with different alkyl chain lengths (DDG, DG and OG0) were investigated.

3.3 Synthesis procedure

Three types of reactions were done to synthesis *p*-DMTBA as depicted in **Figure 3.1**. First step was a substitution reaction at terminal amine group of 4-amino benzoic acid to azide, 4-azido benzoic acid. Second step was Williamson ether reaction for the formation of acetylene as a second reactant. The formation of 1,2,3-triazole linkage was via Copper(I)-catalyzed azide-alkyne cycloaddition (CuAAC) between the reactants produced. The detailed steps for each product was explained in **Figure 3.1**.

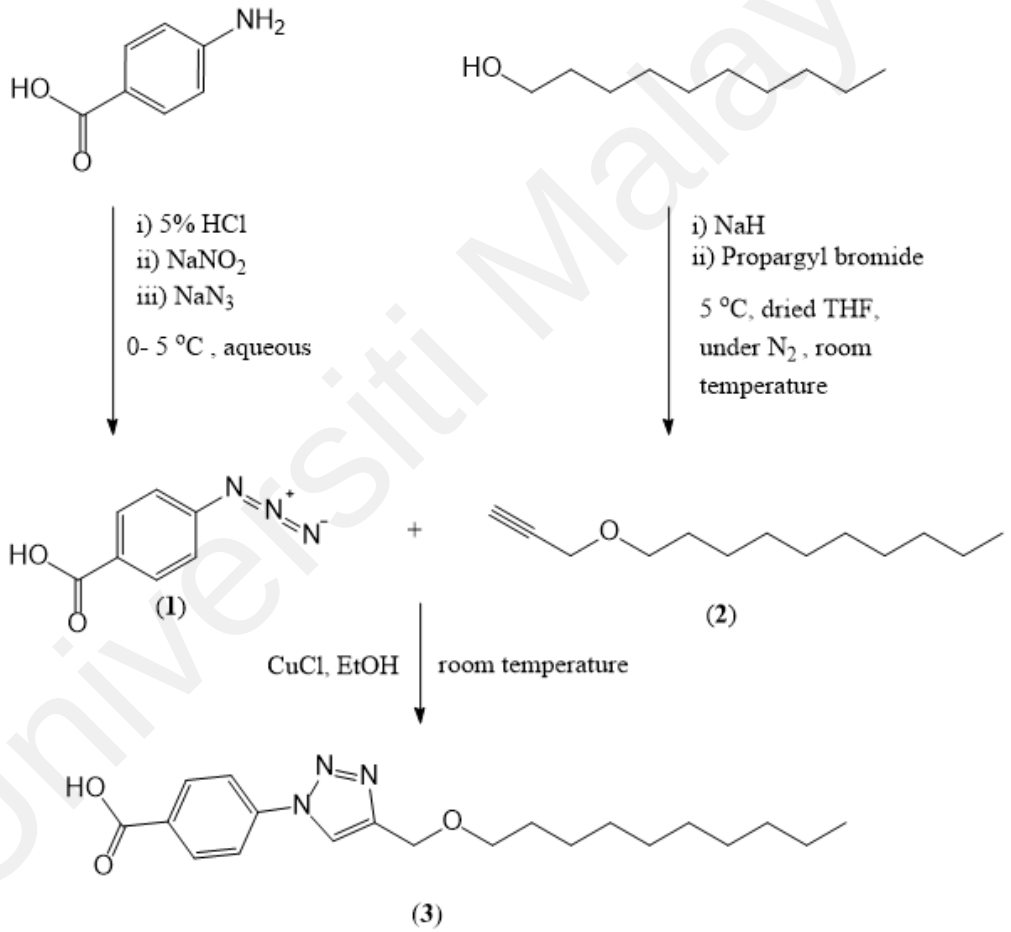

Figure 3.1: Synthesis route of *para*-decyloxymethyl triazolyl benzoic acid (*p*-DMTBA)

4-azidobenzoic acid (**1**) (Loner et al., 2012): 1.00 g (7.3 mmol) of 4-aminobenzoic acid was dissolved in 30 ml of 5% HCl (1.62 M). The mixture was continuously stirred and maintained at a temperature below 5°C. Then, 0.53 g (7.7 mmol) of $NaNO_2$ in 5 ml distilled water was slowly added to the mixture, followed by 0.54 g (8.3 mmol) of NaN_3 in 5 ml distilled water. The yellow foam product was collected and thoroughly rinsed with cold distilled water on a Buchner filtration. The crude was then further purified by solvent extraction from diethyl ether and aqueous. The organic solvent was removed by using a rotatory evaporator and 0.89 g yellowish solid products was obtained (75.4% yield). The product was then kept in the dark under dry condition (*Note: Arylazide should be kept in the dark because it is a light sensitive substance.*). R_f value = 0.6 and m.p = 175-177°C. FT-IR (cm^{-1}): 3531 (-OH carboxylic acid), 3068 - 2357 (-CH aromatic), 2101 ($-N_3$ azide), 1669 (C=O), 1600, 1506, 1423 (C=C ring stretch), 1281 (-C-OH). ^{1}H NMR (400 MHz, $CDCl_3$) δ (ppm): 8.10 - 8.08 (d, J = 8.64 Hz, CH-Ar), 7.11 - 7.09 (d, J= 8.36 Hz, CH-Ar).

1-(prop-2-yn-1-yloxy) decane (**2**) (Ranjan et al., 2017): 4.8 ml (25.2 mmol) of decanol was dissolved in 120 ml dried THF and cooled down with ice-water bath. 1.20 g (30.0 mmol) dispersion of NaH (60% wt in mineral oil) was slowly added into the solution. The mixture was stirred for another 30 minutes before 3.4 ml (30.0 mmol) of propargyl bromide (80.0% w/w in toluene) was slowly added to the mixture. The temperature was slowly elevated to room temperature and left overnight until it turned to a cloudy mixture. The crude product was dissolved in diethyl ether and extracted with distilled water. The organic solvent was removed under vacuum and conduct to further purification by column chromatography using a mixture of hexane and ethyl acetate in 4 to 1 ratio to obtain 2.80 g yellowish liquid (56.2% yield). R_f value = 0.6 and b.p = 248-250°C. FT-IR (cm^{-1}): 3311 (-C≡C-), 2923, 2854 ($-CH_2$), 1102 (C-O-C ether). ^{1}H NMR (400MHz, $CDCl_3$) δ (ppm): 4.06 - 4.05 (d, J = 2.36 Hz, CH_2O), 3.45 - 3.42 (t, J = 6.64 Hz, OCH_2), 2.34 - 2.33 (t, J = 2.36 Hz, HC≡C), 1.55 - 1.19 (m, bulk CH_2), 0.82 - 0.79 (t, J = 6.64 Hz, CH_3).

4-[4-((decyloxy)methyl)-1H-1,2,3-triazol-1-yl) benzoic acid (**3**) (Rostovtsev et al., 2002): 1.00 g (4.4 mmol) of 1-(prop-2-yn-1-yloxy) decane and 1.00 g (6.1 mmol) of 4-azidobenzoic acid were dissolved in 20 ml of ethanol while stirring in the dark. 0.04 g (0.4 mmol) of CuCl was added to the mixture and stirred for overnight. The solvent was evaporated, and the crude extracted three times with DCM and 5% HCl. The combine organic layer was concentrated under vacuum and the product was further purified and recrystallized using mixture of ethyl acetate and hexane as an eluent in 2 to 1 ratio to give the white solid product (1.30 g, 84.0% yield). R_f value = 0.2 and m.p = 220 - 225°C. FT-IR (cm^{-1}): 3152 (-OH), 2940 - 2851 (C-H alkane), 2110 (azide), 1690 - 1681 (C=O), 1608 (C-N triazole), 1519 (C=C aromatic), 1321 - 1227 (C-OH carboxylic acid), 1100 (C-O-C ether). ^{1}H NMR (400 MHz, $CDCl_3$) δ (ppm): 8.29 - 8.27 (d, J = 8.56 Hz, CH-Ar), 8.06 (s, CH-triazole), 7.91 - 7.88 (d, J = 8.56 Hz, CH-Ar), 4.73 (s, CH_2-triazole), 3.60 – 3.57 (t, J = 6.68 Hz, OCH_2), 1.65 (-CH_2), 1.36 - 1.25 (m, 14H, bulk-CH_2), 0.89 – 0.85 (t, J = 6.48 Hz, CH_3). ^{13}C NMR (400 MHz, $CDCl_3$) δ (ppm): 167.41 (C=O), 145.97 (C-triazole), 139.67 (C-Ar), 130.99 (CH-Ar), 128.15 (CH-triazole), 119.29 (CH-Ar), 70.23 (OCH_2), 63.28 (CH_2O), 30.92, 29.03, 28.35 (bulk-CH_2), 25.11 (*β*-CH_2), 21.66 (CH_2-methyl), 13.09 (CH_3). LC-MS: calculated for $C_{20}H_{29}N_3O_3$: 359.2209, found $[M+H]^+$ for $C_{20}H_{30}N_3O_3$ is 360.2292 while found [M-H]- for $C_{20}H_{28}N_3O_3^-$ is 358.2140.

3.4 Stock solutions

3.4.1 Preparation of basic solution

A stock solution of 1.0 M sodium hydroxide, (NaOH) was prepared by dissolving about 2.00 g of NaOH pellets in deionized water in a 50 ml volumetric flask. Then, dilution from the stock solution was performed to produce 2 mM NaOH solutions.

3.4.2 Preparation of *p*-DMTB solution

A stock solution of *p*-DMTB was prepared by dissolving 0.09 g of *p*-DMTBA in 0.5 ml of 1 M NaOH in a 250 ml volumetric flask to produce 1.0 mM of *p*-DMTB solution. It was then stirred and sonicated until the entire solid been dissolved. The solution was kept in dark at room temperature.

3.4.3 Preparation of DDG solution

A stock solution of DDG was prepared by dissolving 0.03 g of DDG in 100 ml deionized water. The final concentration of the DDG solution was 1.00 mM. The solution was stirred and sonicated until completely dissolved.

3.4.4 Preparation of DG solution

A stock solution of DG was prepared by dissolving 0.03 g of DG in 100 ml deionized water. The final concentration of the DG solution was 1.00 mM. The solution was stirred and sonicated until completely dissolved.

3.4.5 Preparation of OG solution

A stock solution of OG was prepared by dissolving 0.03 g of OG in 100 ml deionized water. The final concentration of OG solution was 1.00 mM. The solution was stirred and sonicated until completely dissolved.

3.4.6 Preparation of *p*-DMTB-Glycolipids solutions

A stock solution of *p*-DMTB-glycolipids mixture was prepared by mixing 45 ml of *p*-DMTB solution and 5 ml of glycolipids solutions in a 50 ml volumetric flask. The mixed *p*-DMTB-glycolipids solutions were adjusted and maintained at pH 12. This gave *p*-DMTB to the glycolipids in a volume ratio of 9:1 with a total concentration of 2.0 mM.

3.4.7 Preparation of *p*-DMTB solution for CMC determination

A stock solution of *p*-DMTB was prepared as described in 3.4.2. Then, a set of different concentrations of the *p*-DMTB solution was diluted in deionized water in a 10 ml volumetric flask.

3.4.8 Preparation of *p*-DMTB stock solution for phase transition determination

A stock solution of *p*-DMTB was prepared as described in 3.4.2. A fixed volume of 5 ml of 1.00 mM *p*-DMTB solution was mixed with a specific known volume of 1 mM HCl to give a series of a fixed concentration of *p*-DMTB solution with different HCl concentrations in 10 ml volumetric flask. This gave a series of 0.5 mM *p*-DMTB solution.

3.4.9 Preparation of stock solution of *p*-DMTB-Glycolipids mixture for CMC determination

A series of *p*-DMTB-glycolipids mixtures of different concentrations were prepared by subsequent dilution of the stock mixture solution in 3.4.6.

3.5 Instrumentations

3.5.1 Nuclear Magnetic Resonance (NMR) Spectroscopy

NMR spectroscopy was used to confirm the structure and purity of *p*-DMTBA. A stock solution consisted of 16 mM *p*-DMTBA and 48 mM NaOH was dissolved with D_2O in 20 ml volumetric flask. The molar ratio of *p*-DMTB to NaOH was 1 to 3. The stock solution was sonicated until the entire solid dissolved before dilution was performed. Hydrogen bonding between triazoles and its neighboring molecules was determined from frequency changes at proton triazole in various *p*-DMTB concentrations (0.05 mM, 0.08 mM, 0.09 mM, 0.10 mM, 0.15 mM and 0.20 mM). In addition, π-π interaction was also being determined from protons on phenyl. Deuterated chloroform, $CDCl_3$ and deuterium oxide, D_2O was used as a solvent in *p*-DMTBA structural confirmation and non-covalent interactions (hydrogen bonding and π-π interaction), respectively. The analysis was

conducted by using 400 MHz Bruker AVANCE III with the help of Top Spin 3.5.7 software. The number of scanning was set at 128. **Figure 3.2** shows a schematic diagram of NMR spectroscopy.

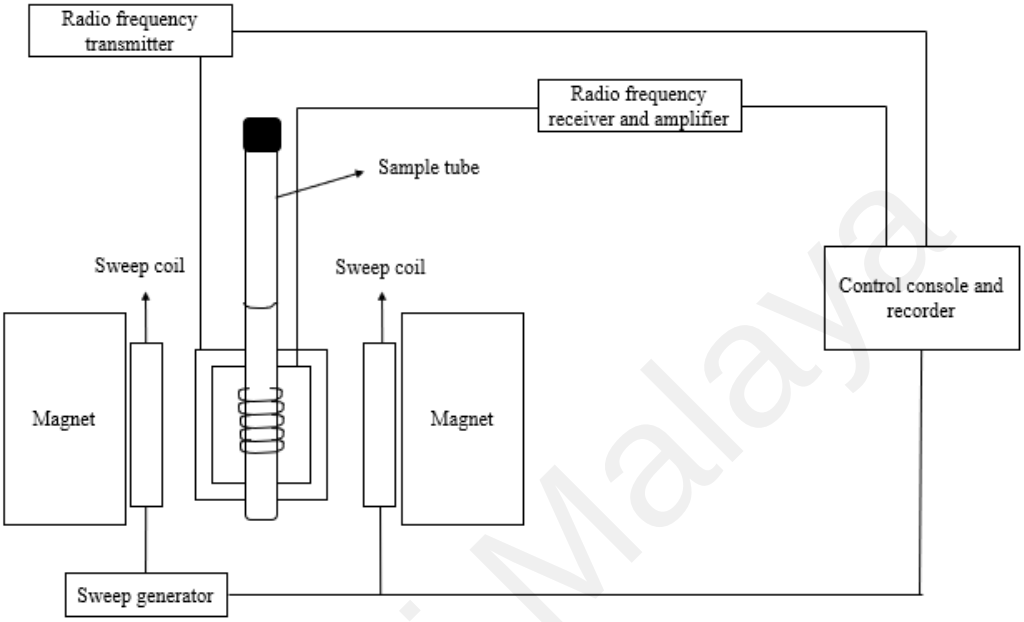

Figure 3.2: A simplified schematic diagram of NMR spectroscopy.

3.5.2 Surface tensiometer

Surface tension is a crucial analysis to determine CMC of a sample solution. By definition, surface tension is a tensile force acting on the surface of a liquid in contact with air (gas or between two immiscible liquids).

$$\gamma = \frac{F}{l} \tag{3.1}$$

γ is surface tension (in N/m), can also be represented by σ or T. F is the tensile force meanwhile l is the length represented by **Equation 3.1**. There are two types of forces that exist which are cohesion and adhesion. Cohesion force is the attractive force between water molecules, whereas adhesion force is the attractive force between water molecules

and air. In a container, water molecules in the bulk experience equally cohesive forces in all directions, while water molecules at the surface only exerted inward cohesive forces that create unbalanced intermolecular forces. The surface tension of the aqueous solution may increase or decrease due to the addition of other components. Typical additional components that can change the surface tension profile can be divided into charged particles, electrolytes, organics and surfactants.

In this study, aggregation of the synthesized surfactant and mixed surfactants with glycolipid showed a reduction in surface tension. A KSV-Sigma 702 tensiometer balance was used to determine the surface tension of *p*-DMTB and *p*-DMTB-glycolipids mixtures. The platinum ring method was used, and it requires calibration with deionized water prior to measurement. The acceptable requirement value for the surface tension of deionized water is between 71 – 72 mN m^{-1} at 25°C. The measurement was conducted at least three times. **Figure 3.3** shows a schematic diagram using the platinum ring method for surface tension analysis.

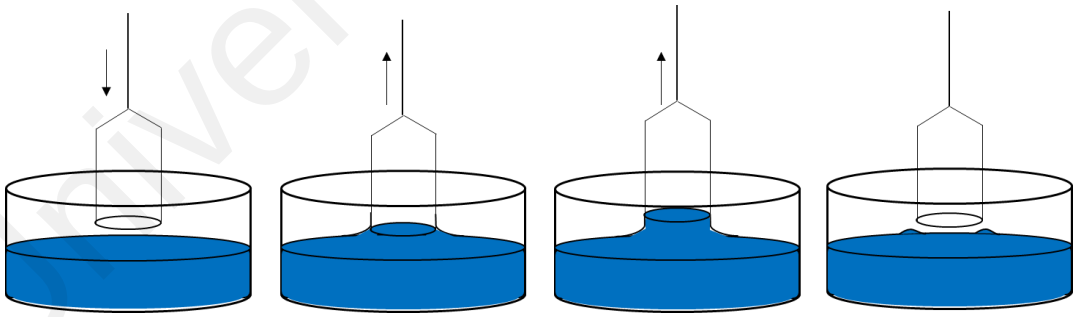

Figure 3.3: A schematic diagram of the platinum ring method used for surface tension analysis.

3.5.3 Conductivity meter

Conductivity study is a measurement of the ability of an aqueous solution to conduct electricity. Electrolytes are substances containing ions which responsible for conducting electric current. The type of electrolytes is divided into strong and weak. Strong

electrolytes are substances that can be fully ionized in solution such as strong acids like hydrochloric acid, HCl and strong base like sodium hydroxide, NaOH. As a result, the concentration of ions in solution is proportional to the concentration of added electrolyte. Weak electrolytes are a substance that is partially ionized in solution. For example, acetic acid is partially dissociating into acetate ions and hydrogen ions, therefore acetic acid contains both ions and molecules. Many factors influence the conductivity study such as the concentration and mobility of ions, presence of matter such as organic alcohol, salt, temperature, etc. Conductivity analysis can be explained by using Kohlrausch's law as defined in **Equation 3.2**, where κ is conductivity (S/cm), c is concentration and Λ is molar conductivity.

$$\Lambda = \frac{\kappa}{c} \tag{3.2}$$

In this study, conductivity analysis was performed to determine the presence of monomer and micelle by analyzing the number of ions present in the *p*-DMTB by using Eutech Cond 6+ Conductivity meter. Prior to measurement, the conductivity meter probe was rinsed with deionized water and calibrated with a standard conductivity buffer solution of 1413 μS cm^{-1} at room temperature. The probe was rinsed with clean deionized water for each sample measurement. The measurement was conducted at least three times.

3.5.4 Ultraviolet-Visible (UV-VIS) Spectrophotometer

Ultraviolet (UV) and visible radiation are a part of the electromagnetic spectrum, in which also include other radiation such as radio, infrared (IR) and X-ray. Electromagnetic radiation can be considered as a combination of alternating electric and magnetic fields that travel through space with a wave motion. There are two equations (**Equation 3.3** and **Equation 3.4**) that related to the electromagnetic radiation:

$$E = hv \quad (3.3)$$

where E is energy (in joule), h is Planck constant (6.62 x 10^{-34} Js) and v is the frequency (in seconds) and

$$v = c/\lambda \quad (3.4)$$

where v is frequency (in seconds), c is the speed of light (3 x 10^{8} ms^{-1}), and λ is wavelength (in meters).

In UV-VIS, wavelength is expressed in nanometres (1nm = 10^{-9} m). UV and visible regions fall between 190 – 380 nm and 380 – 750 nm, respectively. From the equation, the shorter the wavelength, the higher is the energy, therefore in UV-VIS spectroscopy, a shorter wavelength of UV light has the highest energy. By using UV-VIS spectroscopy, some processes occur when radiation is applied to a matter such as reflection, scattering, absorbance, fluorescence/phosphorescence (absorption and reemission) and photochemical reaction (absorbance and bond breaking). However, in UV-VIS spectra, we usually want absorption to occur. This can be explained by the concept of Beer-Lambert equation as stated in **Equation 3.5**:

$$I = I_o e^{-\tau l} \quad (3.5)$$

where I is the intensity of light, I_o is the incident light, τ is the turbidity and l is the path length of light through a solution. The above equation also applied to turbidity concept where turbidity is caused by scattering of light in all direction and reduction in transmitted.

In our study, UV-VIS spectroscopy was used to determine the CMC and phase transition equilibrium. It was performed with the help of a Varian Cary 60 UV-VIS

Spectrophotometer and data were collected at 500 nm to show the turbidity property. The plotting of spectrum was performed with the help of Cary WinUV software. The measurement was conducted at least three times. **Figure 3.4** below is a schematic diagram of UV-VIS analysis for CMC and phase transition measurements.

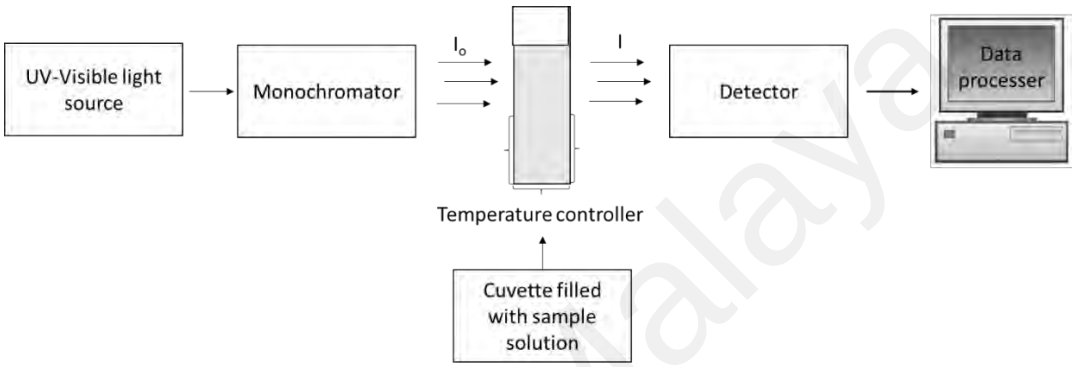

Figure 3.4: A schematic diagram of turbidity measurement for determination of CMC and phase transition formation.

3.5.5 Fluorescence Spectrophotometer

Fluorescence spectroscopy is based on a light emitting process that is triggered by the absorption of the excited radiation. It is measured by exciting the sample at absorption wavelength (also known as excitation wavelength) and measuring the emission at a longer wavelength (fluorescence wavelength). Fluorophore or chromophore is a part or moiety of the molecule that responsible for absorbing light and re-emission of light upon deactivation. Chromophore is usually contained several aromatics, planar or cyclic groups with several pi bonds. It is usually used as a tracer in fluids, a dye for staining or as a probe or indicator. There are several factors that influence emission intensity in fluorescent studies such as the solvent, pH, and concentration of a solution. A triazole and benzene groups act as our chromophores due to the presence of π bonds and it is predicted that the triazolyl benzoic acid will release fluorescent emission signals in the visible

range. Fluorescence behavior of the surfactant in different phases of self-assembly structures will also be explored by using this method.

In our study, investigation on CMC of *p*-DMTB, CMC of mixture of *p*-DMTB-glycolipids solution and phase transition behavior of *p*-DMTB was performed using the Cary Eclipse Fluorescence Spectrophotometer. The solutions were kept in a water bath at 25℃ for 30 minutes before measurement. The data of fluorescence emission was recorded at an emission intensity wavelength of 420 nm for an excitation wavelength of 257 nm. The measurement was detected by altering the settings of the instrument at the 800 V PMT voltage and smoothing factor of 5 with slit width of 10 nm. The PMT was changed to 600 V for phase transition because the emission exceeded the measurable value. At least three measurement were carried out for each concentration. A simplified diagram of the fluorescence spectrophotometer is shown in **Figure 3.5**.

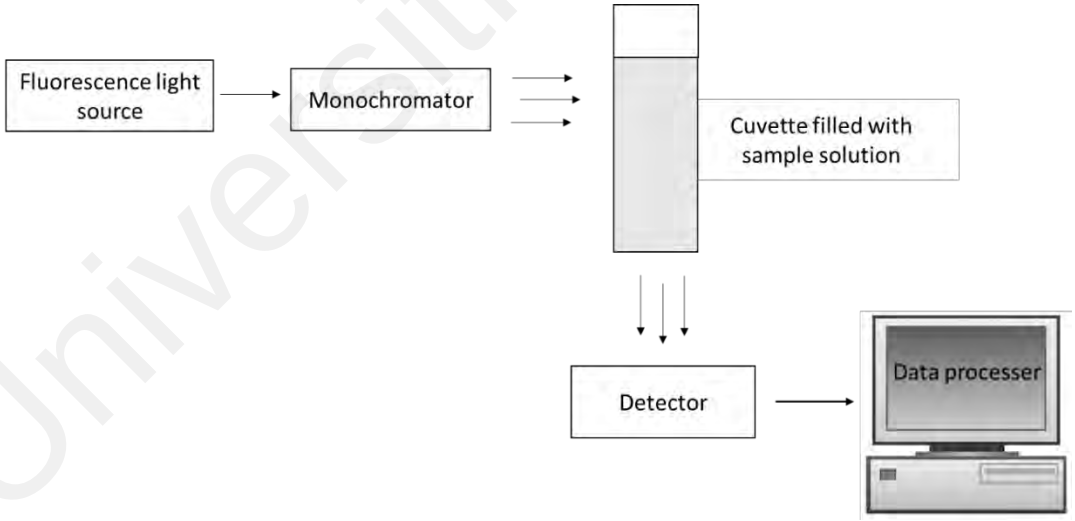

Figure 3.5: A simplified diagram of the fluorescence study for determination of CMC and phase transition.

3.5.6 Optical Polarizing Microscope (OPM)

Optical polarizing microscopy is the most suitable equipment for analyzing the presence of aggregate structures such as vesicles. It has the advantage of illustrating the

particle size and shape of particles. It differs from the regular microscope because it uses polarized light that cannot be seen by the naked eyes. Polarized light has a wave that vibrating in one direction using a polarizer. The polarizer is the place between the light source and the specimen, while the analyzer (also known as an adjustable polarizer) is place between the lens and the objectives. Sample preparation for the technique is straightforward. A drop of sample solution was placed on a clean and dried glass slide. A cover slip was then gently placed on the drip without trapping the air bubbles. The glass slide was placed on the stage of the microscope with the drop just underneath the objective lens. 10X, 20X and 50X magnification objective lenses were used to determine the morphology of the sample solution. The aggregation of synthesized surfactants was observed and determined under optical microscopic images. Images were captured from a Leica DMRXP polarizing light microscope and analyzed with Leica QWin software. **Figure 3.6** depicted is a schematic diagram of the sample observation under optical polarizing microscope.

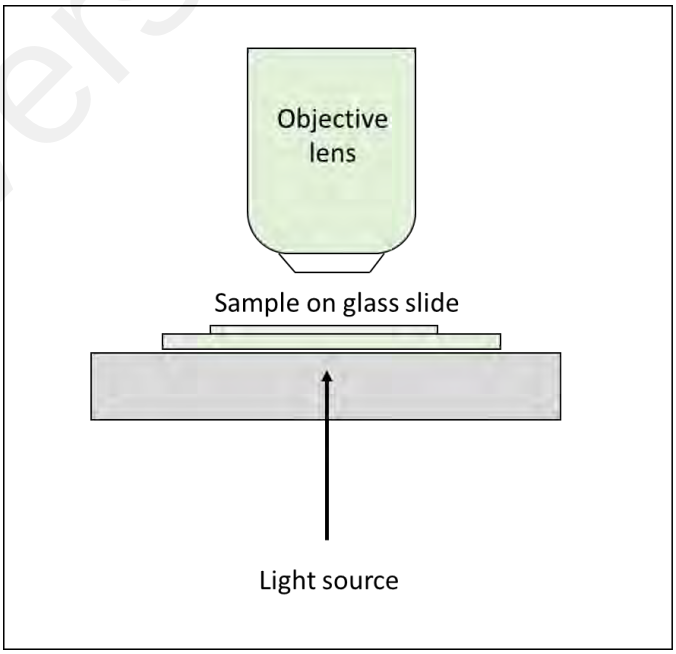

Figure 3.6: A schematic diagram for the observation of the sample under an optical polarizing microscope.

3.5.7 pH Meter

pH is a unit of measurement to describe the acidity and alkalinity of a solution. It is measured on a scale of 0 to 14. By the **Equation 3.6** below, pH is a negative logarithm of hydrogen ion concentration.

$$\mathrm{pH} = -\log\ [\mathrm{H}^+] \tag{3.6}$$

Eutech pH 700 pH meter was used to study the phase transition and CMC of the synthesized surfactant and mixed surfactants. A series of dilution was performed to observe changes in pH values. The pH meter was calibrated with pH 4.0, pH 7.0 and pH 10.0 buffer solutions at room temperature.

3.5.8 Fourier-Transform Infra-Red (FT-IR) Spectroscopy

Different functional groups of molecular structure are determined using FT-IR spectroscopy. Infrared radiation is passes through the sample material and trigger the vibration of specific molecular bonds. Two types of vibration motion are stretching and bending modes. The modes of the sample material were measured in infrared region wavelength in a range of 4000 to 400 cm^{-1} interpreted by a FT-IR spectrometer.

In our study, Perkin Elmer Spectrum 400 FT-IR spectrometer with attenuated total reflectance (ATR) accessory was used. The ATR method provides a powerful sampling technique that nearly eliminates sample preparation with solid and liquid. Furthermore, maximum durability, fast and easy cleanup was offered by the ATR.

The plate was cleaned with alcohol before measurement. A small amount of sample e.g. 1 mg was placed on the cleansed plate such that the diamond is covered by the sample. FT-IR spectrum was measured in the range of 400 to 4000 cm^{-1} with a scanning number

of 4 and was analyzed using Spectrum software. **Figure 3.7** is a simplified diagram of the FT-IR measurement.

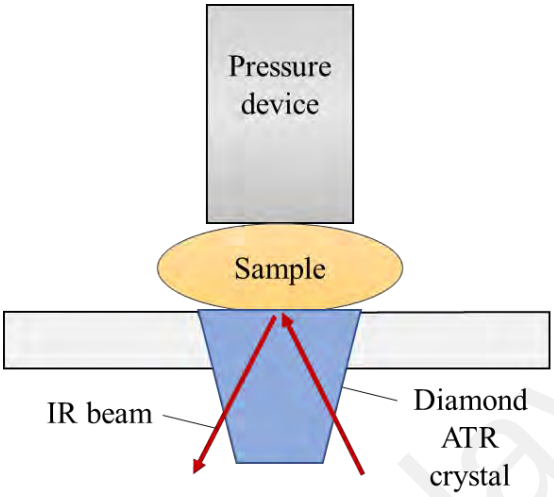

Figure 3.7: A simplified diagram of the FT-IR measurement with ATR method.

3.5.9 Liquid Chromatography-Mass Spectrometry (LC-MS)

Liquid chromatography is conducted to separate sample components to their relatively purified forms before being introduced into the mass spectrometer. Charge ion from the sample is generated by applying electrospray ionization (ESI) or atmospheric pressure chemical ionization (APCI). The ions then pass into the mass analyzer. The identity of the target ion is determined by comparing its mass to charge (*m/z*) ratio against a spectral database.

In our study, High Resolution Electrospray Ionization Mass Spectrometer (HRESIMS) technique from the Agilent 6550 iFunnel Q-TOF mass spectrometer equipped with the Agilent 1200 series Rapid Resolution LC system was applied. 20 µL of the sample was injected with a flowrate of 0.2 mL/min in ambient temperature with Zorbax SB-18 column (2.1 x 50mm, 1.8 µm). The mobile phase used was 100% acetonitrile. The mass spectrum data was analyzed using Mass Hunter Workstation software (B.06.01).

CHAPTER 4: RESULTS AND DISCUSSION

4.1 Formation of *Para*- decyloxymethyl triazolyl benzoic acid (*p*-DMTBA)

4.1.1 Structural analysis of *p*-DMTBA

Copper(I)-catalyzed azide-alkyne cycloaddition is one of the 'Click' reaction that can provide high yield of product and regiospecifically for the formation of 1,4-disubstituted 1,2,3- triazole. The reaction proceeded in a mild condition by connecting the terminal alkyne and organic azides to produce triazolyl benzoic acid amphiphile, namely 4-(4-decyloxymethyl-1H-1,2,3-triazo-1-yl benzoic acid.

Organic azide was preformed by azidation reaction, which converted the amine group of 4-aminobenzoic acid to the azide group of 4-azidobenzoic acid (**1**). A yellowish solid with a percentage yield of 75.4% was obtained. **Figure 4.1** represents the doublet signals at 8.10 ppm and 7.11 ppm of ^{1}H-NMR spectrum, which indicates protons at the benzene ring for 4-azidobenzoic acid. FT-IR spectra show the absence of a broad signal at 3361-3460 cm^{-1} and a new sharp peak at 2101 cm^{-1} indicating the transformation of amine to azide group as depicted in **Figure 4.2**.

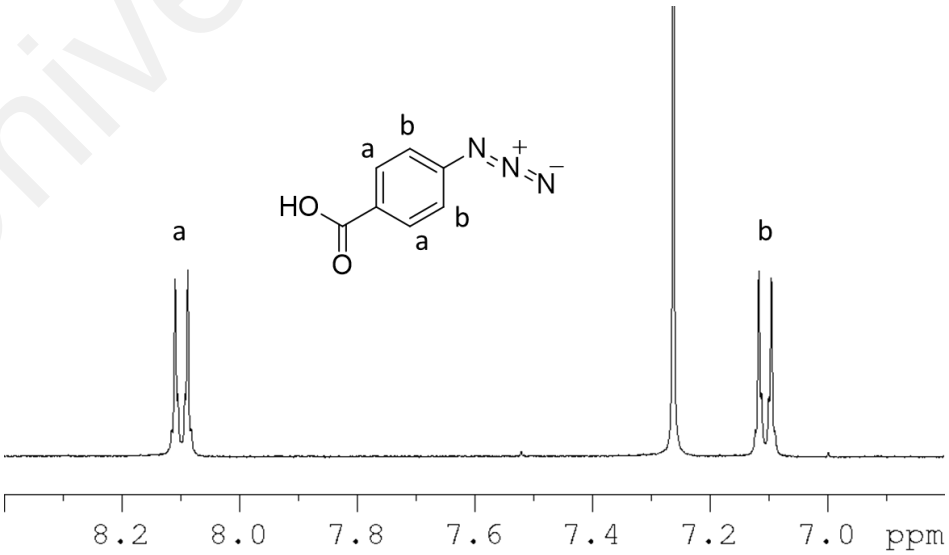

Figure 4.1: ^{1}H-NMR spectrum of 4-azidobenzoic acid (1).

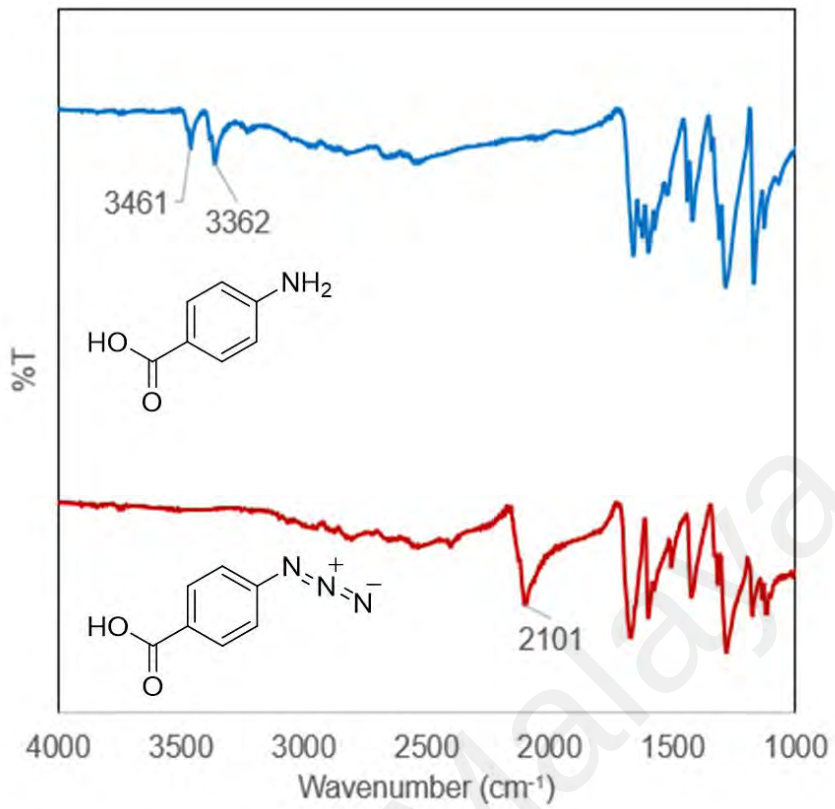

Figure 4.2: FT-IR spectra of 4-aminobenzoic acid (blue) and 4-azidobenzoic acid (red).

Williamson ether reaction was performed to produce yellowish liquid acetylene (**2**) by substitution between propargyl bromide and 1-decanol. **Figure 4.3** shows the doublet signals at 4.06 ppm and triplet signal at 3.45 ppm of ^{1}H-NMR spectrum indicating the ether linkage formation. FT-IR spectrum of liquid acetylene (**2**) shows that the terminal alkyne of C≡C is at 3311 cm^{-1}, alkyl chain of CH_2 band is between 2923 until 2854 cm^{-1} and the strong absorption band for the ether linkage of C-O-C is at 1102 cm^{-1}. The full ^{1}H-NMR and FT-IR spectra are supplied in **Appendix A** and **Appendix B**.

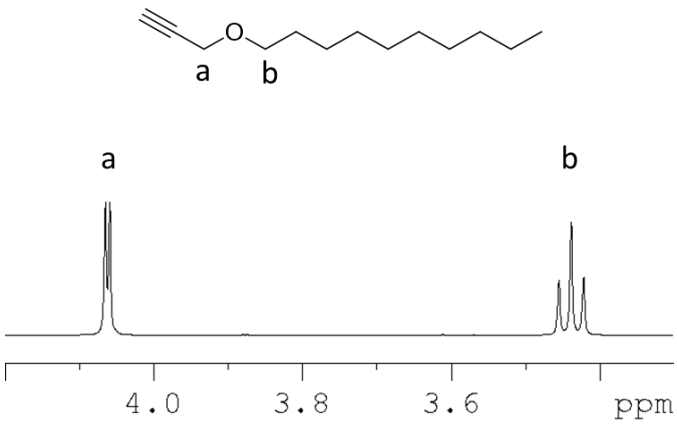

Figure 4.3: ^{1}H-NMR spectrum of acetylene (2).

The white solid product was obtained from the cycloaddition reaction with a percentage yield of 84.0% by using 10% of copper(I) catalyst. From ^{1}H-NMR spectrum in **Figure 4.4**, the key signals of the synthesized *p*-DMTBA were at 8.06 ppm, 4.73 ppm and 3.60-3.57 ppm indicating that a singlet proton signal of triazole, α-protons of triazole and β-protons of the ether linkage, respectively. **Figure 4.5** shows the ^{13}C-NMR spectrum of *p*-DMTBA. At 63.28 ppm indicated for ether linkage near the aliphatic group -OCH_2. The presence of oxygen and triazole atom causes a deshielding effect to 70.23 ppm. Two carbon atoms of triazole were detected at the lower field at 128.15 ppm and 145.97 ppm.

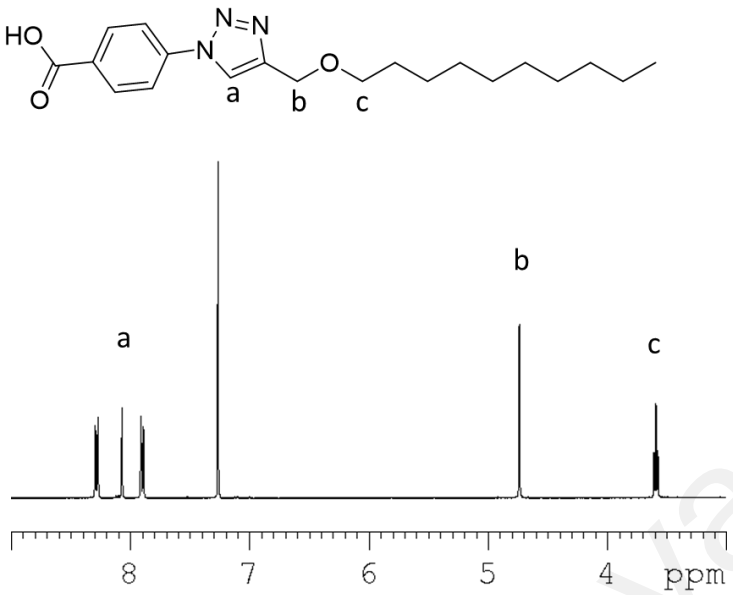

Figure 4.4: ^{1}H-NMR of key signals for *p*-DMTBA.

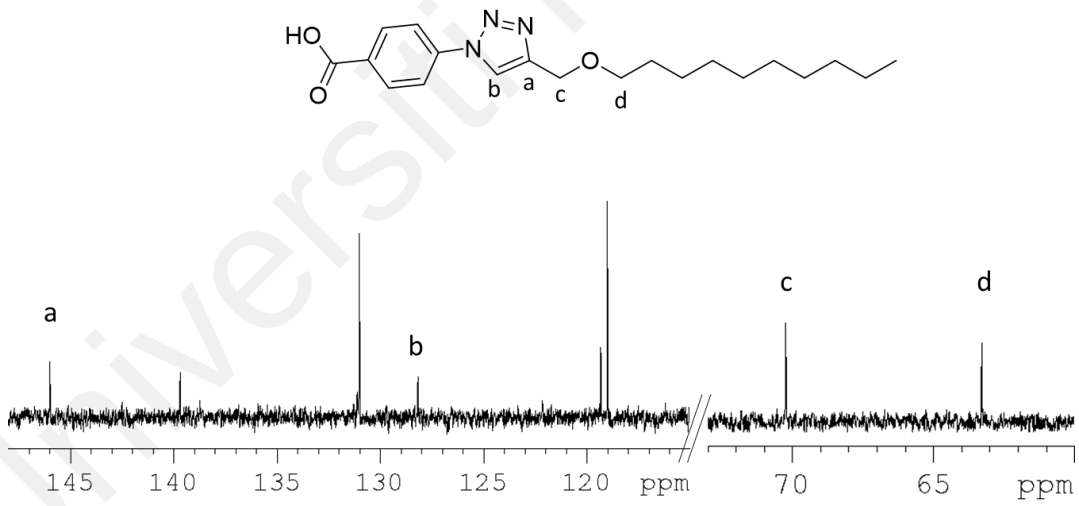

Figure 4.5: ^{13}C-NMR of key signals for *p*-DMTBA.

FT-IR spectrum indicating the main absorption bands at 3152 cm^{-1} for OH stretch, 2940-2851 cm^{-1} for C-H stretching of methylene group, 2110 cm^{-1} for N=N=N stretching, 1690-1681 cm^{-1} for C=O stretch, 1608 cm^{-1} for C-N stretching and at 1100 cm^{-1} for C-O-C ether. All signals are represented in the FT-IR spectrum in **Appendix B**. The

synthesized product has been further analyzed using the elemental analyzer and LCMS for confirmation.

LC-MS study is one of the studies to determine the purity of the synthesized compound. From the result, it was shown that calculated molecular weight for the product [M], $C_{20}H_{29}N_3O_3$ is 359.2209 m/z. We found that the molecular weight for $[M+H]^+$ of $C_{20}H_{30}N_3O_3$ is 360.2286 m/z at 30.1 sec, whereas the molecular weight for $[M-H]^-$ of $C_{20}H_{28}N_3O_3^-$ is 358.2136 m/z at 31.0 sec. For elemental studies, the percentage elements obtained were (66.24 $\pm$ 0.01)% for carbon atom with 0.58% of difference from the theoretical value, (8.23% $\pm$ 0.01)% for hydrogen with a slight difference of 0.10% and (11.48 $\pm$ 0.01)% for nitrogen with a deviation of 0.21%. The total elements present for carbon, hydrogen, nitrogen was 20, 29, and 3 respectively.

4.2 Critical Micellar Concentration (CMC) of *p*-DMTB

Different methods to determine *p*-DMTB micellization have been carried out in this study including absorbance spectroscopy, ion conductivity, fluorescence intensity, and surface tension. ^{1}H-NMR study also has been conducted to confirm the interaction that occur between *p*-DMTB molecules.

4.2.1 Aggregation of *p*-DMTB observed from absorbance intensity

The absorbance of the *p*-DMTB solution at different concentrations is presented in **Figure 4.6**. The absorbance intensity was taken at A_{500} nm to represent possible absorption, scattering, and reflection of the sample solution. Below 0.13 mM, absorbance intensity was detected at (0.002 $\pm$ 0.0001) a.u. indicating the light source almost completely passes the sample solution. As the *p*-DMTB concentration exceeded 0.13 mM, the absorbance intensity started to increase up to (0.012 $\pm$ 0.01 a.u). drastically. The increment of the absorbance value was due to light absorption and scattering by the samples. The trend proposes the transition of *p*-DMTB molecules from monomers into

micellar phases. The correlation between the changes in absorbance intensity with the micellization process is supported by Namani & Walde (2005) where they found that the absorbance intensity value was at 0.05 a.u. in pH 11.5 (Namani & Walde, 2005). The absorbance intensity was much lower than the reported elsewhere (Gajowy et al., 2014; Rather et al., 2015; Ysambertt et al., 1998) indicated that the *p*-DMTB was completely soluble and eliminates possibility of as macrophase.

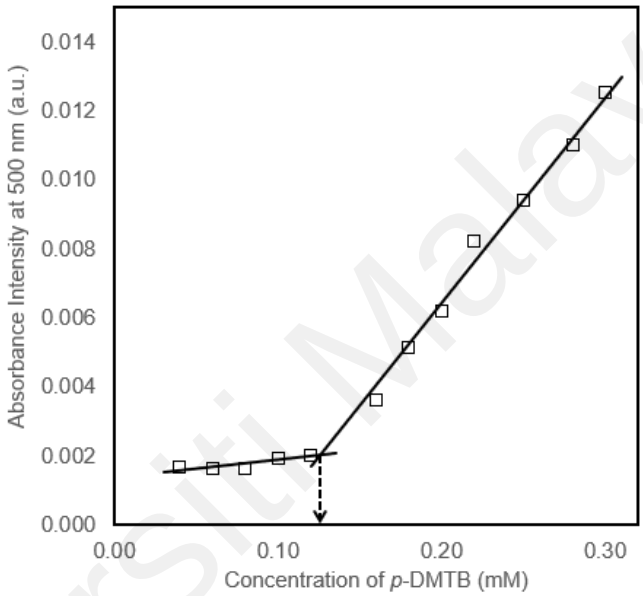

Figure 4.6: Absorbance intensity at 500 nm as a function of *p*-DMTB concentration.

4.2.2 Evaluating ionic conductivity of *p*-DMTB headgroup with aggregation process

Conductivity study was performed to determine ionic property and conversion that could occur at the amphiphile headgroup. **Figure 4.7** below demonstrated molar conductivity of *p*-DMTB solution with increasing concentration. The plot follows Kohlrausch's law where molar conductivity value decreased with the increase of *p*-DMTB concentration. However, the plot did not linearly decrease as an intersection occurred at 0.10 mM, indicating CMC of *p*-DMTB. Before the CMC value is reached,

the fully ionized headgroup of the amphiphile was moving freely in the aqueous solution. As the amphiphile started to self-aggregate, the mobility of the free ions in the solution is restricted. This is shown by the further lower molar conductivity above the CMC value with a deviated slope.

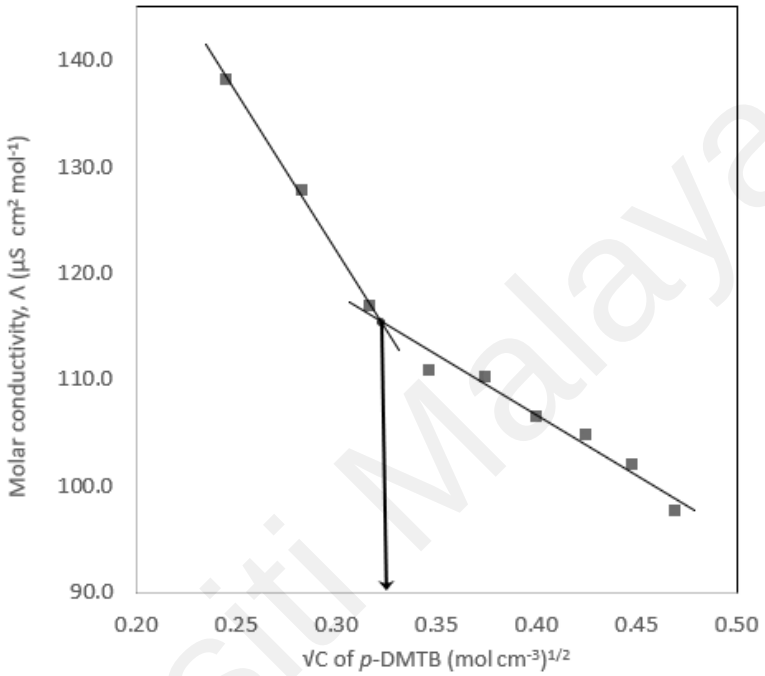

Figure 4.7: Variation of molar conductivity of *p*-DMTB at room temperature.

The CMC value obtained from the absorbance intensity and ionic conductivity are constant within a range of 0.10-0.13 mM. The value range suggested that *p*-DMTB absorb light during the pre-collision of the micellization process, while less effective electron transfers only occurred after the aggregation. In order to ensure the measured CMC value of the amphiphile, the behavior of the amphiphile was further conducted using fluorescence emission and surface tension study.

4.2.3 Effect of emission intensity of triazole with aggregation behavior of *p*-DMTB

Triazole and its derivatives are potentially fluoresced. These fluorescents have been applied in various fields (Meisner et al., 2018; Yan et al., 2011; Zhang et al., 2017b). For that reason, the fluorescence emission measurement for CMC determination is reasonably included in this study to highlight the contribution of triazole to the micellization of *p*-DMTB.

In this research, the fluorescence of triazole has been utilized to examine the aggregation of the amphiphile capturing direct interaction between the heterocyclic. The interaction is hardly detectable if the measurement is not involving the property of triazole itself. **Figure 4.8** s4.25hows the plot of the emission intensity of the triazole with increasing *p*-DMTB concentrations. In the monomer state, the number of triazole moiety is as low as the amphiphile molecules. The emission intensity obtained is constant at 90 a.u. before it immediately elevated to 150 a.u. as a result of the aggregation of *p*-DMTB. It is evident that the aggregation of the *p*-DMTB has induced increased emission intensity of the triazole, also known as aggregation-induced emission (AIE). AIE can be one of the indicators for CMC determination with the assistance of fluorescent probes (Tang et al., 2009). It can occur mainly from the restriction of internal rotation macrostructures that were promoted through extensive non-covalent interaction during the self-aggregation process (Wu et al., 2019).

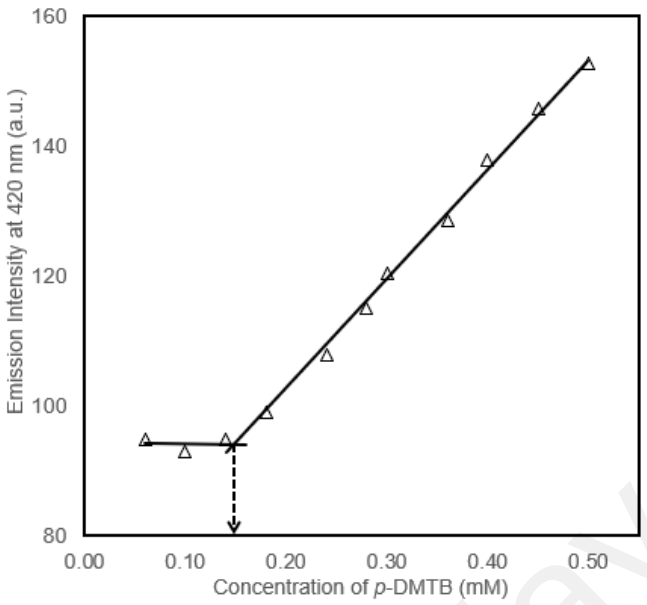

Figure 4.8: Emission intensity at 420 nm with increasing *p*-DMTB concentration at 25℃. The graph shows that triazole emission intensified from monomer to micelle formation.

From the observed results, it is plausible that the distance between the triazoles is suspected to be closer when in aggregated form. The self-aggregated molecules could have normal micellar morphology with triazole moieties closer to each other, hence allowing intermolecular interactions between the amphiphilic molecules. The molecule could exist in planar, where the phenyl and the triazole are almost in eclipse configuration. If the aromatic and the heteroaromatic groups in staggered configuration or non-planar, the triazoles could be distanced. Hence, the intermolecular interaction between the amphiphilic molecules would be unachievable.

The planar configuration of the molecule is also related to AIE behavior. In this interesting aspect, it is expected that emission could be either quenched or enhanced due to the aggregation process. Since the triazole itself fluoresce, any interaction and electron transfer could directly be observed from the emission trend. In the monomer phase, the

molecules have minimum molecular interaction, particularly on the triazole which is indicated by the constant low value of emission. Above the CMC value, the triazoles are getting closer, and the emission increased drastically due to the AIE. The most plausible interaction is through hydrogen bonding from the proton at C5 position to the second nitrogen, N2 of the adjacent molecules. The N2 has lone pairs that act as a proton acceptor. The interaction requires sufficient distance with parallel arrangement and planar molecule structures as illustrated in **Scheme 4.1**.

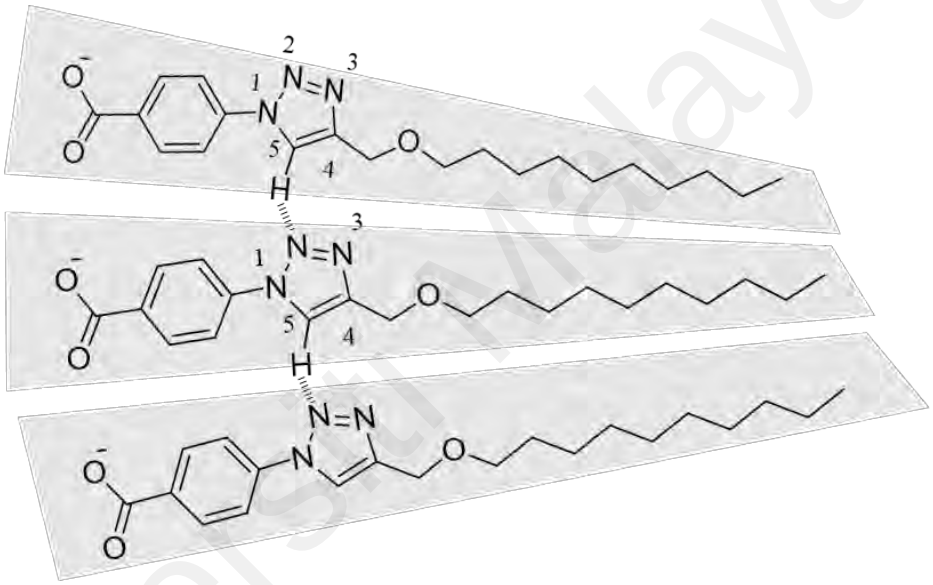

Scheme 4.1: Hydrogen bonding at C5 position of triazole to N2 of neighboring molecules may occurred provided that the molecular arrangement is in parallel and planar.

From the obtained results, it was strongly suggested that the embedded triazole group in *p*-DMTB molecule has contribution in lowering the CMC value of the amphiphile. However, the status quo of an amphiphile or surfactant is not reached if without surface tension measurement. Therefore, surface tension analysis of *p*-DMTB was carried out in aqueous solution.

4.2.4 Effect of *p*-DMTB on water surface tension

Figure 4.9 shows a plot of surface tension for the solution of *p*-DMTB with different concentrations in the log scale. If the triazole in *p*-DMTB can assist in decreasing the surface tension value, the amphiphile could behave similarly to natural fatty acid. It was observed that the surface tension value decreased with concentration but started to become constant at 0.10 mM. Water surface tension was disturbed by *p*-DMTB monomers that affect the cohesive force of water molecules. The surface tension at the CMC was relatively higher compared to the similar hydrophobic length of natural fatty acids with C14 (Chumpitaz et al., 1999).

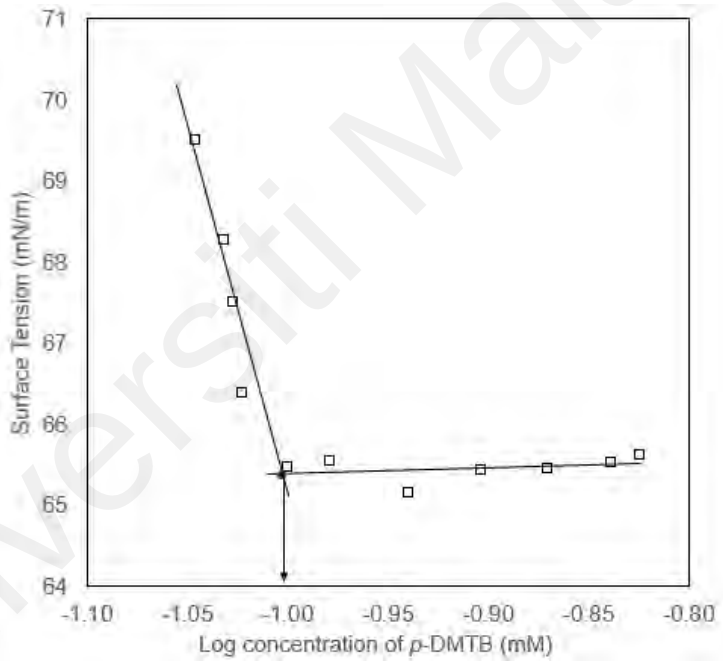

Figure 4.9: Surface tension against log concentration of *p*-DMTB at 25℃.

When *p*-DMTB monomers occupy all interfaces and surface, the *p*-DMTB monomers in the bulk start to aggregate into micelles. The aggregation of *p*-DMTB occurred by avoiding their hydrophobic tails to be in contact with water. Micelles are formed with the hydrophobic tails facing inwards while the hydrophilic headgroups pointing outwards.

The formation of micelles from the *p*-DMTB monomers is facilitated by the favorable interaction between the hydrophobic tails and repulsive interaction between the charged headgroups. The surface tension at the CMC of the *p*-DMTB amphiphile achieved the optimum value at (65.38 $\pm$ 0.01) mN m^{-1}.

The surface tension values remained constant due to saturation of the solution surface by the adsorbed molecules. Although the surface tension value at CMC is not reduced significantly, the CMC value obtained is ten-fold lower compared to alkyl benzoic acid with similar alkyl chain length (Hatzopoulos et al., 2011). In addition, a small reduction in surface tension value was supported by Matsuoka and colleagues, (Matsuoka et al., 2003). They found that higher surface tension at CMC was due to the presence of strong electrostatic repulsion between the hydrophilic segment at the monolayer and the formation of highly stable micelles in the bulk solution.

The measured surface tension at the CMC value also indicates the low surface activity of the amphiphile. The surface activity can be described by the interactions between water molecules and *p*-DMTB's headgroups. For an anionic headgroup such as carboxylate, the repulsive interaction also exists due to the same charge species. The charge balances the attractive forces gained from the hydrophobic region.

From the possible interactions, the mechanism of micellization and surface activity of *p*-DMTB could be foreseen. It has been stated elsewhere (Wang et al., 2008), the repulsive headgroup interaction can be reduced by the adsorption of the anions to the surface of the micelle. Hypothetically, if the amphiphile experience closer arrangement, the carboxylate headgroups have to encounter much higher repulsion forces. Adsorption of sodium counterions to the micellar surfaces could condense the polarizability and repulsive forces between the headgroups. Hence, it decreases the hydration of water to the aggregation surface and results in higher surface tension at CMC.

In this amphiphile molecule, there are also phenyl and triazolyl functional groups that potentially become the additional attractive forces between the molecules. *p*-DMTB also could probably engage with the strong hydrogen bonding interaction, particularly between the triazolyl groups. Studies have reported that hydrogen bonding between triazole moieties intermolecularly exists in oligomers (Hua & Flood, 2010). Therefore, ^{1}H-NMR measurement was applied to confirm the hypothesis about the potential existence of the hydrogen bond between triazolyl and phenyl groups interaction within *p*-DMTB molecules.

4.2.5 Hydrogen bonding and π–π interaction in *p*-DMTB aggregate

NMR was used in aggregation studies of aggregation by examining the chemical shift of protons in monomer and micellar states (Chachaty, 1987; Hatzopoulos et al., 2011; Wanka et al., 1994). A simple approach to NMR in this study was to interpret the chemical shift to demonstrate the possible interactions between the surfactant molecules. The interest of interactions was precisely dictated to the hydrogen of triazole and phenyl ring.

Figure 4.10 (a) represents the resonance frequency of hydrogen at the C5 position of a triazole with an increasing concentration of *p*-DMTB. In monomer form, where the concentration was below CMC value, frequency of proton nuclei at C5 position was detected above 3405 Hz. The proton nuclei tend to spin relatively higher frequency and therefore reflect their uninterrupted condition freely with less interaction from other molecules. The frequency of the proton nuclei started to decrease down to 3405 Hz and becomes constant when reaching the CMC value at 0.10 mM. The value obtained was consistent with the CMC value determined earlier from surface tension, conductivity, absorbance and fluorescence emission analyses.

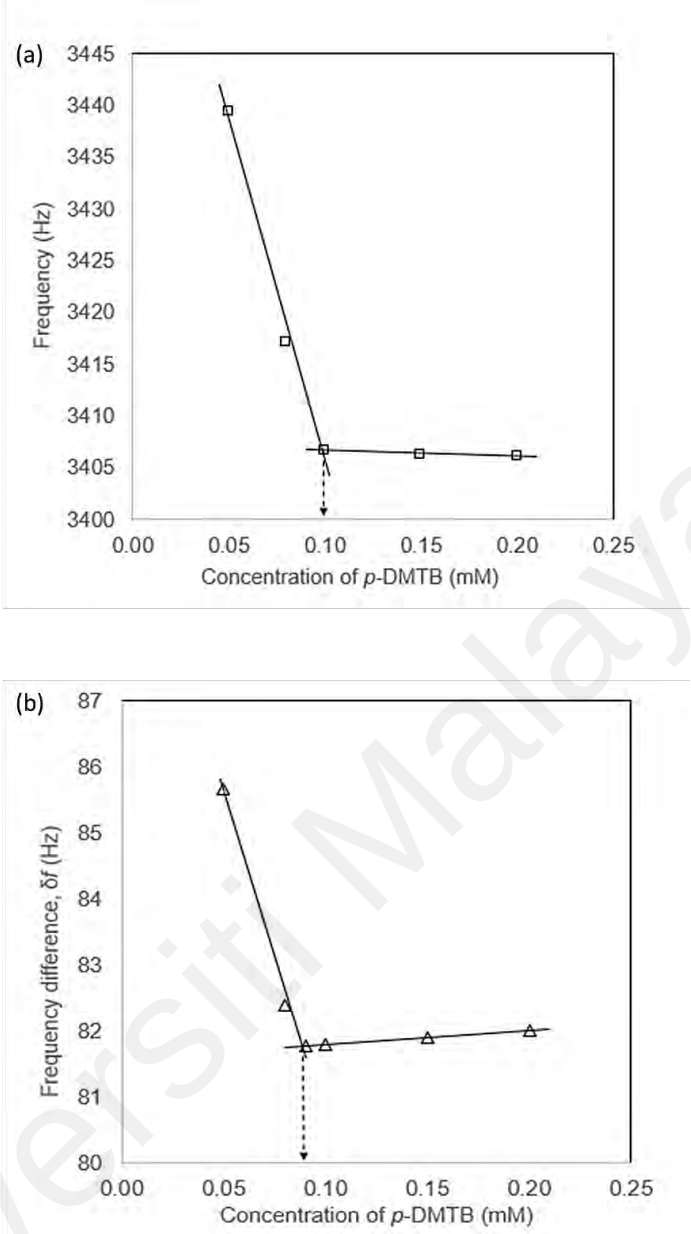

Figure 4.10: (a) Frequency changes of proton at C5 position of triazole and (b) frequency difference of protons at ortho and meta positions of phenyl group with various concentrations of *p*-DMTB at 25℃.

If the proton is not further disturbed due to self-aggregation, the frequency could be further decreased after the CMC value. The results show that the frequency of the proton nuclei was constant at above CMC value indicating the interruption of the spinning of the

proton. The interruption was due to the hydrogen bonding formed from the proton at C5 position to N2 of an adjacent amphiphile molecule as shown previously in **Scheme 4.1**.

As suggested in fluorescence analysis, the planar conformation on the triazole and phenyl is more reasonable than the non-planar conformation. This conformation may also encourage the π–π interaction between the phenyl groups simultaneously (Meyer et al., 2003). Therefore, the NMR signals were also analyzed for protons at the phenyl groups. The π–π interaction can be defined by the frequency difference of the protons on the ortho and meta positions, also referred to as δ*f*. **Figure 4.10 (b)** shows the δ*f* of *p*-DMTB at various concentrations. The plot showed an identical trend as proposed hydrogen bonding formed between the triazole moieties.

δ*f* can be correlated to the ring current effect due to the aggregation of monomers that cause the phenyl to come close together. The distance between the phenyl groups should be sufficient to induce π-π interaction, which results in the stable aggregation of macrocyclic structures such as phenylene ethylene (Pickholz & Stafström, 2001). The similar π-π interaction has also been studied in solutions through self-association of the phenylacetylene macrocyclic molecule (Shetty et al., 1996). They have determined the influence of ring current from neighboring molecules resulting in the shift of aromatic protons to upfield.

From the plot, it showed that δ*f* decreased from 86 to 82 Hz at concentration 0.05 to 0.09 mM before δ*f* becomes constant even though the concentration of the amphiphile keeps increasing. The δ*f* value was higher at a concentration below CMC value, suggesting uninterrupted spinning of ortho and meta proton nuclei (Hatzopoulos et al., 2011). When the aggregation occurred, the δ*f* was constant, which caused the spinning at ortho and meta protons to be shielded by adjacent molecules. A slight increase in frequency difference after 0.10 mM is probably due to neighboring atoms at meta and

ortho protons. After aggregation, the spherical shape of micelle may slightly interrupt the π–π interaction of the benzene. Thus, a slight increase in the frequency difference after the CMC reached has occurred.

Scheme 4.2 showed that the ring current from adjacent molecules was produced only when phenyl-phenyl is closer and parallel to each other. The parallel orientation is more reasonable than the perpendicular orientation. In other words, the parallel orientation of the phenyl-phenyl groups causes *p*-DMTB to assemble in more stable arrangements. Therefore, the hydrogen bonding formation between triazoles and π–π interaction in phenyl groups are confirmed to exist in *p*-DMTB during the aggregation process. The self-assembly of *p*-DMTB in planar conformation has also led to the parallel orientation of phenyl groups that drive the molecules to be packed together closely.

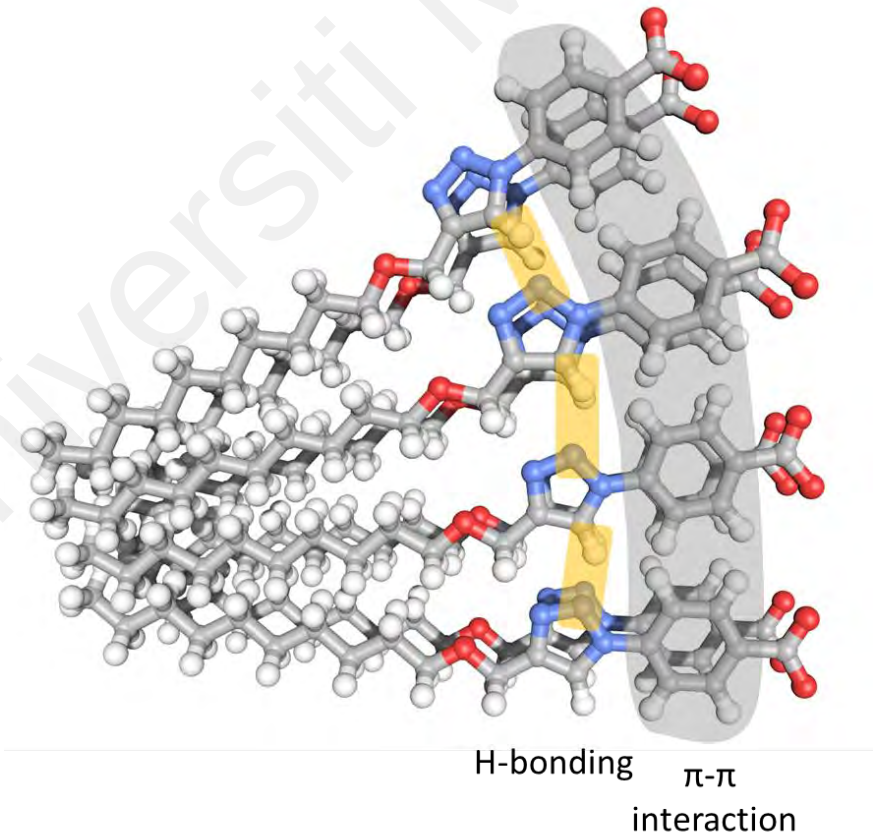

Scheme 4.2: Grey and yellow regions represent π–π interaction and intermolecular hydrogen bonding between triazoles of *p*-DMTB, respectively.

Micellization of *p*-DMTB affects the intermolecular hydrogen bonding and π–π interaction of phenyl groups to be strengthened within themselves although in the presence of the repulsion amongst the headgroup.

This finding was significantly important to justify how the presence of nonionic co-surfactant such as glycolipids interact and incorporated with the amphiphile. By disruption of the hydrogen bonding networking and aromatic interaction, the CMC value was higher towards the CMC value of natural fatty acid. Prior to the study of the amphiphile in a mixed system, a simple investigation of phase transition would be worth to explore especially for emphasizing the contribution of the interaction in a larger self-aggregation structure such as vesicles. In order to determine whether the attained interactions in *p*-DMTB molecules are still in well-packed manner, the transition of micelle-to-vesicle need to be investigated by titration similar like fatty acid systems.

4.3 Micelle-to-Vesicle transition of *p*-DMTB

Self-aggregation in most fatty acid systems can be induced by changing the pH value. With the variation of pH, the conversion of fatty acid headgroups can be manipulated. Besides that, pH variation also changes the morphology of the aggregate from worm-like micelle to spherical micelle at higher pH and form vesicle structure at lower pH value. The aggregation process may occur from interaction among amphiphiles and by the interaction of amphiphiles with solvents.

In order to study the equilibrium phase transition of *p*-DMTB, different volumes of 1 mM HCl solution were titrated into the alkaline *p*-DMTB solution to produce a series of solutions with different pH. Then, each sample was tested with pH meter, the turbidity of the samples by UV-VIS spectroscopy at 500 nm and the fluorescence emission of *p*-DMTB.

Figure 4.11 shows that the turbidity of *p*-DMTB solutions varied with HCl concentrations by the titration method. The amphiphile solution changed from optically clear to turbid with decreasing pH values. The titration was started from basic (pH 10) to neutral (pH 7) conditions. It has been discovered that micellar structure was predominant when *p*-DMTB was dissolved between pH 9.50–10.50. At this stage, it is suggested that *p*-DMTB has been entirely in micellar formation due to complete deprotonation of the carboxylic group of *p*-DMTB by addition of NaOH in the solution to form $RCOO^{-}Na^{+}$.

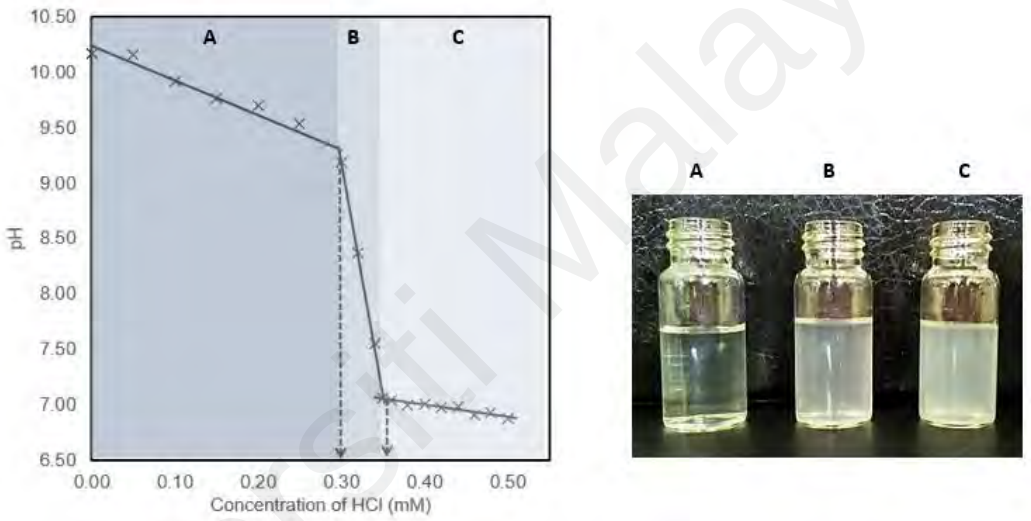

Figure 4.11: Titration graph of 0.5 mM *p*-DMTB stock solution with HCl at room temperature. Three types of regions representing the opacity of *p*-DMTB solution vary with increase of HCl concentration from clear to turbid as shown in vial A, B and C.

Addition of the acid gradually changes the solution turbidity in which the pH value was decreased and affected a partial protonation of $RCOO^{-}Na^{+}$ and ionic interaction of $COOH---COO^{-}$. The turbidity was observed from pH 9.50 to nearly neutral pH. It has been stated that the turbid solution appearance indicated the conversion of small aggregates to the larger size of aggregates (Chen et al., 2017). Further addition of HCl has made the complete protonation of COO^{-} to COOH in the solution. Effect of HCl in

the solution can be evaluated from the three types of regions i.e. A, B and C from the pH profile. The regions were then correlated with the opacity of the *p*-DMTB solutions in the vials. Vial A did not show any significant opacity compared to vials B and C. Thus, both solutions in vial B and C were further observed under an optical polarizing microscope (OPM) with HCl concentration of 0.32 mM and 0.39 mM, respectively.

Small vesicles are detected in vial B before the size significantly increases to more than 20 µm in vial C (**Figure 4.12**). The small vesicle is observed under the microscope due to the coexistence of micelle and vesicle, which results from the neutralization process at the headgroup that converts COO^- into partially COOH. The neutralization causes the electrostatic interaction of COO^----COOH to become weak. In previous reports, stable oleate/oleic acid vesicles were formed around pH 8.5 (Fukuda et al., 2001), where the stability was explained in terms of intermolecular H-bond occurred between protonated and ionized species in aqueous solution (Apel et al., 2002).

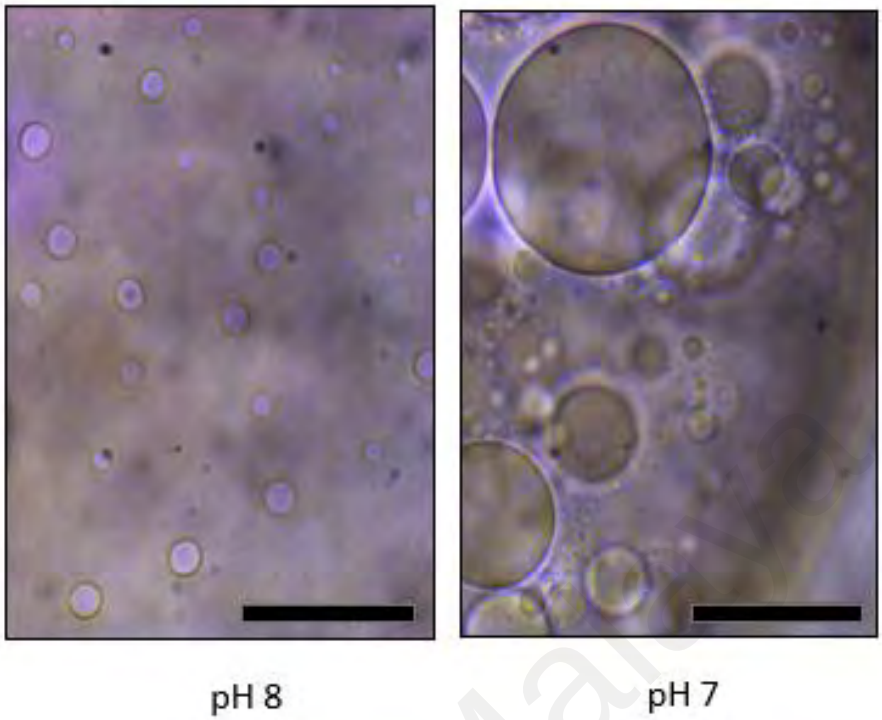

Figure 4.12: Morphology of *p*-DMTB at pH 8 and pH 7 with HCl concentration of 0.32 mM and 0.39 mM, respectively. Small to giant vesicles were observed with decreasing pH value at room temperature. The scale bar is 20 µm.

As more acid is added into the solution, the carboxylate COO^{-} headgroup becomes fully protonated into COOH. Surprisingly, more vesicles were formed with giant size at a diameter of 20 µm. This observation could be because the protonation has reduced repulsive interactions between the headgroup, which transforms the small size of vesicles to giant vesicles. Giant vesicles were reported by Marques and co-researchers using two different charges of surfactants with resulting diameter sizes up to 5 µm (Marques et al., 1999). Besides that, formation of double-chained amphiphile through a mixture of amphiphilic imine and amphiphilic aldehyde has led to giant vesicle growth in a diameter range of 2.5-20 µm (Takakura et al., 2014). Furthermore, a mixture of alkyl amines and fatty acids at extreme environment conditions e.g. strongly basic and acidic pH with divalent ionic strength has been reported but did not contribute to significant giant-sized

vesicle compared to our work (Namani & Deamer, 2008). Thus, *p*-DMTB could be the first report on the spontaneous growth of giant vesicles with more than 20 µm by a single amphiphile.

Besides using pH measurement to determine micelle-to-vesicle transition, turbidity determine by absorbance UV-VIS spectroscopy was another alternative that serves to study the same purpose. **Figure 4.13** shows the plot of absorbance intensity at 500 nm against HCl concentration. Lower absorbance intensity was determined around 0.02 a.u due to low scattering in solution. During this condition, *p*-DMTB was presumed not fully aggregate in the micellar formation. Above 0.10 mM HCl, the absorbance value started to increase because the aggregation of micelle is slowly increased. The highest absorbance was observed at around 0.18 a.u. when the solution was at 0.32 mM HCl. This observation was probably due to the complete micelle-to-vesicle transition in the solution.

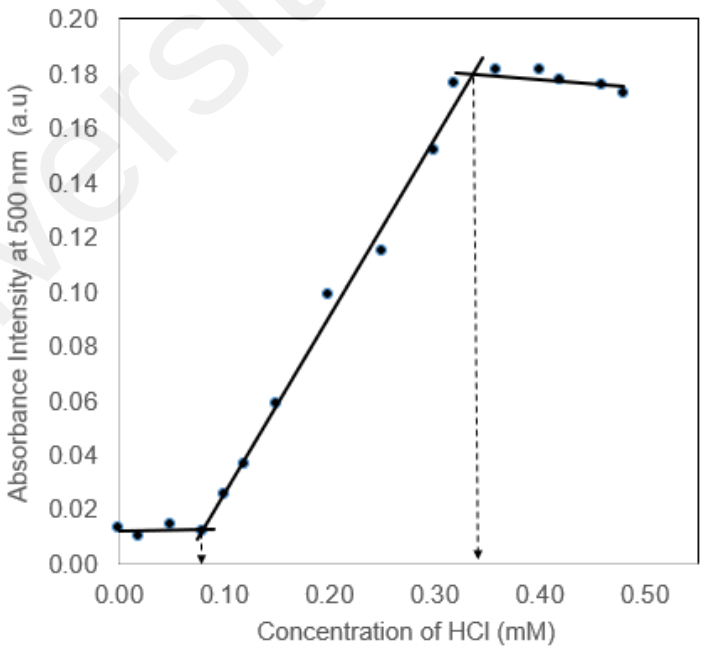

Figure 4.13: Turbidity profile of *p*-DMTB at 500 nm with addition of HCl.

Figure 4.14 represents the emission intensity of triazole moiety by changing the HCl concentration. Titration of acid induces the protonation of COO^- to COOH at the *p*-DMTB headgroup. Below 0.15 mM HCl, the headgroup conversion to COOH was in a smaller amount due to the low amount of H^+ presents in the solution. When the titration reached above 0.15 mM, the quantity of the conversion to COOH keeps increased, thus resulting in drastic emission intensity of 200 a.u. From the finding, we can deduce that although the headgroup has been disturbed by pH changing, the emission from triazole moiety has not been interrupted. Besides, the triazole produces emission intensity trend similar to our previous CMC finding.

A sudden rise of the emission intensity is affected by the conversion of COO^- to COOH at the headgroup. The triazole molecules in micelles become more concentrated and compact in structure with a side by side formation. Although CH---X (X= O, N, Cl, or S) interaction tends to form short intermolecular contact (Taylor & Kennard, 1982), the hydrogen bonding CH---N of triazole moieties in *p*-DMTB can be strengthened with the help of protonated headgroups. Therefore, it is confirmed that the intermolecular interactions of triazoles are stronger due to the transition of micelle-to-vesicle.

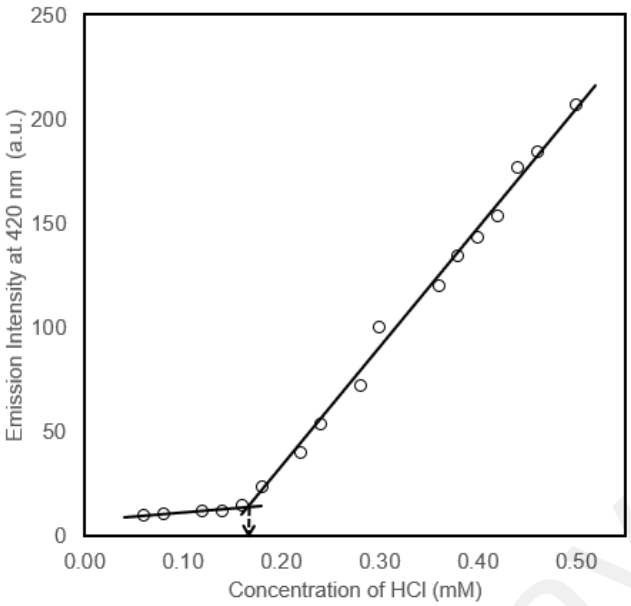

Figure 4.14: Emission intensity at 420 nm of 0.5 mM *p*-DMTB plot with increasing concentration of HCl at 25℃.

From the previous results, the contribution of hydrogen bonding between triazoles, π–π interaction in phenyl groups and protonation at the headgroups has surprisingly led to giant vesicle formation suggested in planar conformation with parallel orientation (**Scheme 4.3**).

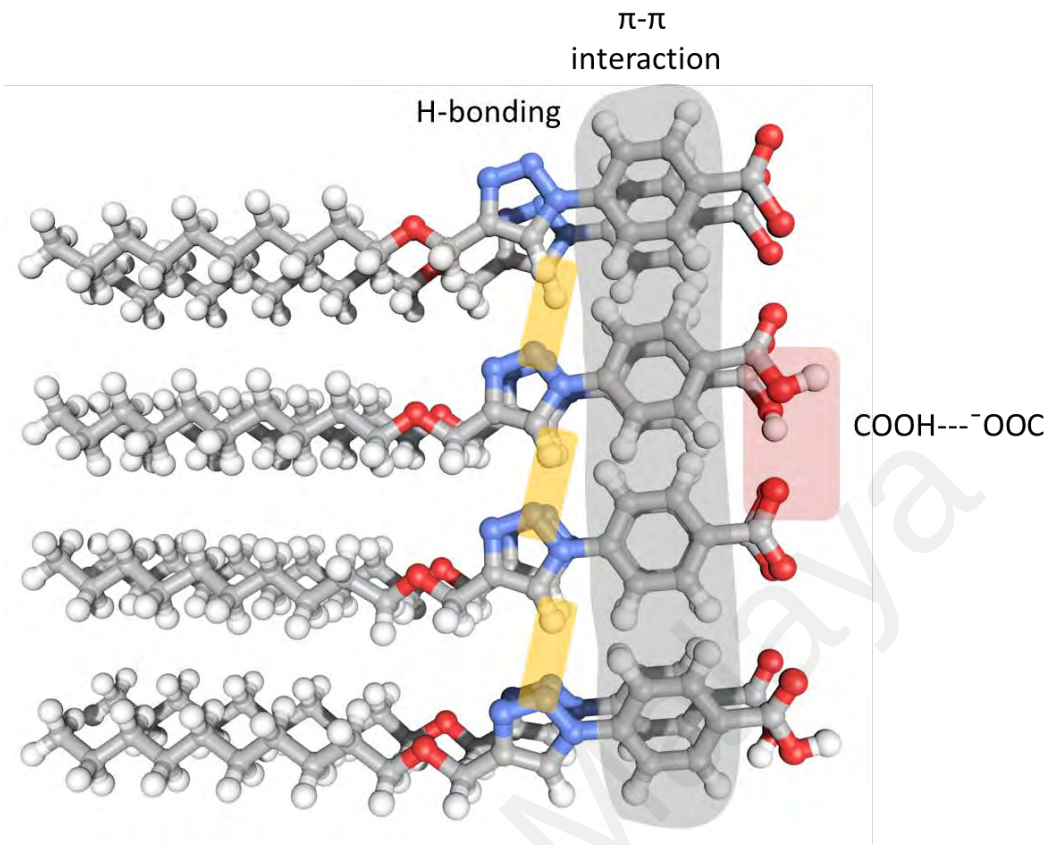

Scheme 4.3: Hydrogen bonding, π–π interaction and headgroup neutralization COOH---COO⁻ at pH 7 induced giant vesicle formation in planar conformation with parallel orientation.

These interactions certainly helped *p*-DMTB to self-aggregate at much lower concentration in micellar form, while having an extremely large self-assembling structure of vesicles. The self-aggregation of the amphiphile, however, could potentially have limitations if incorporated with a co-surfactant. It is known and typical that a mixed amphiphile system would be incorporated and well blended into a uniform shape. But, as of the finding on the interactions, the presence of minor amount of nonionic co-surfactant could be as a competitor to the strength of the interactions.

In the following sub-chapter, the main subject of the thesis will be discussed. Hypothetically, if the hydrogen bonding network between triazoles is in a continuous manner and strong, intermolecular interaction will not be disturbed by another co-

surfactant. Therefore, glycolipids co-surfactant was introduced into *p*-DMTB solution to investigate whether the existing intermolecular interaction can be retained.

4.4 *p*-DMTB-Glycolipids mixture solutions

4.4.1 Critical Micellar Concentration of *p*-DMTB-Glycolipids mixture solutions

A series of glycolipids with different hydrophobic chain lengths were mixed with *p*-DMTB in aqueous solution to determine changes in aggregation behavior of *p*-DMTB. The three selected glycolipids were DDG, DG and OG with 12, 10 and 8 saturated alkyl chains, respectively. The study was carried out by using UV-Visible spectrophotometer, fluorescence spectrophotometer and tensiometer. Aggregation behavior in the aqueous solution of mixed *p*-DMTB-glycolipids system was being determined and compared to a single amphiphile system of the *p*-DMTB solution.

The surface tension of water was tested with a mixture of *p*-DMTB-glycolipids at 25℃. The CMC values from the mixture of *p*-DMTB-glycolipids were increased from 0.10 mM to 0.31 mM, 0.49 mM and 0.59 mM with decreasing glycolipids alkyl chain length compared to the CMC of a single system of *p*-DMTB. **Figure 4.15** shows the surface tension plot of those three mixture solutions. The increment in CMC value was attributed to a disturbance between *p*-DMTB molecules with glycolipids. In other words, the arrangement of *p*-DMTB at the interface was disturbed by glycolipids. Therefore, micelle formation in the mixture solution has influenced the increment of CMC value.

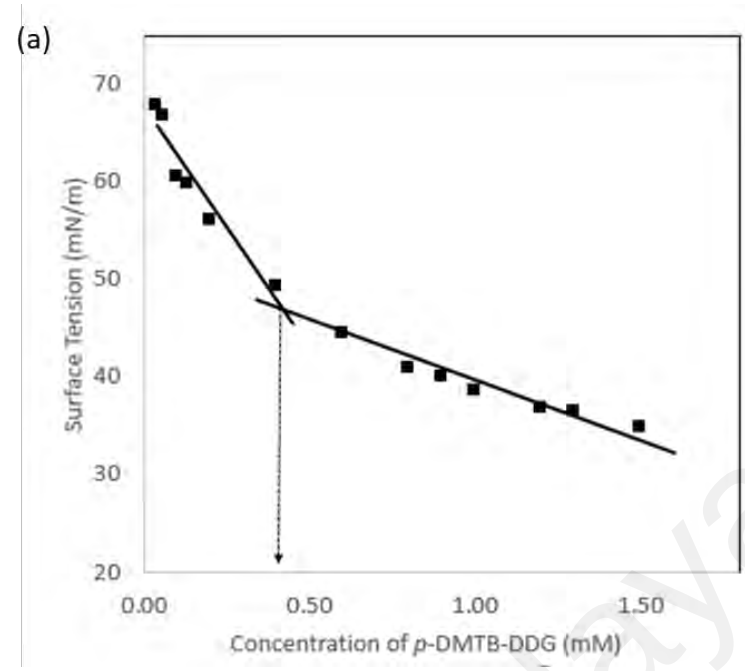

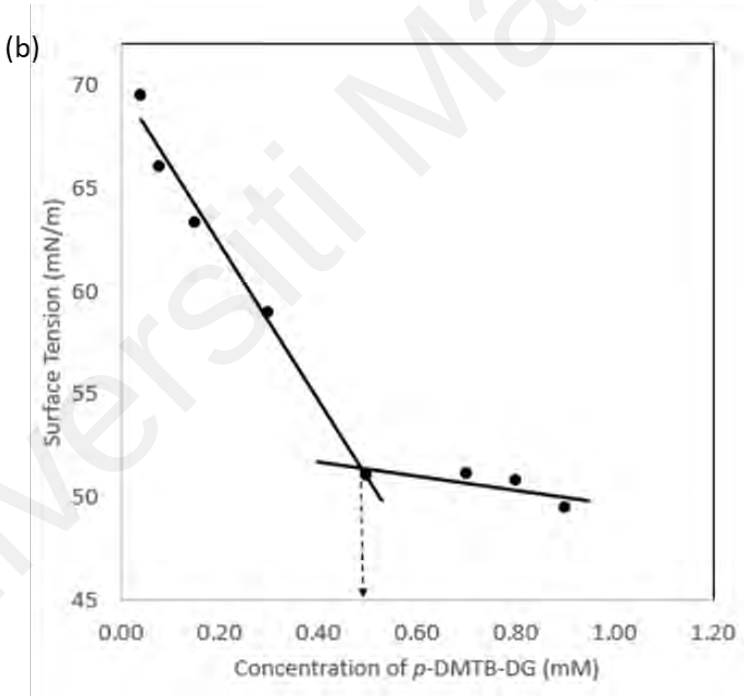

Figure 4.15: Surface tension of (a) *p*-DMTB-DDG, (b) *p*-DMTB-DG and (c) *p*-DMTB-OG in aqueous solution at 25 ℃.

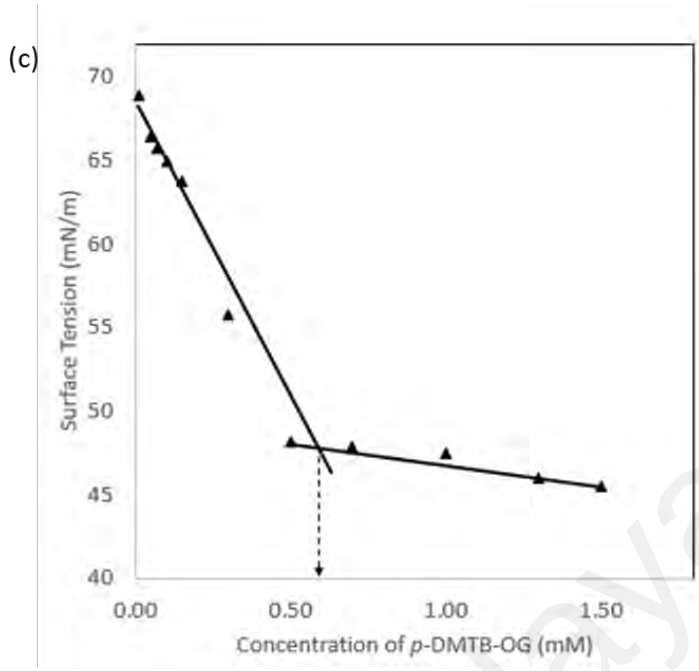

Figure 4.15, continued.

Amongst the mixture of *p*-DMTB-DDG, *p*-DMTB-DG and *p*-DMTB-OG, the mixture of the *p*-DMTB-DDG solution showed the lowest CMC value. The reason could be from the differences in alkyl chain length of the glycolipids used. DDG with 12 alkyl chains influenced more significantly in hydrophobic effect towards alkyl chain of *p*-DMTB. In addition, surface tension at the CMC value of *p*-DMTB-DDG was the lowest at 43.34 mN m^{-1} as being compared to the other two mixtures and single *p*-DMTB solutions. It shows that although CMC for the mixture *p*-DMTB-DDG was increased three times higher than single system *p*-DMTB, the surface tension value was decreased with the presence of DDG.

Figure 4.16 showed absorbance of *p*-DMTB-DDG, *p*-DMTB-DG and *p*-DMTB-OG solutions. The CMC value of *p*-DMTB-DDG, *p*-DMTB-DG and *p*-DMTB-OG was determined at 0.18, 0.35 and 0.38 mM, respectively. The mixture of *p*-DMTB-OG has the highest CMC value among other *p*-DMTB-glycolipids mixtures. The observation indicated that hydrophobic tail of OG has the lowest impact to promote the micellization of *p*-DMTB-OG at low concentrations. Besides that, the shortest alkyl chain length of

glycolipid also reduces the efficiency of hydrophobic attraction between *p*-DMTB and OG.

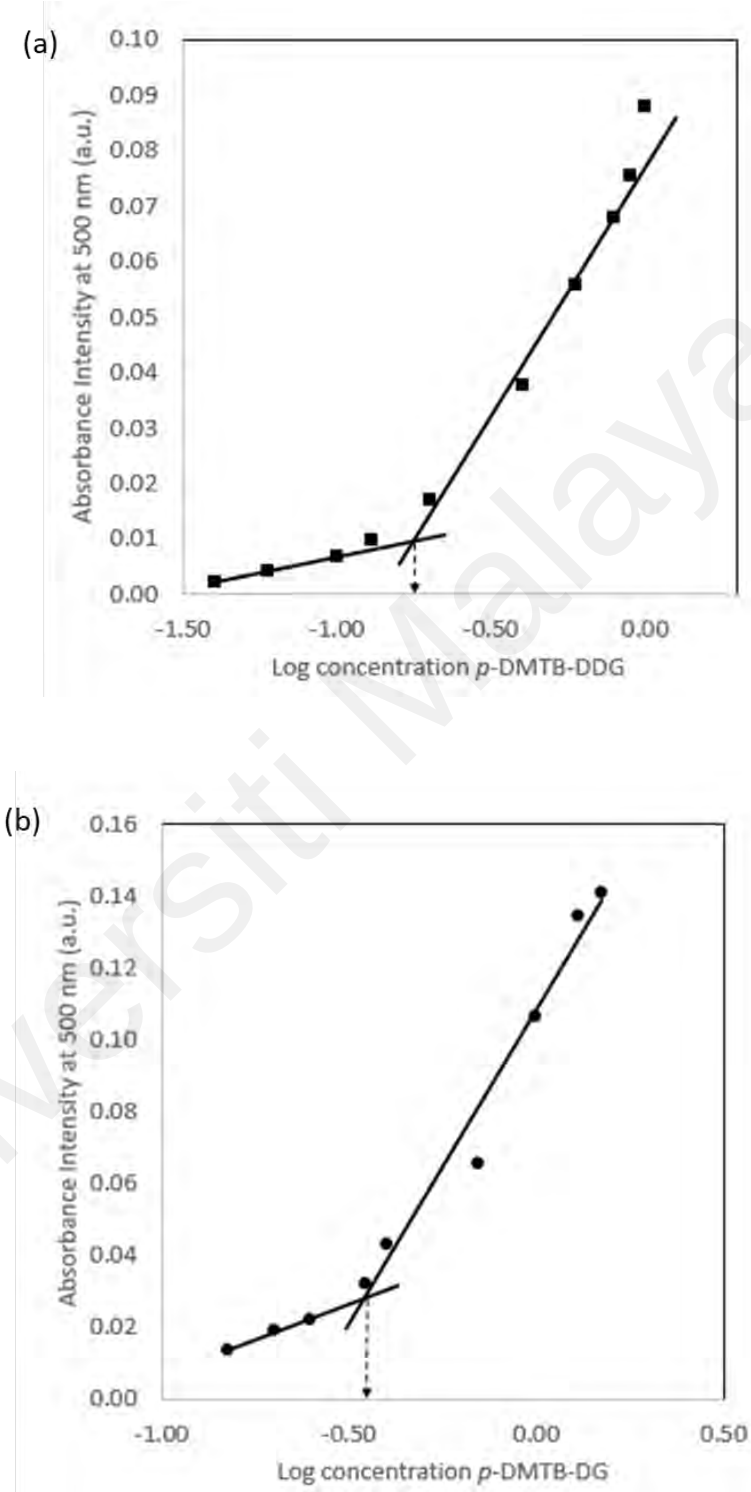

Figure 4.16: Absorbance intensity at 500 nm with log concentration of mixture (a) *p*-DMTB-DDG, (b) *p*-DMTB-DG and (c) *p*-DMTB-OG at 25℃.

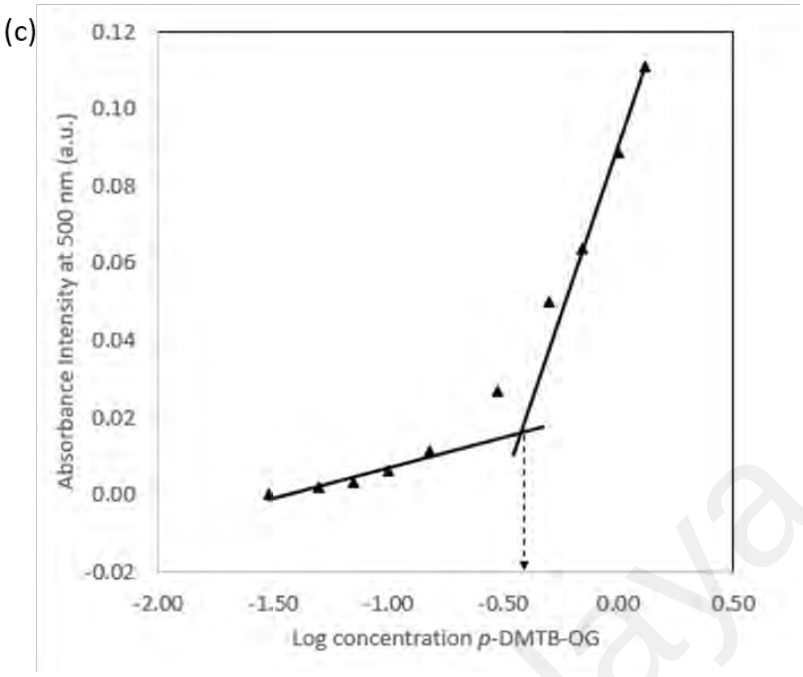

Figure 4.16, continued.

Addition of glycolipids in *p*-DMTB solution shifted the *p*-DMTB CMC value. From the previous result and discussion, the possibility of hydrogen bonding happened between triazoles has been confirmed through the drastic increase of absorbance intensity *p*-DMTB. The aggregation of *p*-DMTB was influenced by CH···N hydrogen bonding, π-π interaction, hydrophobic attraction between alkyl tails. Thus, glycolipids can form another additional hydrogen bonding between glucose headgroup of glycolipids bonded with carboxylate headgroup of *p*-DMTB. Therefore, this possibility has led to interruption and delaying *p*-DMTB micelle aggregation.

The mixtures were further analyzed based on emission intensity study to discover whether emission intensity of triazole is being enhanced in the presence of the glycolipids. From the previous single system of *p*-DMTB, aggregation of *p*-DMTB led to inducing emission intensity of the triazole. The drastic emission intensity was confirmed being influenced by hydrogen bonding between triazoles molecules.

Figure 4.17 shows the plot of emission intensity at 420 nm with increasing concentration of *p*-DTMB-glycolipids. From the plot, emission intensities from the three mixtures were decreased compared to *p*-DMTB. The value of emission intensity has reduced significantly, almost 20-fold in mixture solutions. All three mixtures have almost similar emission intensity values, 5 a.u.. Previously, aggregation-induced emission (AIE) from *p*-DMTB was attributed by intermolecular interaction between triazoles. Thus, in the mixture of the *p*-DMTB-glycolipids, AIE could not be supported by the addition of glycolipids. Intermolecular interaction between triazoles has been disturbed by glycolipids. Therefore, the emission intensity values obtained for *p*-DMTB-DDG, *p*-DMTB-DG and *p*-DMTB-OG can be explained by the overall quenching of emission from triazole to interact with each other due to the presence of co-surfactant.

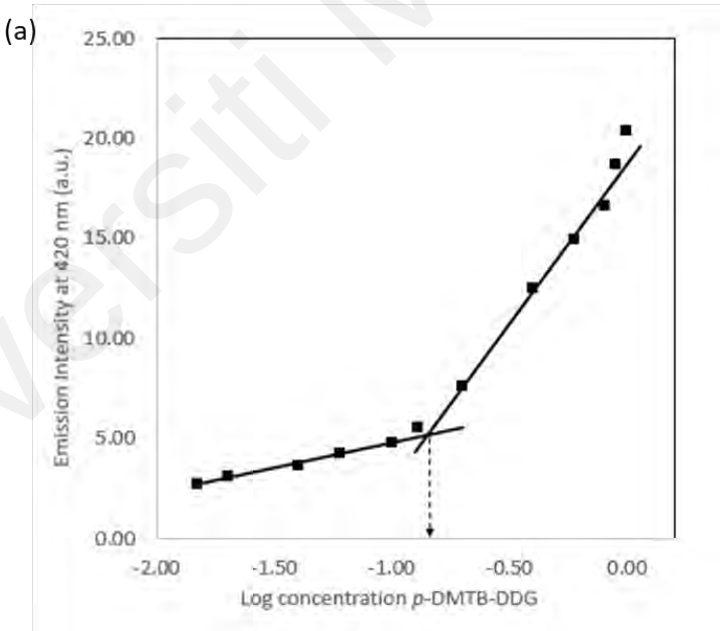

Figure 4.17: Emission intensity at 420 nm for mixture of (a) *p*-DMTB-DDG, (b) *p*-DMTB-DG and (c) *p*-DMTB-OG at 25℃.

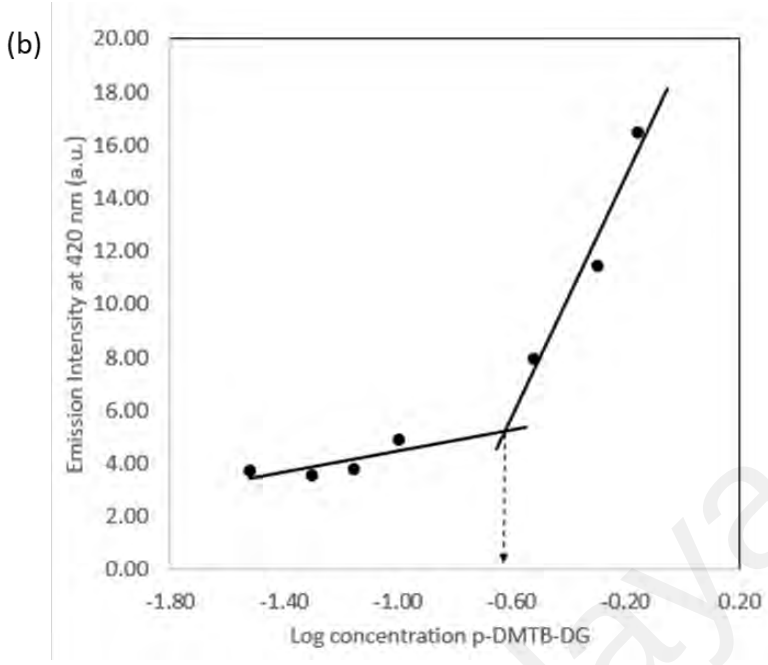

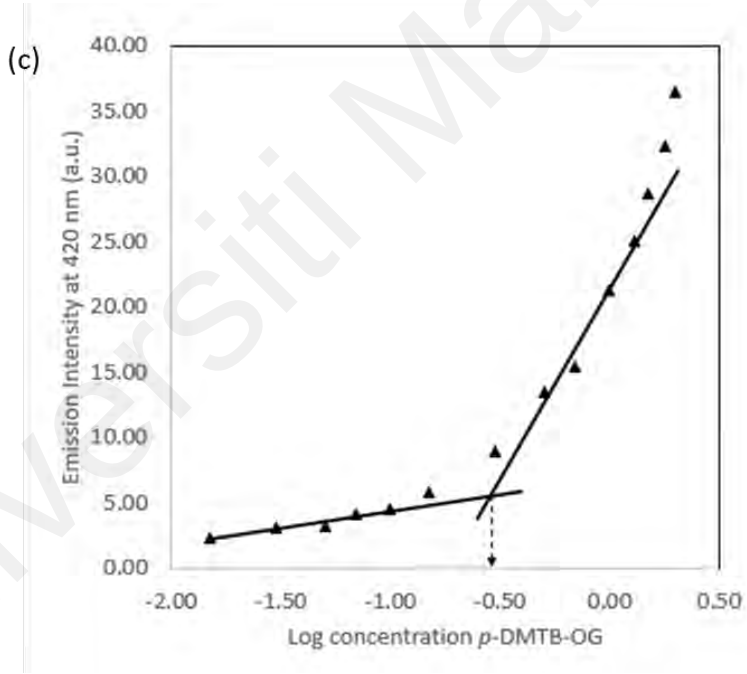

Figure 4.17, continued.

Figure 4.18 shows the overall CMC values obtained based on three methods applied for *p*-DMTB-glycolipids mixtures. From the graph, the CMC values for each *p*-DMTB-glycolipids mixture showed a huge inconsistency with different measurement techniques compared to the pure *p*-DMTB. For example, the *p*-DMTB-OG solution had the widest gap of CMC values with a standard deviation of 0.15. Meanwhile, the *p*-DMTB solution

has a standard deviation of only 0.03 based on surface tension, absorbance, and fluorescence emission measurement techniques. The inconsistency of these CMC values may be due to the different arrangement of *p*-DMTB and glycolipids molecules during the micellization process. It is reasonable that during the formation of the micelle, the arrangement of *p*-DMTB and glycolipids is not in the ordered array or random distribution and most probably subjected to the molecules nearby to interact.

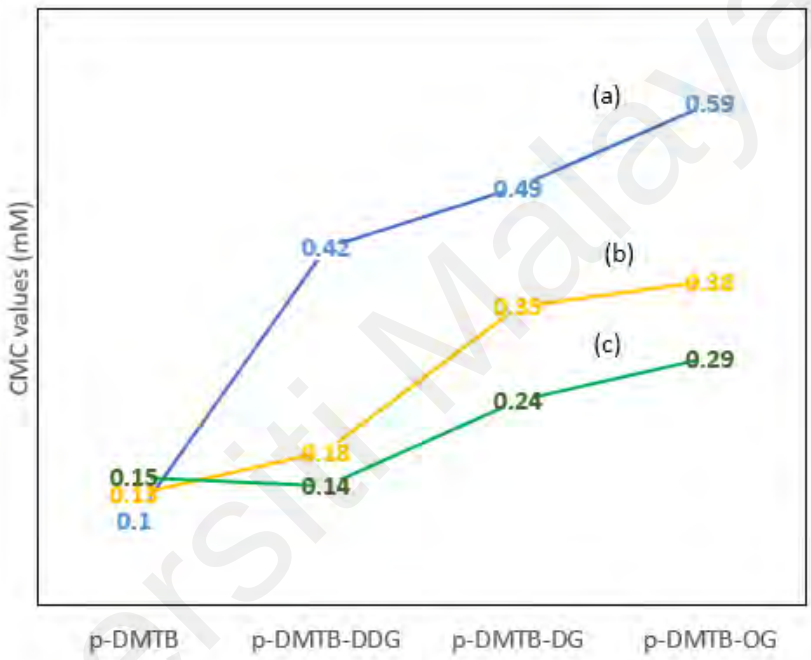

Figure 4.18: Overall CMC values determined from three methods applied for mixture of *p*-DMTB-glycolipids compared to pure *p*-DMTB. (a) CMC values based on surface tension, (b) CMC values based on UV-VIS and (c) CMC values based on fluorescence emission.

Based on results obtained and the possible micellization arrangement mentioned previously in **Figure 1.5**, the combination of *p*-DMTB and glycolipids to form micelle is the most appropriate model to represent the arrangement of *p*-DMTB-glycolipids mixture.

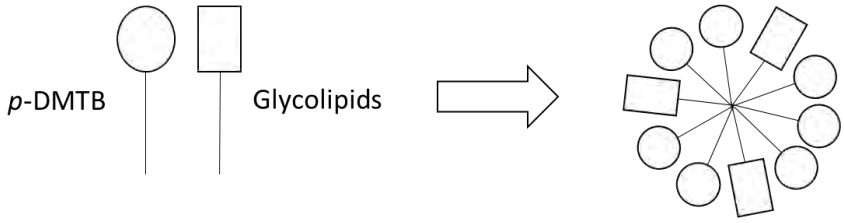

Figure 4.19: Arrangement of *p*-DMTB-glycolipids mixture in aqueous solution.

The detailed arrangement in **Figure 4.19** was furthered illustrated in **Figure 4.20**. **Figure 4.20** shows the proposed aggregation may happen between *p*-DMTB-glycolipids solution. **Figure 4.20**(a) represents interaction between triazolyl proton and sugar headgroup of glycolipids while **Figure 4.20**(b) is carboxylate-hydroxyl group interactions. Based on the results acquired, **Figure 4.20**(a) was selected as the most reasonable arrangement for the glycolipids that disrupted the intermolecular interactions of triazoles. The presence of four hydroxyl groups at sugar headgroup led to interruption of *p*-DMTB to aggregate in the solution. Existing hydrogen bonding between the triazole groups has been interfered by one of the hydroxyl glycolipids headgroup. Although the volume ratio of glycolipids is only 10% of the mixture, the *p*-DMTB-glycolipids CMC value acquired was increased above than 0.10 mM relative to a single *p*-DMTB system. Therefore, glycolipids did not significantly take part in enhancing aggregation behavior of *p*-DMTB by disrupting the existing hydrogen bonding formed from the triazole proton at C5 position to N2 of an adjacent amphiphile molecule.

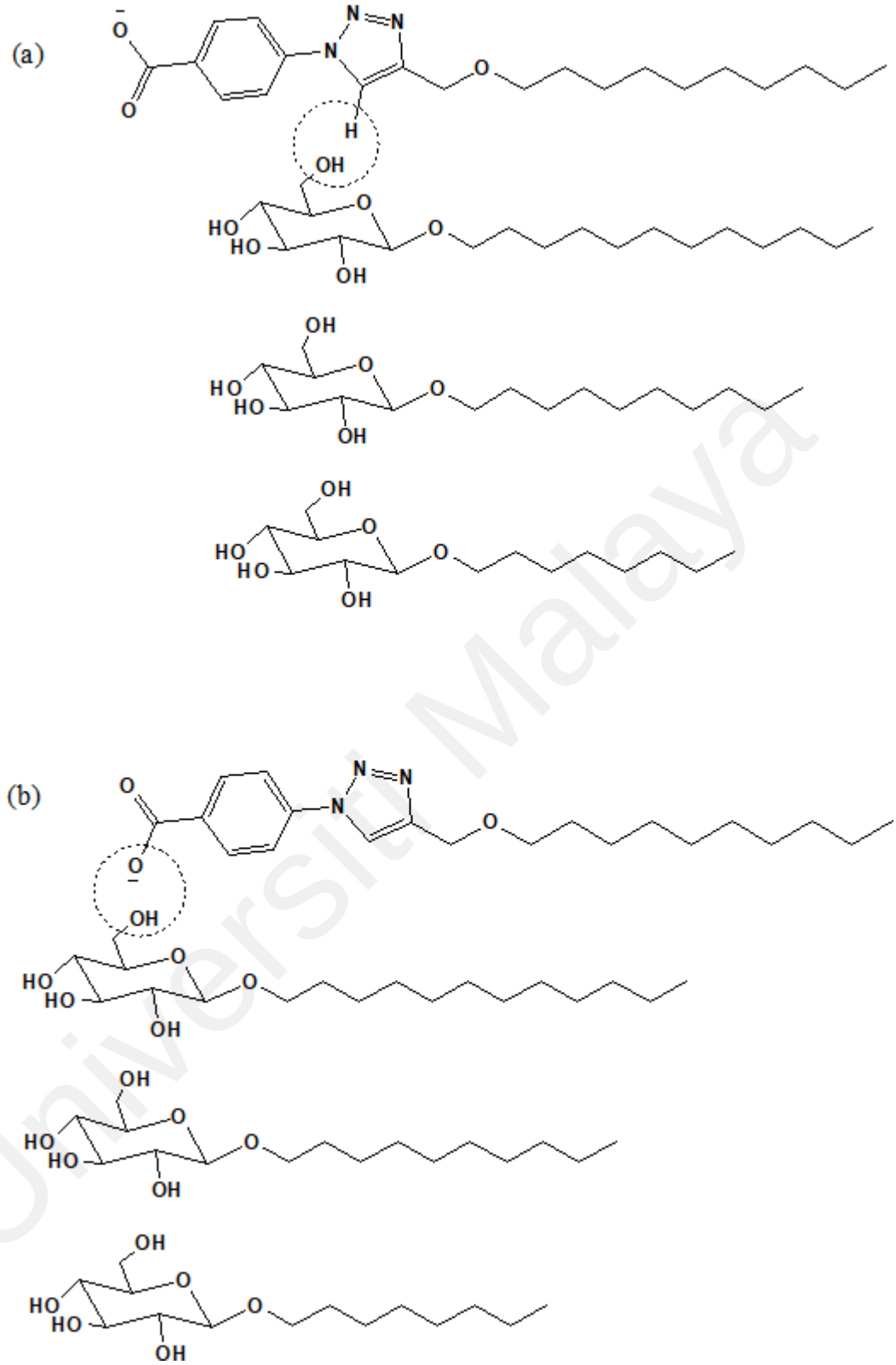

Figure 4.20: Proposed possible aggregations that may happen between *p*-DMTB-glycolipids solution. (a) Interaction between triazolyl proton and glucose of glycolipids and (b) carboxylate-hydroxyl group interactions.

CHAPTER 5: CONCLUSIONS

Para-decyloxymethyl triazolyl benzoic acid (*p*-DMTBA) was successfully synthesized from Copper(I)–catalyzed cycloaddition reaction with 84.0% yield. The important NMR signals were detected at 8.06 ppm, 4.73 ppm and 3.57 ppm, which represented triazole linkage and ether bond.

p-DMTBA was conducted in aqueous solution to investigate its self-aggregation behavior. Critical micellar concentration (CMC) of the *p*-DMTB occurred in the range of 0.10 mM-0.15 mM. The surface tension of the amphiphile was determined at 65.38 mN m^{-1} much lower surface activity compared to other similar amphiphilic molecules or surfactants mainly attributed to additional interactions from triazole and phenyl groups within the aggregation process.

The interactions of internal triazole and phenyl groups require a planar configuration and induced drastic emission intensity above 0.15 mM. The interaction is hydrogen bonding from proton at C5 position to the second, N2 of the adjacent triazole molecule. The resonance frequency of proton nuclei at C5 of triazole has been confirmed through ^{1}H-NMR. The frequency plot became constant at 0.10 mM similar to the CMC value obtained from other methods. The planar configuration and the hydrogen bonding networking within the aggregation are in agreement with the π-π interaction that occurred between phenyl groups in the parallel orientation promotes the *p*-DMTB molecules to assemble in more stable arrangements.

Phase transition of micelle-to-vesicle also has been investigated from pH 10 to pH 7. A complete protonation at the carboxylate headgroup did not disturb the emission intensity from the triazole group. Therefore, hydrogen bonding between the triazole

moieties is strong and stable enough to induce the formation of giant vesicle size up to 20 μm.

Self-aggregation of the *p*-DMTB was then investigated in the presence of glycolipids (OG, DG and DDG) as co-surfactants. A series of the mixture *p*-DMTB-glycolipids in a fixed 9:1 volume ratio was analyzed from the surface tension, absorbance and emission intensity. The results clearly suggesting that the addition of the glycolipids affects the aggregation stability of *p*-DMTB where the CMC of the mixtures are much higher than that of the amphiphile only. In a sequence, the mixture of *p*-DMTB-DDG was determined to have the lowest CMC values compared to *p*-DMTB-OG and *p*-DMTB-DG using the three methods. These observations were due to the hydrophobic effect from the alkyl chain of DDG.

The *p*-DMTB solution has shown consistent CMC values varying in the methods of determination than *p*-DMTB-DDG. The presence of co-surfactant did not enhance the aggregation of *p*-DMTB in terms of CMC value. Thus, as demonstrated by this research work, the *p*-DMTB solution has a remarkable ability to self-aggregate more effectively by additional interactions particularly hydrogen bonding and π–π interaction from heteroaromatic and aromatic groups without the assistance of any additional amphiphile or co-surfactant. In fact, the presence of co-surfactant in a small amount may cause the susceptibility to the hydrogen bonding networking and π–π interaction region. Therefore, presence of additional interactions by embedding new moieties to the amphiphile could help formulation, biological or sensor device applications towards growing of development industry.

Suggestion for future work, we would like to recommend thermodynamics and kinetics investigation as well as in different organic solvents environment. It would be interesting to analyze the potential formation of *p*-DMTB monolayer using Langmuir Blodget along

with computational approach. Furthermore, *p*-DMTB may also potentially beneficial in cellular and biomolecular tagging as it fluoresces through aggregation. With the proposed suggestion for the future work, we would discover ability of the amphiphile to respond towards external factors such as temperature, humidity, mechanical pressure or frictional force. These approaches are crucial if we would like to pursue the amphiphile usage in medical, coating, painting industries and etc.

REFERENCES

Ahmad, N., Muhammad, R., Tajuddin, H. A., & Misran, M. (2014). Effect of glycolipids on the stability and electrophoretic mobility of decanoic acid vesicles. *Colloids and Surfaces A: Physicochemical and Engineering Aspects, 443*, 96-101.

Akbarzadeh, A., Rezaei-Sadabady, R., Davaran, S., Joo, S. W., Zarghami, N., Hanifehpour, Y., Samiei, M., Kouhi, M., & Nejati-Koshki, K. (2013). Liposome: classification, preparation, and applications. *Nanoscale research letters, 8*(1), 102.

Al-Soufi, W., Piñeiro, L., & Novo, M. (2012). A model for monomer and micellar concentrations in surfactant solutions: Application to conductivity, NMR, diffusion, and surface tension data. *Journal of Colloid and Interface Science, 370*(1), 102-110.

Anneken, D. J., Both, S., Christoph, R., Fieg, G., Steinberner, U., & Westfechtel, A. (2006). Fatty Acids. *Ullmann's Encyclopedia of Industrial Chemistry, 14*, 73-116.

Apel, C. L., Deamer, D. W., & Mautner, M. N. (2002). Self-assembled vesicles of monocarboxylic acids and alcohols: conditions for stability and for the encapsulation of biopolymers. *Biochimica et Biophysica Acta (BBA)-Biomembranes, 1559*(1), 1-9.

Averko-Antonovich, I. Y., Ziganshina, L., Rakhmatullina, A., & Akhmed'yanova, R. (2004). Surface activity of fatty acid salts in aqueous solutions. *Russian Journal of Applied Chemistry, 77*(4), 595-598.

Brown, G. M., Dubreuil, P., Ichhaporia, F. M., & Desnoyers, J. E. (1970). Synthesis and properties of some α-D-alkyl glucosides and mannosides: apparent molal volumes and solubilization of nitrobenzene in water at 25°C. *Canadian Journal of Chemistry, 48*(16), 2525-2531.

Butt, H. J., Graf, K., & Kappl, M. (2004). Surfactants, micelles, emulsions, and foams. *Physics and Chemistry of Interfaces* (pp. 246-279). Federal Republic of Germany: Wiley-VCH Verlag GmbH & Co. KGaA.

Chachaty, C. (1987). Applications of NMR methods to the physical-chemistry of micellar solutions. *Progress in Nuclear Magnetic Resonance Spectroscopy, 19*, 183-222.

Chen, L. C., Wang, H. P., Deng, Y. H., & Deng, S. P. (2017). Vesicle formation by proton transfer driven short-tailed fatty acids of C4-C8 chain length in water. *Soft Matter, 13*(6), 1291-1298.

Chumpitaz, L. D., Coutinho, L. F., & Meirelles, A. J. (1999). Surface tension of fatty acids and triglycerides. *Journal of the American Oil Chemists' Society, 76*(3), 379-382.

Cui, X., Mao, S., Liu, M., Yuan, H., & Du, Y. (2008). Mechanism of Surfactant Micelle Formation. *Langmuir, 24*(19), 10771-10775.

De, S., Aswal, V. K., & Ramakrishnan, S. (2010). Phenyl-ring-bearing cationic surfactants: effect of ring location on the micellar structure. *Langmuir, 26*(23), 17882-17889.

Deng, C., Niu, Y., Peng, Q., Qin, A., Shuai, Z., & Tang, B. Z. (2011). Theoretical study of radiative and non-radiative decay processes in pyrazine derivatives. *The Journal of Chemical Physics, 135*(1), 014304.

Du Vernet, R., & Boekelheide, V. (1974). Nuclear magnetic resonance spectroscopy. ring-current effects on carbon-13 chemical shifts. *Proceedings of the National Academy of Sciences, 71*(8), 2961-2964.

Ek, K., Bjellqvist, B., & Righetti, P. G. (1983). Preparative isoelectric focusing in immobilized pH gradients. I. General principles and methodology. *Journal of Biochemical and Biophysical Methods, 8*(2), 135-155.

Evans, H. (1956). 117. Alkyl sulphates. Part I. Critical micelle concentrations of the sodium salts. *Journal of the Chemical Society (Resumed)*, 579-586.

Fameau, A.-L., Arnould, A., & Saint-Jalmes, A. (2014). Responsive self-assemblies based on fatty acids. *Current Opinion in Colloid & Interface Science, 19*(5), 471-479.

Fisher, L., & Oakenfull, D. (1977). Micelles in aqueous solution. *Chemical Society Reviews, 6*(1), 25-42.

Frisken, B. J., Asman, C., & Patty, P. J. (2000). Studies of Vesicle Extrusion. *Langmuir, 16*(3), 928-933.

Fu, N., Wang, S., Zhang, Y., Zhang, C., Yang, D., Weng, L., Zhao, B., & Wang, L. (2017). Efficient click chemistry towards fatty acids containing 1,2,3-triazole: Design and synthesis as potential antifungal drugs for *Candida albicans*. *European Journal of Medicinal Chemistry, 136*, 596-602.

Fukuda, H., Goto, A., Yoshioka, H., Goto, R., Morigaki, K., & Walde, P. (2001). Electron spin resonance study of the pH-induced transformation of micelles to vesicles in an aqueous oleic acid/oleate system. *Langmuir, 17*(14), 4223-4231.

Fukuda, H., Kawata, K., Okuda, H., & Regen, S. L. (1990). Bilayer-forming ion-pair amphiphiles from single-chain surfactants. *Journal of the American Chemical Society, 112*(4), 1635-1637.

Gabriel, N. E., & Roberts, M. F. (1984). Spontaneous formation of stable unilamellar vesicles. *Biochemistry, 23*(18), 4011-4015.

Gajowy, J., Bolikal, D., Kohn, J., & Fray, M. E. (2014). Synthesis and characterization of fatty acid/amino acid self-assemblies. *Journal of Functional Biomaterials, 5*(4), 211-231.

Gaudin, T., Rotureau, P., Pezron, I., & Fayet, G. (2017). Conformations of n-alkyl-*α*/*β*-D-glucopyranoside surfactants: Impact on molecular properties. *Computational and Theoretical Chemistry, 1101*, 20-29.

Gazit, E. (2002). A possible role for π-stacking in the self-assembly of amyloid fibrils. *The FASEB Journal, 16*(1), 77-83.

Han, C. M., Dong, S. P., Zhang, W. S., & Chen, Z. (2018). One-pot synthesis of 1-monosubstituted 1,2,3-triazoles from propargyl alcohol. *Synlett, 29*(5), 673-677.

Han, N. S., Heidelberg, T., & Salman, A. A. (2017). Spacer effect on triazole-linked sugar-based surfactants. *Journal of Dispersion Science and Technology, 38*(1), 105-109.

Hanzhen, Y., Youru, D., Sui, Z., & Jiayong, Y. (1999). Self-aggregation of surfactants in water solution by NMR. *Science in China Series A: Mathematics, 42*(3), 319-324.

Hargreaves, W. R., & Deamer, D. W. (1978). Liposomes from ionic, single-chain amphiphiles. *Biochemistry, 17*(18), 3759-3768.

Hatzopoulos, M. H., Eastoe, J., Dowding, P. J., Rogers, S. E., Heenan, R., & Dyer, R. (2011). Are hydrotropes distinct from surfactants? *Langmuir, 27*(20), 12346-12353.

Hensing, J. T. (2004). The discovery of lecithin, the first phospholipid. *Bulletin for the History of Chemistry, 29*(1), 9-14.

Hoffmann, Grabner, D., Hornfeck, U., & Platz, G. (1999). Novel vesicles from single-chain surfactants. *Journal of Physical Chemistry B, 103*(4), 611-614.

Hoffmann, H., & Ebert, G. (1988). Surfactants, micelles and fascinating phenomena. *Angewandte Chemie International Edition in English, 27*(7), 902-912.

Holmberg, K., Jonsson, B., Kronberg, B., & Lindman, B. (2003). Surfactant micellization. *Surfactants and Polymers in Aqueous Solution* (pp. 39-66): John Wiley & Sons Ltd.

Horne, W. S., Yadav, M. K., Stout, C. D., & Ghadiri, M. R. (2004). Heterocyclic peptide backbone modifications in an alpha-helical coiled coil. *Journal of the American Chemical Society, 126*(47), 15366-15367.

Hua, Y., & Flood, A. H. (2010). Click chemistry generates privileged CH hydrogen-bonding triazoles: the latest addition to anion supramolecular chemistry. *Chemical Society Reviews, 39*(4), 1262.

Hunter, C. A., & Sanders, J. K. (1990). The nature of. pi.-. pi. interactions. *Journal of the American Chemical Society, 112*(14), 5525-5534.

Hunter, D. G., & Frisken, B. J. (1998). Effect of Extrusion Pressure and Lipid Properties on the Size and Polydispersity of Lipid Vesicles. *Biophysical Journal, 74*(6), 2996-3002.

Israelachvili, J. N., Mitchell, D. J., & Ninham, B. W. (1976). Theory of self-assembly of hydrocarbon amphiphiles into micelles and bilayers. *Journal of the Chemical Society, Faraday Transactions 2: Molecular and Chemical Physics, 72*, 1525-1568.

Juwarker, H., Lenhardt, J. M., Pham, D. M., & Craig, S. L. (2008). 1,2,3-triazole CH···Cl− contacts guide anion binding and concomitant folding in 1,4-diaryl triazole oligomers. *Angewandte Chemie International Edition, 47*(20), 3740-3743.

Kagatikar, S., & Sunil, D. (2019). Aggregation-induced emission of azines: An up-to-date review. *Journal of Molecular Liquids, 292*, 111371.

Kaler, E. W., Murthy, A. K., Rodriguez, B. E., & Zasadzinski, J. A. (1989). Spontaneous vesicle formation in aqueous mixtures of single-tailed surfactants. *Science, 245*(4924), 1371-1374.

Kanicky, J., & Shah, D. (2003). Effect of premicellar aggregation on the pKa of fatty acid soap solutions. *Langmuir, 19*(6), 2034-2038.

Kano, K., & Ishimura, T. (1995). Properties of alkyl β-D-glucoside and alkyl β-D-maltoside micelles. *Journal of the Chemical Society, Perkin Transactions 2*(8), 1655-1660.

Kautny, P., Glöcklhofer, F., Kader, T., Mewes, J.-M., Stöger, B., Fröhlich, J., Lumpi, D., & Plasser, F. (2017). Charge-transfer states in triazole linked donor–acceptor materials: strong effects of chemical modification and solvation. *Physical Chemistry Chemical Physics, 19*(27), 18055-18067.

Khalil, R. A., & Hammad, F. J. (2014). Critical intermolecular forces: A new physical insight for the formation of wormlike micelles. *Journal of the Chemical Society of Pakistan, 36*(2).

Khalil, R. A., & Saadoon, F. A. (2015). Effect of presence of benzene ring in surfactant hydrophobic chain on the transformation towards one dimensional aggregate. *Journal of Saudi Chemical Society, 19*(4), 423-428.

Klein, R., Touraud, D., & Kunz, W. (2008). Choline carboxylate surfactants: Biocompatible and highly soluble in water. *Green Chemistry, 10*(4), 433-435.

Kondo, Y., Uchiyama, H., Yoshino, N., Nishiyama, K., & Abe, M. (1995). Spontaneous vesicle formation from aqueous solutions of didodecyldimethylammonium bromide and sodium dodecyl sulfate mixtures. *Langmuir, 11*(7), 2380-2384.

Kontogeorgis, G. M., & Kiil, S. (2016). Surfactants and self-assembly. detergents and cleaning. *Introduction to Applied Colloid and Surface Chemistry* (pp. 96-120): John Wiley & Sons, Ltd.

Kronberg, B., Holmberg, K., & Lindman, B. (2014). Types of Surfactants, their Synthesis, and Applications. *Surface Chemistry of Surfactants and Polymers* (pp. 1-47): John Wiley & Sons, Ltd.

Lawless, J. G., & Yuen, G. U. (1979). Quantification of monocarboxylic acids in the Murchison carbonaceous meteorite. *Nature, 282*(5737), 396-398.

Leigh, D. A., Robertson, C. C., Slawin, A. M., & Thomson, P. I. (2013). AAAA-DDDD quadruple hydrogen-bond arrays featuring NH⋯ N and CH⋯ N hydrogen bonds. *Journal of the American Chemical Society, 135*(26), 9939-9943.

Li, X., Gu, L., Xu, Y., & Wang, Y. (2009). Preparation of fenofibrate nanosuspension and study of its pharmacokinetic behavior in rats. *Drug Dev Ind Pharm, 35*(7), 827-833.

Li, Y., Reeve, J., Wang, Y., Thomas, R. K., Wang, J., & Yan, H. (2005). Microcalorimetric study on micellization of nonionic surfactants with a benzene ring or adamantane in their hydrophobic chains. *The Journal of Physical Chemistry B, 109*(33), 16070-16074.

Liu, Q.-Y., Jia, Q.-Y., Zhu, J.-Q., Shao, Q., Fan, J.-F., Wang, D.-M., & Yin, Y.-S. (2014). Highly ordered arrangement of meso-tetrakis (4-aminophenyl) porphyrin in self-assembled nanoaggregates via hydrogen bonding. *Chinese Chemical Letters, 25*(5), 752-756.

Logan, J. W., & Moya, F. R. (2009). Animal-derived surfactants for the treatment and prevention of neonatal respiratory distress syndrome: summary of clinical trials. *Ther Clin Risk Manag, 5*(1), 251-260.

Loner, C. M., Luzzio, F. A., & Demuth, D. R. (2012). Preparation of azidoaryl- and azidoalkyloxazoles for click chemistry. *Tetrahedron Letters, 53*(42), 5641-5644.

López, O., Cócera, M., Parra, J. L., & de la Maza, A. (2001). Influence of the alkyl chain length of alkyl glucosides on their ability to solubilize phosphatidylcholine liposomes. *Colloids and Surfaces A: Physicochemical and Engineering Aspects, 193*(1), 221-229.

Maibaum, L., Dinner, A. R., & Chandler, D. (2004). Micelle formation and the hydrophobic effect. *The Journal of Physical Chemistry B, 108*(21), 6778-6781.

Marques, E. F., Regev, O., Khan, A., da Graça Miguel, M., & Lindman, B. (1999). Vesicle formation and general phase behavior in the catanionic mixture SDS−DDAB−water. the cationic-rich side. *The Journal of Physical Chemistry B, 103*(39), 8353-8363.

Matsuoka, H., Matsutani, M., Mouri, E., & Matsumoto, K. (2003). Polymer micelle formation without Gibbs monolayer formation: Synthesis and characteristic behavior of an amphiphilic diblock copolymer having strong acid groups. *Macromolecules, 36*(14), 5321-5330.

Mei, J., Leung, N. L., Kwok, R. T., Lam, J. W., & Tang, B. Z. (2015). Aggregation-induced emission: together we shine, united we soar! *Chemical reviews, 115*(21), 11718-11940.

Meisner, Q. J., Accardo, J. V., Hu, G., Clark, R. J., Jiang, D.-e., & Zhu, L. (2018). Fluorescence of hydroxyphenyl-substituted "click" triazoles. *The Journal of Physical Chemistry A, 122*(11), 2956-2973.

Meyer, E. A., Castellano, R. K., & Diederich, F. (2003). Interactions with aromatic rings in chemical and biological recognition. *Angewandte Chemie International Edition, 42*(11), 1210-1250.

Moises de Oliviera, H. P., & H., G. M. (2002). Characterization of mixed micelles of sodium dodecyl and tetraoxyethylene dodecyl ether in aqueous solution. *Langmuir, 18*(10), 3792-3796.

Mukerjee, P. (1967). The nature of the association equilibria and hydrophobic bonding in aqueous solutions of association colloids. *Advances in Colloid and Interface Science, 1*(3), 242-275.

Myers, D. (1999). Surface activity and surfactant structures. *Surfaces, Interfaces and Colloids: Principle and Applications* (pp. 21-39): John Wiley & Sons, Inc.

Nagarajan, R. (2002). Molecular packing parameter and surfactant self-assembly: The neglected role of the surfactant tail. *Langmuir, 18*(1), 31-38.

Namani, T., & Deamer, D. W. (2008). Stability of model membranes in extreme environments. *Origins of Life and Evolution of Biospheres, 38*(4), 329-341.

Namani, T., & Walde, P. (2005). From decanoate micelles to decanoic acid/dodecylbenzenesulfonate vesicles. *Langmuir, 21*(14), 6210-6219.

Nishihata, T., Rytting, J. H., Takahashi, K., & Sakai, K. (1988). Effects of dithiothreitol and ascorbate on the penetration of diclofenac across excised rat dorsal skin. *Pharmaceutical Research, 5*(11), 738-740.

Nishikido, N. (1992). Thermodynamic equations expressing the synergistic solubilization effect by surfactant mixtures. 2. Further Information. *Langmuir, 8*(7), 1718-1723.

Ohta, A., Matsubara, H., Ikeda, N., & Aratono, M. (2001). Miscibility of binary surfactant mixtures in the adsorbed film and micelle the effect of size of polar head group. *Colloids and Surfaces A: Physicochemical and Engineering Aspects, 183 - 185*, 403 - 413.

Oldham, E. D., Seelam, S., Lema, C., Aguilera, R. J., Fiegel, J., Rankin, S. E., Knutson, B. L., & Lehmler, H. J. (2013). Synthesis, surface properties, and biocompatibility of 1,2,3-triazole-containing alkyl beta-D-xylopyranoside surfactants. *Carbohydrate Research, 379*, 68-77.

Ozkal, E., Llanes, P., Bravo, F., Ferrali, A., & Pericàs, M. A. (2014). Fine-Tunable Tris(triazolyl)methane Ligands for Copper(I)- Catalyzed Azide-Alkyne Cycloaddition Reactions. *Advanced Synthesis & Catalysis, 356*(4), 857-869.

Palla, B. J., & Shah, D. O. (2000). Stabilization of high ionic strength slurries using the synergistic effects of a mixed surfactant system. *Journal of Colloid Interface Science, 223*(1), 102-111.

Peterson, B., & Marzzacco, C. (2007). The effect of hydrocarbon chain length on the critical micelle concentration of cationic surfactants: An undergraduate physical chemistry experiment. *The Chemical Educator, 12*, 80-84.

Pickholz, M., & Stafström, S. (2001). Theoretical investigation of the role of π–π interactions for the stability of phenylene ethynylene aggregates. *Chemical Physics, 270*(2), 245-251.

Pokhodylo, N. T., Matiychuk, V. S., & Obushak, M. D. (2010). Synthesis of 1-(r-phenyl)-5-(r-methyl)-1 h-1, 2, 3-triazole-4-carboxylic acids by one-pot tandem reaction. *Synthetic Communications®, 40*(13), 1932-1938.

Ranjan, N., Story, S., Fulcrand, G., Leng, F., Ahmad, M., King, A., Sur, S., Wang, W., Tse-Dinh, Y.-C., & Arya, D. P. (2017). Selective inhibition of *Escherichia coli* rna and DNA Topoisomerase I by hoechst 33258 derived mono- and bisbenzimidazoles. *Journal of Medicinal Chemistry, 60*(12), 4904-4922.

Rather, M. A., Rather, G. M., Pandit, S. A., Bhat, S. A., & Bhat, M. A. (2015). Determination of cmc of imidazolium based surface active ionic liquids through probe-less UV–vis spectrophotometry. *Talanta, 131*, 55-58.

Resende, G. O., Teixeira, S. F., Figueiredo, I. F., Godoy, A. A., Lougon, D. J. F., Cotrim, B. A., & Souza, F. C. d. (2019). Synthesis of 1, 2, 3-triazole derivatives and its evaluation as corrosion inhibitors for carbon steel. *International Journal of Electrochemistry, 2019,*12.

Reshad, M., Nesbit, M., Petrie, A., & Setchell, D. (2009). Chlorhexidine gluconate mouthwashes as a surfactant for addition-reaction silicone impressions. *The European Journal of Prosthodontics and Restorative Dentistry, 17*(1), 2-8.

Rosen, M. J. (1972). The relationship of structure to properties in surfactants. *Journal of the American Oil Chemists' Society, 49*(5), 293-297.

Rosen, M. J. (2004). Micelle formation by surfactants. *Surfactants and Interfacial Phenomena*. Hoboken, New Jersey: John Wiley & Sons.

Rosen, M. J., & Sulthana, S. B. (2001). The interaction of alkylglycosides with other surfactants. *Journal of Colloid and Interface Science, 239*(2), 528-534.

Rosen, M. J., & Zhou, Q. (2001). Surfactant− surfactant interactions in mixed monolayer and mixed micelle formation. *Langmuir, 17*(12), 3532-3537.

Rostovtsev, V. V., Green, L. G., Fokin, V. V., & Sharpless, K. B. (2002). A Stepwise Huisgen Cycloaddition Process: Copper(I) - Catalyzed Regioselective "Ligation" of Azides and Terminal Alkynes. *Angewandte Chemie, 114*(14), 2708-2711.

Rustan, A. C., & Drevon, C. A. (2005). Fatty Acids: Structures and Properties.

Sani, F. A., Heidelberg, T., & Hashim, R. (2012). Alkyl triazole glycosides (ATGs)—a new class of bio-related surfactants. *Colloids and Surfaces B: Biointerfaces, 97*, 196-200.

Schmidt-Lassen, J., & Lindhorst, T. K. (2014). Exploring the meaning of sugar configuration in a supramolecular environment: comparison of six octyl glycoside

micelles by ITC and NMR spectroscopy. *Medicinal Chemistry Communications, 5*(8), 1218-1226.

Sharpless, K. B., Fokin, V., Rostovtsev, V. A., Green, L., & Himo, F. (2008). United States Patent Patent No. US 7375234. T. S. R. Institute.

Shetty, A. S., Zhang, J., & Moore, J. S. (1996). Aromatic π-stacking in solution as revealed through the aggregation of phenylacetylene macrocycles. *Journal of the American Chemical Society, 118*(5), 1019-1027.

Shinoda, K. (1954). The effect of alcohols on the critical micelle concentrations of fatty acid soaps and the critical micelle concentration of soap mixtures. *The Journal of Physical Chemistry, 58*(12), 1136-1141.

Shinoda, K., Yamaguchi, T., & Hori, R. (1961). The surface tension and the critical micelle concentration in aqueous solution of *β*-D-alkyl glucosides and their mixtures. *Bulletin of the Chemical Society of Japan, 34*(2), 237-241.

Takakura, K., Yamamoto, T., Kurihara, K., Toyota, T., Ohnuma, K., & Sugawara, T. (2014). Spontaneous transformation from micelles to vesicles associated with sequential conversions of comprising amphiphiles within assemblies. *Chemical Communications, 50*(17), 2190-2192.

Tanford, C. (1974). Theory of micelle formation in aqueous solutions. *The Journal of Physical Chemistry, 78*(24), 2469-2479.

Tang, L., Jin, J., Zhang, S., Mao, Y., Sun, J., Yuan, W., Zhao, H., Xu, H., Qin, A., & Tang, B. Z. (2009). Detection of the critical micelle concentration of cationic and anionic surfactants based on aggregation-induced emission property of hexaphenylsilole derivatives. *Science in China Series B: Chemistry, 52*(6), 755-759.

Taylor, R., & Kennard, O. (1982). Crystallographic evidence for the existence of CH. cntdot.. cntdot.. cntdot. O, CH. cntdot.. cntdot.. cntdot. N and CH. cntdot.. cntdot.. cntdot. Cl hydrogen bonds. *Journal of the American Chemical Society, 104*(19), 5063-5070.

Tornoe, C. W., Christensen, C., & Meldal, M. (2002). Peptidotriazoles on solid phase: [1,2,3]-triazoles by regiospecific copper(i)-catalyzed 1,3-dipolar cycloadditions of terminal alkynes to azides. *Journal of Organic Chemistry, 67*(9), 3057-3064.

Van Koningsveld, H., Jansen, J., & Straathof, A. (1988). Structure of anhydrous octyl α-d-glucopyranoside. A comparison with its hemi-and monohydrate. *Acta Crystallographica Section C: Crystal Structure Communications, 44*(6), 1054-1057.

Verma, S. K., & Ghosh, K. K. (2011). Micellar and surface properties of some monomeric surfactants and a gemini cationic surfactant. *Journal of Surfactants and Detergents, 14*(3), 347-352.

Wang, H., Wang, J., Zhang, S., & Xuan, X. (2008). Structural effects of anions and cations on the aggregation behavior of ionic liquids in aqueous solutions. *The Journal of Physical Chemistry B, 112*(51), 16682-16689.

Wanka, G., Hoffmann, H., & Ulbricht, W. (1994). Phase-diagrams and aggregation behavior of poly(oxyethylene)-poly(oxypropylene)-poly(oxyethylene) triblock copolymers in aqueous-solutions. *Macromolecules, 27*(15), 4145-4159.

Wu, T., Huang, J., & Yan, Y. (2019). Self‐assembly of aggregation‐induced‐emission molecules. *Chemistry‐An Asian Journal, 14*(6), 730-750.

Yan, J. F., & Palmer, M. B. (1969). A nuclear magnetic resonance method for determination of critical micelle concentration. *Journal of Colloid and Interface Science, 30*(2), 177-182.

Yan, W., Wang, Q., Lin, Q., Li, M., Petersen, J. L., & Shi, X. (2011). N‐2‐aryl‐1, 2, 3‐triazoles: A novel class of UV/blue‐light‐emitting fluorophores with tunable optical properties. *Chemistry‐A European Journal, 17*(18), 5011-5018.

Yang, C.-M., Lee, I.-W., Chen, T.-L., Chien, W.-L., & Hong, J.-L. (2013). Enhanced emission of organic and polymeric luminogens containing 2, 4, 6-triphenylpyridine moieties: crystallization-and aggregation-enhanced emission. *Journal of Materials Chemistry C, 1*(16), 2842-2850.

Ysambertt, F., Vejar, F., Paredes, J., & Salager, J.-L. (1998). The absorbance deviation method: a spectrophotometric estimation of the critical micelle concentration (CMC) of ethoxylated alkylphenol surfactants. *Colloids and Surfaces A: Physicochemical and Engineering Aspects, 137*(1-3), 189-196.

Yuasa, H., Asakura, K., & Banno, T. (2017). Sequential dynamic structuralisation by in situ production of supramolecular building blocks. *Chemical Communications, 53*(61), 8553-8556.

Zhai, L., Zhao, M., Sun, D., Hao, J., & Zhang, L. (2005). Salt-induced vesicle formation from single anionic surfactant SDBS and its mixture with LSB in aqueous solution. *The Journal of Physical Chemistry B, 109*(12), 5627-5630.

Zhang, Q., Ning, Z., & Tian, H. (2009). 'Click'synthesis of starburst triphenylamine as potential emitting material. *Dyes and Pigments, 81*(1), 80-84.

Zhang, R., Zhang, L., & Somasundaran, P. (2004). Study of mixtures of n-dodecyl-beta-D-maltoside with anionic, cationic, and nonionic surfactant in aqueous solutions using surface tension and fluorescence techniques. *Journal of Colloid and Interface Science, 278*(2), 453-460.

Zhang, T. J., Wu, Q. X., Li, S. Y., Wang, L., Sun, Q., Zhang, Y., Meng, F. H., & Gao, H. (2017a). Synthesis and evaluation of 1-phenyl-1H-1,2,3-triazole-4-carboxylic acid derivatives as xanthine oxidase inhibitors. *Bioorganic & Medicinal Chemistry, 27*(16), 3812-3816.

Zhang, Y.-C., Jin, R., Li, L.-Y., Chen, Z., & Fu, L.-M. (2017b). Study on the fluorescent activity of N^2-indolyl-1, 2, 3-triazole. *Molecules, 22*(9), 1380.

Zhou, T., Li, F., Fan, Y., Song, W., Mu, X., Zhang, H., & Wang, Y. (2009). Hydrogen-bonded dimer stacking induced emission of aminobenzoic acid compounds. *Chemical Communications*(22), 3199-3201.

LIST OF PUBLICATIONS AND PAPERS PRESENTED

List of Publications

1. **Zul, N. F.,** Tajuddin, H. A., Ahmad, N., Abidin, Z. H. Z., Sadidarto, A. B., Abdullah, Z. (2020). Influence of hydrogen bonding on low critical micellar concentration value and formation of giant vesicle of triazole-contained amphiphile. *Journal of Surfactants and Detergents* (Vol. 24, p. 243-253).
2. Tajuddin, H. A., Idris, T., **Zul, N. F**., Sadidarto, A. B., Abdullah, Z., & Ahmad, N. (2017, December). Self-aggregation behavior of synthetic amphiphile derived from triazolylbenzoic acid: CMC and phase transition. In *AIP Conference Proceedings* (Vol. 1901, No. 1, p. 080002). AIP Publishing LLC.

Papers Presented

1. Physicochemical investigations of self-aggregations alkylated triazolyl benzoate. 15th International Conference on Frontier of Polymers and Advanced Materials (ICFPAM 2019), 17-21st June 2019, Penang, Malaysia. (Presenter)
2. Physicochemical investigations of triazolyl benzoate anionic surfactant and its mixture with glycolipids. 31st International Conference of Analytical Sciences 2018 (SKAM31), 17-19th August 2018, Kuantan, Pahang.
3. Low Critical Aggregation and pH-induced Phase transition when alkyl triazolyl benzoic acid in aqueous. 7th Asian Conference on Colloid and Interface Science (ACCIS 2017), 8-10th August 2017, Berjaya Times Square, Kuala Lumpur, Malaysia. (Presenter).